International Telecommunication Union

ITU-T

TELECOMMUNICATION
STANDARDIZATION SECTOR
OF ITU

Series G
Supplement 39
(02/2016)

SERIES G: TRANSMISSION SYSTEMS AND MEDIA,
DIGITAL SYSTEMS AND NETWORKS

Optical system design and engineering considerations

ITU-T G-series Recommendations – Supplement 39

Supplement 39 to ITU-T G-series Recommendations

Optical system design and engineering considerations

Summary

Supplement 39 to ITU-T G-series Recommendations provides information on the background and methodologies used in the development of optical interface Recommendations such as ITU-T G.691, ITU-T G.957 and ITU-T G.959.1. This edition adds further information on modulation formats; clarifies power budget parameters for systems with optical amplifiers; provides further information on the optical signal-to-noise ratio (OSNR) measurement; updates information on concatenation of non-linear effects; adds bit error ratio (BER) estimation technique based on constellation and makes other miscellaneous corrections.

History

Edition	Recommendation	Approval	Study Group	Unique ID[*]
1.0	ITU-T G Suppl. 39	2003-10-31	15	11.1002/1000/7049
2.0	ITU-T G Suppl. 39	2006-02-17	15	11.1002/1000/8749
3.0	ITU-T G Suppl. 39	2008-12-12	15	11.1002/1000/9684
4.0	ITU-T G Suppl. 39	2012-09-21	15	11.1002/1000/11765
5.0	ITU-T G Suppl. 39	2016-02-26	15	11.1002/1000/12840

---

[*] To access the Recommendation, type the URL http://handle.itu.int/ in the address field of your web browser, followed by the Recommendation's unique ID. For example, http://handle.itu.int/11.1002/1000/11830-en.

FOREWORD

The International Telecommunication Union (ITU) is the United Nations specialized agency in the field of telecommunications, information and communication technologies (ICTs). The ITU Telecommunication Standardization Sector (ITU-T) is a permanent organ of ITU. ITU-T is responsible for studying technical, operating and tariff questions and issuing Recommendations on them with a view to standardizing telecommunications on a worldwide basis.

The World Telecommunication Standardization Assembly (WTSA), which meets every four years, establishes the topics for study by the ITU-T study groups which, in turn, produce Recommendations on these topics.

The approval of ITU-T Recommendations is covered by the procedure laid down in WTSA Resolution 1.

In some areas of information technology which fall within ITU-T's purview, the necessary standards are prepared on a collaborative basis with ISO and IEC.

NOTE

In this publication, the expression "Administration" is used for conciseness to indicate both a telecommunication administration and a recognized operating agency.

Compliance with this publication is voluntary. However, the publication may contain certain mandatory provisions (to ensure, e.g., interoperability or applicability) and compliance with the publication is achieved when all of these mandatory provisions are met. The words "shall" or some other obligatory language such as "must" and the negative equivalents are used to express requirements. The use of such words does not suggest that compliance with the publication is required of any party.

INTELLECTUAL PROPERTY RIGHTS

ITU draws attention to the possibility that the practice or implementation of this publication may involve the use of a claimed Intellectual Property Right. ITU takes no position concerning the evidence, validity or applicability of claimed Intellectual Property Rights, whether asserted by ITU members or others outside of the publication development process.

As of the date of approval of this publication, ITU had not received notice of intellectual property, protected by patents, which may be required to implement this publication. However, implementers are cautioned that this may not represent the latest information and are therefore strongly urged to consult the TSB patent database at http://www.itu.int/ITU-T/ipr/.

Table of Contents

Supplement 39 to ITU-T G-series Recommendations

Optical system design and engineering considerations

1 Scope

This Supplement is not a Recommendation and does not have the status of a standard. In case of conflict between the material contained in this Supplement and the material of the relevant Recommendations, the latter always prevails. This Supplement should not be used as a normative reference; only the relevant Recommendations can be referenced.

This Supplement describes design and engineering considerations for unamplified and amplified single-channel and multichannel digital optical line systems supporting plesiochronous digital hierarchy (PDH), synchronous digital hierarchy (SDH) and optical transport network (OTN) signals in intra-office, inter-office and long-haul terrestrial networks.

One intent of this Supplement is to consolidate and expand on related material that is currently included in several Recommendations, including [ITU-T G.691], [ITU-T G.692], [ITU-T G.955], [ITU-T G. 957] and [ITU-T G.959.1]. This Supplement is also intended to allow a better correlation of the specifications of the fibre, components and system interface Recommendations currently developed in ITU-T.

2 References

[ITU-T G.650.1]   Recommendation ITU-T G.650.1 (2010), *Definitions and test methods for linear, deterministic attributes of single-mode fibre and cable.*

[ITU-T G.650.2]   Recommendation ITU-T G.650.2 (2015), *Definitions and test methods for statistical and non-linear related attributes of single-mode fibre and cable.*

[ITU-T G.652]   Recommendation ITU-T G.652 (2009), *Characteristics of a single-mode optical fibre and cable.*

[ITU-T G.653]   Recommendation ITU-T G.653 (2010), *Characteristics of a dispersion-shifted, single-mode optical fibre and cable.*

[ITU-T G.654]   Recommendation ITU-T G.654 (2012), *Characteristics of a cut-off shifted single-mode optical fibre and cable.*

[ITU-T G.655]   Recommendation ITU-T G.655 (2009), *Characteristics of a non-zero dispersion-shifted single-mode optical fibre and cable.*

[ITU-T G.661]   Recommendation ITU-T G.661 (2007), *Definitions and test methods for the relevant generic parameters of optical amplifier devices and subsystems.*

[ITU-T G.662]   Recommendation ITU-T G.662 (2005), *Generic characteristics of optical amplifier devices and subsystems.*

[ITU-T G.663]   Recommendation ITU-T G.663 (2011), *Application-related aspects of optical amplifier devices and subsystems.*

[ITU-T G.671]   Recommendation ITU-T G.671 (2012), *Transmission characteristics of optical components and subsystems.*

[ITU-T G.691]   Recommendation ITU-T G.691 (2006), *Optical interfaces for single channel STM-64 and other SDH systems with optical amplifiers.*

[ITU-T G.692]   Recommendation ITU-T G.692 (1998), *Optical interfaces for multichannel systems with optical amplifiers.*

[ITU-T G.693]	Recommendation ITU-T G.693 (2009), *Optical interfaces for intra-office systems*.
[ITU-T G.694.1]	Recommendation ITU-T G.694.1 (2012), *Spectral grids for WDM applications: DWDM frequency grid*.
[ITU-T G.694.2]	Recommendation ITU-T G.694.2 (2003), *Spectral grids for WDM applications: CWDM wavelength grid*.
[ITU-T G.695]	Recommendation ITU-T G.695 (2015), *Optical interfaces for coarse wavelength division multiplexing applications*.
[ITU-T G.697]	Recommendation ITU-T G.697 (2012), *Optical monitoring for dense wavelength division multiplexing systems*.
[ITU-T G.698.1]	Recommendation ITU-T G.698.1 (2009), *Multichannel DWDM applications with single-channel optical interfaces*.
[ITU-T G.698.2]	Recommendation ITU-T G.698.2 (2009), *Amplified multichannel dense wavelength division multiplexing applications with single channel optical interfaces*.
[ITU-T G.707]	Recommendation ITU-T G.707/Y.1322 (2007), *Network node interface for the synchronous digital hierarchy (SDH)*.
[ITU-T G.709]	Recommendation ITU-T G.709/Y.1331 (2012), *Interfaces for the optical transport network*.
[ITU-T G.798]	Recommendation ITU-T G.798 (2012), *Characteristics of optical transport network hierarchy equipment functional blocks*.
[ITU-T G.826]	Recommendation ITU-T G.826 (2002), *End-to-end error performance parameters and objectives for international, constant bit-rate digital paths and connections*.
[ITU-T G.828]	Recommendation ITU-T G.828 (2000), *Error performance parameters and objectives for international, constant bit-rate synchronous digital paths*.
[ITU-T G.872]	Recommendation ITU-T G.872 (2012), *Architecture of optical transport networks*.
[ITU-T G.955]	Recommendation ITU-T G.955 (1996), *Digital line systems based on the 1544 kbit/s and the 2048 kbit/s hierarchy on optical fibre cables*.
[ITU-T G.957]	Recommendation ITU-T G.957 (2006), *Optical interfaces for equipments and systems relating to the synchronous digital hierarchy*.
[ITU-T G.959.1]	Recommendation ITU-T G.959.1 (2012), *Optical transport network physical layer interfaces*.
[ITU-T G.975]	Recommendation ITU-T G.975 (2000), *Forward error correction for submarine systems*.
[ITU-T G.983.1]	Recommendation ITU-T G.983.1 (2005), *Broadband optical access systems based on Passive Optical Networks (PON)*.
[ITU-T G.8080]	Recommendation ITU-T G.8080/Y.1304 (2012), *Architecture for the automatically switched optical network*.
[ITU-T G.8201]	Recommendation ITU-T G.8201 (2011), *Error performance parameters and objectives for multi-operator international paths within optical transport networks*.

[ITU-T L.302]	Recommendation ITU-T L.302/L.40 (2000), *Optical fibre outside plant maintenance support, monitoring and testing system*.
[ITU-T L.301]	Recommendation ITU-T L.301/L.41 (2000), *Maintenance wavelength on fibres carrying signals*.
[IEC 61291-4]	IEC 61291-4 (2011), *Optical amplifiers – Part 4: Multichannel applications – Performance specification template*. <http://webstore.iec.ch/webstore/webstore.nsf/Artnum_PK/45812>
[IEC/TR 61282-3]	IEC/TR 61282-3 (2006), *Fibre optic communication system design guides – Part 3: Calculation of link polarization mode dispersion*. <http://webstore.iec.ch/Webstore/webstore.nsf/ArtNum_PK/37065!opendocument&preview=1>
[IEC/TR 61292-3]	IEC/TR 61292-3 (2003), *Optical amplifiers – Part 3: Classification, characteristics and applications*. <http://webstore.iec.ch/webstore/webstore.nsf/Artnum_PK/30718>

3 Terms and definitions

Formal definitions are found in the Recommendations referenced in clause 2.

4 Abbreviations and acronyms

This Supplement uses the following abbreviations and acronyms:

1R	Regeneration of power
2R	Regeneration of power and shape
3D-Simplex	3-Dimensional Simplex
3R	Regeneration of power, shape and timing
6PolSK-QPSK	6-Polarization Shift Keying QPSK
ADC	Analogue-to-Digital Converter
ADM	Add/Drop Multiplexer
APR	Automatic Power Reduction
ASE	Amplified Spontaneous Emission
ASK	Amplitude Shift Keying
AWGN	Additive White Gaussian Noise
BCH	Bose-Chaudhuri-Hocquenghem
BER	Bit Error Ratio
BPM	Beam Propagation Method
BSC	Binary Symmetric Channel
CD	Chromatic Dispersion
CS-RZ	Carrier Suppressed Return to Zero
CWDM	Coarse Wavelength Division Multiplexing
DA	Dispersion Accommodation
DAa	Amplifier-Aided Dispersion Accommodation
DAc	Channel Dispersion Accommodation

DAC	Digital-to-Analogue Converter
DC	Direct Current
DCD	Dispersion compensation device
DCF	Dispersion-Compensating Fibre
DGD	Differential Group Delay
DI	Delay and add MZ differential interferometer
DP-QAM	Dual Polarization QAM
DP-QPSK	Dual Polarization Quadrature Phase Shift Keying
DPSK	Differential Phase Shift Keying
DQPSK	Differential Quadrature Phase Shift Keying
DSP	Digital Signal Processing
DST	Dispersion-Supported Transmission
DWDM	Dense Wavelength Division Multiplexing
E/O	Electrical to Optical conversion
EDC	Error Detection Code
EDFA	Erbium-Doped Fibre Amplifier
FEC	Forward Error Correction
FFE	Feed Forward Equalizer
FFT	Forward Fourier Transform
FSK	Frequency Shift Keying
FWHM	Full Width at Half Maximum
FWM	Four-Wave Mixing
GEF	Generalized Exponential Function
GVD	Group Velocity Dispersion
HD	Hard-Decision
HIPPI	High-Performance Parallel Interface
ICI	Interchannel Interference
IFT	Inverse Fourier Transform
IL	Interleaver
IrDI	Inter-Domain Interface
IPP	Integrated Power Product value
ISI	Intersymbol Interference
LD	Laser Diode
LO	Local Oscillator
MAP	Maximum A posteriori Probability
MC	Multichannel
MI	Modulation Instability

MLM	Multi-Longitudinal Mode
MLSD	Maximum Likelihood Sequence Detection
MPI	Multi-Path Interferance
MPI-R	Multi-Path Interface at the Receiver
MPI-S	Multi-Path Interface at the Source
MPN	Mode Partition Noise
M-Rx	Multichannel Receiver equipment
M-Tx	Multichannel Transmitter equipment
MZI	Mach-Zehnder interferometer
MZM	Mach-Zehnder Modulator
NCG	Net Coding Gain
NLT	Non-Linear Threshold
NNI	Network Node Interface
NRZ	Non-Return to Zero
NRZ-DPSK	Non-Return to Zero Differential Phase Shift Keying
NRZ-DQPSK	Non-Return to Zero Differential Quadrature Phase Shift Keying
O/E	Optical to Electrical conversion
OA	Optical Amplifier
OAC	Optical Auxiliary Channel
OADM	Optical ADM (also WADM)
OBM-OFDM	Orthogonal-Band-Multiplexed Orthogonal Frequency Division Multiplexing
OCh	Optical Channel
OD	Optical Demultiplexer
ODB	Optical Duobinary
ODUk	Optical channel Data Unit of order k
OFA	Optical Fibre Amplifier
OLS	Optical Label Switching
OM	Optical Multiplexer
OMS	Optical Multiplex Section
ONE	Optical Network Element
O-OFDM	Optical Orthogonal Frequency Division Multiplexing
OPFDM-DQPSK	Orthogonal Polarization Frequency Division Multiplexing Differential Quadrature Phase Shift Keying
OSC	Optical Supervisory Channel
OSNR	Optical Signal-to-Noise Ratio
OSSB	Optical Single Side-Band
OTDR	Optical Time Domain Reflectometer

OTN	Optical Transport Network
OTS	Optical Transmission Section
OTUk	Optical channel Transport Unit of order k
OXC	Optical Cross Connect (also WSXC)
P/S	Parallel to Serial
PBC	Polarization beam combiner
PBS	PBS: Polarization beam splitter
PDC	Passive Dispersion Compensator
pdf	probability density function
PDFFA	Praseodymium-Doped Fluoride Fibre Amplifiers
PDH	Plesiochronous Digital Hierarchy
PDL	Polarization Dependent Loss
PDM-BPSK	Polarization Division Multiplexed Binary Phase Shift Keying
PDM-16QAM	Polarization Division Multiplexed 16-state Quadrature Amplitude Modulation
P-DPSK	Partial Differential Phase Shift Keying
PIN	P type-intrinsic-n type
PMD	Polarization Mode Dispersion
PM-QPSK	Polarization Multiplexed Quadrature Phase Shift Keying
PRBS	Pseudo-Random Bit Sequence
PS-QPSK	Polarization-Switched QPSK
PSBT	Phase Shaped Binary Transmission
PSK	Phase Shift Keying
ptp	point-to-point
QAM	Quadrature Amplitude Modulation
QPSK	Quadrature Phase Shift Keying
R	single-channel optical interface point at the Receiver
RF	Radio Frequency
RFA	Raman Fibre Amplifier
RX	(optical) Receiver
RZ	Return to Zero
RZ-AMI	Return to Zero Alternate Mark Inversion
RZ-DPSK	Return-to-Zero Differential Phase Shift Keying
RZ-DQPSK	Return to Zero Differential Quadrature Phase Shift Keying
S	single-channel optical interface at the Source
S/P	Serial to Parallel
SBS	Stimulated Brillouin Scattering
SC	Single Channel

SCM	Sub-Carrier Multiplexing
SD	Soft-Decision
SDH	Synchronous Digital Hierarchy
SLM	Single Longitudinal Mode
SOA	Semiconductor Optical Amplifier
SPM	Self-Phase Modulation
SRS	Stimulated Raman Scattering
STM	Synchronous Transport Module
TDM	Time Division Multiplex
TX	(optical) Transmitter
WADM	Wavelength ADM (also OADM)
WDM	Wavelength Division Multiplex
WSS	Wavelength-Selective Switch
WSXC	Wavelength-Selective XC (also OXC)
WTM	Wavelength Terminal Multiplexer
XC	Cross-Connect
XPM	Cross-Phase Modulation

5 Definition of spectral bands

5.1 General considerations

Consider optical transmitters. From the viewpoint of semiconductor laser diodes, the GaAlAs material system can cover the wavelength range from 700 nm to 1000 nm, while InGaAsP can cover 1000 nm to 1700 nm. Fibre lasers may later be added to this list. For optical receivers, the quantum efficiency of detector materials is important, and Si is used from 650 nm to about 950 nm, InGaAsP from 950 nm to 1150 nm, Ge from about 1100 nm to 1550 nm, and InGaAs from 1300 nm to 1700 nm. Thus, there is no technical problem for transmitters and receivers over a wide wavelength range of interest to optical communications.

With optical amplifiers (OAs), activity has been mainly in the longer-wavelength regions used with single-mode fibre. The original doped-fibre amplifiers, erbium-doped fibre amplifiers (EDFAs) around 1545 nm and praseodymium-doped fluoride fibre amplifiers (PDFFAs) around 1305 nm have been joined by other dopants such as Te, Yt or Tu. Consequently, the spectral region from about 1440 nm to above 1650 nm can be covered, though not with equal efficiency, and not all amplifiers may yet be commercially available. Semiconductor optical amplifiers (SOAs) and lower-noise Raman fibre amplifiers (RFAs) can extend from below 1300 nm to above 1600 nm. For some applications, combinations of OA types are used to achieve wide and flat-band low-noise operation.

[IEC/TR 61292-3] gives further details.

5.2 Allocation of spectral bands for single-mode fibre systems

Examine the limitations to spectral bands as imposed by the fibre types. In [ITU-T G.957], which does not include optical amplifiers, the wavelength range of 1260 nm to 1360 nm was chosen for ITU-T G.652 fibres. [ITU-T G.983.1] on passive optical networks also uses this range. The lower limit is determined by the cable cut-off wavelength, which is 1260 nm. The worst-case absolute dispersion coefficient curve for ITU-T G.652 fibre is shown in Figure A.2 of [ITU-T G.957]. The

worst-case dispersion coefficient at that wavelength is −6.42 ps/nm · km, and the worst-case dispersion coefficient of +6.42 ps/nm · km occurs at 1375 nm. However, this wavelength was on the rising edge of the "water" attenuation band peaked at 1383 nm, so 1360 nm was chosen as the upper limit. Various application codes could have more restricted wavelength ranges depending on dispersion requirements. This defines the:

–   "Original" O-band, 1260 nm to 1360 nm.

[ITU-T G.652] also includes fibres with a low water attenuation peak as subcategory ITU-T G.652.C. It is stated that "This subcategory also allows ITU-T G.957 transmissions to portions of the band above 1360 nm and below 1530 nm." The effects of a small water peak are negligible at wavelengths beyond about 1460 nm. This defines the:

–   "Extended" E-band, 1360 nm to 1460 nm.

At longer wavelength, the experts writing [ITU-T G.957] chose the ranges 1430 nm to 1580 nm for short-haul applications with ITU-T G.652 fibre, and 1480 nm to 1580 nm for long-haul applications with ITU-T G.652, ITU-T G.653 and ITU-T G.654 fibres. These were limited by attenuation considerations, and could be further restricted by dispersion in particular applications.

For applications with optical amplifiers, utilizing single-channel transmission as in [ITU-T G.691] and multichannel transmission as in [ITU-T G.692], these ranges were later subdivided. Initially, erbium-doped fibre amplifiers (EDFAs) had useful gain bands beginning at about 1530 nm and ending at about 1565 nm. This gain band had become known as the "C-band" and the boundaries varied in the literature and commercial specifications. The range 1530 nm to 1565 nm has been adopted for ITU-T G.655 fibre and ITU-T G.691 systems, and specifications have been developed for the range. This defines the:

–   "Conventional" C-band, 1530 nm to 1565 nm.

EDFAs have become available with relatively flatter and wider gains, and no limitation of EDFAs to this band is implied. Some EDFA designs can be said to exceed the C-band.

A region below the C-band became known as the "S-band". In particular applications, not all of this band may be available for signal channels. Some wavelengths may be utilized for pumping of optical fibre amplifiers, both of the active-ion type and the Raman type. Some wavelengths may be reserved for the optical supervisory channel (OSC). The lower limit of this band is taken to be the upper limit of the E-band, and the upper limit is taken to be the lower limit of the C-band. This defines the:

–   "Short wavelength" S-band, 1460 nm to 1530 nm.

For the longest wavelengths above the C-band, fibre cable performance over a range of temperatures is adequate to 1625 nm for current fibre types. Furthermore, it is desirable to utilize as wide a wavelength range as feasible for signal transmission. This defines the:

–   "Long wavelength" L-band, 1565 nm to 1625 nm.

For fibre cable outside plants, [ITU-T L.302] defines a number of maintenance functions – preventive, after installation, before service and post-fault. These involve surveillance, testing and control activities utilizing optical time domain reflectometer (OTDR) testing, fibre identification, loss testing and power monitoring. Maintenance wavelengths have been defined in [ITU-T L.301] in which there are the following statements:

–   "This Recommendation deals with maintenance wavelength on fibres carrying signals without in-line optical amplifiers."

–   "The maintenance wavelength assignment has a close relationship with the transmission wavelength assignment selected by Study Group 15."

–   "The maximum transmission wavelength is under study in Study Group 15, but is limited to less than or equal to 1625 nm."

In some cases, the test signal may overlap with the transmission signals if the testing power is sufficiently weaker than the transmission power. In other cases, the test wavelength may be in a region not occupied by the transmission channels for the particular application. In particular, a region that is intended to be never occupied by these channels may be attractive for maintenance, even if enhanced loss occurs. This defines the:

–   "Ultra-long wavelength" U-band, 1625 nm to 1675 nm.

Table 5-1 summarizes single-mode systems:

Table 5-1 – Single-mode spectral bands

Band	Descriptor	Range [nm]
O-band	Original	1260 to 1360
E-band	Extended	1360 to 1460
S-band	Short wavelength	1460 to 1530
C-band	Conventional	1530 to 1565
L-band	Long wavelength	1565 to 1625
U-band	Ultra-long wavelength	1625 to 1675

1)   The definition of spectral bands is to facilitate discussion and is not for specification. The specifications of operating wavelength bands are given in the appropriate system Recommendations.

2)   The ITU-T G.65x fibre Recommendations have not confirmed the applicability of all these wavelength bands for system operation or maintenance purposes.

3)   The boundary (1460 nm) between the E-band and the S-band remains under study.

4)   The U-band is for possible maintenance purposes only, and transmission of traffic-bearing signals is not currently foreseen. The use for non-transmission purposes must be done on a basis of causing negligible interference to transmission signals in other bands. Operation of the fibre in this band is not ensured.

5)   It is anticipated that in the near future, various applications, with and without optical amplifiers, will utilize signal transmission covering the full range of 1260 nm to 1625 nm.

5.3   Bands for multimode fibre systems

Multimode fibres are not limited by cut-off wavelength considerations, and although the values of attenuation coefficient are higher than for single-mode fibres, there can be more resistance to bending effects. The main wavelength limitation is one or more bandwidth windows, which can be designed for particular fibre classifications. In Table 5-2 wavelength windows are specified for several applications:

Table 5-2 – Wavelength ranges for some multimode applications

Application	Window (in nm) around 850 nm	Window (in nm) around 1300 nm
IEEE Serial Bus[a]	830-860	–
Fibre Channel[b]	770-860	(single-mode)
10BASE-F, -FB, -FL, -FP[c]	800-910	–
100BASE-FX[c, d], FDDI[d]	–	1270-1380
1000BASE-SX[c] (GbE)	770-860	–
1000BASE-LX[c] (GbE)	–	1270-1355
HIPPI[e]	830-860	1260-1360
[a] [b-IEEE 1394b] [b] [b-ANSI INCITS 450] [c] [b-IEEE 802.3] [d] [b-ISO/IEC 9314-3] [e] [b-ANSI INCITS 338]		

The classification for multimode fibres is for further study. The region 770 nm to 910 nm has been proposed.

6 Parameters of system elements

6.1 Line coding

Line coding for systems defined in [ITU-T G.957], [ITU-T G.691], [ITU-T G.692] and [ITU-T G.959.1] is performed using two different types of line codes:

– non-return to zero (NRZ);

– return to zero (RZ).

More information on this topic can be found in clause 7.

6.2 Transmitters

6.2.1 Transmitter types

Types of transmitters, using both multi-longitudinal mode (MLM) and single longitudinal mode (SLM) laser diodes, and the relevant specifications as well as implementation-related aspects are specified in [ITU-T G.691], [ITU-T G.692], [ITU-T G.957] and [ITU-T G.959.1].

6.2.2 Transmitter parameters

Transmitter parameters are defined at the transmitter output reference points S or multi-path interface at the source (MPI-S) as explained in [ITU-T G.957], [ITU-T G.691], [ITU-T G.692] and [ITU-T G.959.1].

6.2.2.1 System operating wavelength range

The operating wavelength ranges for single-channel SDH systems up to 10 Gbit/s are given in [ITU-T G.691] and [ITU-T G.957]. The operating wavelength ranges for single-channel and multichannel inter-domain interfaces (IrDIs) up to 40 Gbit/s are defined in [ITU-T G.959.1]. Other applications may use different wavelength bands and ranges within bands as defined in this Supplement.

For dense wavelength division multiplexing (DWDM) systems, the channel frequency grid is given in [ITU-T G.694.1]. For coarse wavelength division multiplexing (CWDM) systems, the channel

wavelength grid is given in [ITU-T G.694.2]. For DWDM systems, the channel frequency grid is summarized as follows:

$$193.1 + n \times Sp_j \ [\text{THz}]$$

where:

n is a positive or negative integer including 0

j is any one of the following integers: 1, 2 or 3

Sp_j is a factor to derive the generic channel spacing on a fibre

$$Sp_j = \begin{cases} 2^{-j} \times 0.1 \ [\text{THz}], \text{ when channel spacing is narrower than 100 GHz, or} \\ 0.1 \ [\text{THz}] , \text{ when channel spacing is 100 GHz or wider} \end{cases}$$

The nominal central frequencies defined by the formulae above consist of the frequency grid for dense wavelength division multiplex (WDM) systems. When the value of j is selected, the related channel spacing and nominal central frequencies of a DWDM system are determined. Values of $j = 1$, 2 and 3 correspond to 50, 25 and 12.5 GHz grids, respectively.

6.2.2.2   Spectral characteristics

Spectral characteristics of single-channel SDH interfaces up to 10 Gbit/s are given in [ITU-T G.691] and [ITU-T G.957]. For higher bit rates and longer distances, in particular in a WDM environment, additional specifications may be needed.

6.2.2.3   Maximum spectral width of SLM sources

This parameter is defined for single-channel SDH systems in [ITU-T G.691].

6.2.2.4   Maximum spectral width of MLM sources

This parameter is defined for single-channel SDH systems in [ITU-T G.691].

6.2.2.5   Chirp

This parameter is defined in [ITU-T G.691]. For higher bit rate or longer distance systems, possibly also operating on other line codes, it is likely that additional specification of a time-resolved dynamic behaviour might be required. This, as well as the measurement of this parameter, is for further study.

6.2.2.6   Side-mode suppression ratio

The side-mode suppression ratio of a single longitudinal mode optical source is defined in [ITU-T G.691], [ITU-T G.957] and [ITU-T G.959.1]. Values are given for SDH and OTN IrDI systems up to 40 Gbit/s.

6.2.2.7   Maximum spectral power density

Maximum spectral power density is defined in [ITU-T G.691].

6.2.2.8   Maximum mean channel output power

Maximum mean output power of a multichannel optical signal is specified and defined in [ITU-T G.959.1].

6.2.2.9   Minimum mean channel output power

This property of a multichannel optical signal is specified and defined in [ITU-T G.959.1].

6.2.2.10   Central frequency

Central frequencies of WDM signals are given in [ITU-T G.694.1] and [ITU-T G.959.1]. Here, frequencies are given down to 12.5 GHz spacing.

6.2.2.11   Channel spacing

Channel spacing for DWDM is defined in [ITU-T G.694.1] and for CWDM in [ITU-T G.694.2]. Other possibilities (wider or denser) are for further study.

6.2.2.12   Maximum central frequency deviation

Maximum central frequency deviation for NRZ-coded optical channels is defined in [ITU-T G.692] and [ITU-T G.959.1]. Other possibilities using asymmetrical filtering may require a different definition which is for further study.

6.2.2.13   Minimum extinction ratio

The minimum extinction ratio, as a per channel value for NRZ-coded WDM systems, is defined in [ITU-T G.959.1]. For RZ coded signals, the same method applies. For other line codes, this definition is for further study.

6.2.2.14   Eye pattern mask

The eye pattern masks of SDH single-channel systems are given in [ITU-T G.691], [ITU-T G.693] and [ITU-T G.957], as well as other Recommendations. The eye pattern mask for NRZ coded IrDI multichannel and single-channel interfaces is defined in [ITU-T G.959.1].

6.2.2.15   Polarization

This parameter gives the polarization distribution of the optical source signal. This parameter might influence the polarization mode dispersion (PMD) tolerance and is important in case of polarization multiplexing.

6.2.2.16   Optical signal-to-noise ratio of optical source

This value gives the ratio of optical signal power relative to optical noise power of an optical transmitter in a given bandwidth coupled into the transmission path.

6.3   Optical amplifiers

6.3.1   Amplifier types

Types of optical amplifiers and the relevant specifications as well as implementation-related aspects of optical fibre amplifiers and semiconductor amplifiers are given in [ITU-T G.661] and [ITU-T G.662] as well as [ITU-T G.663], respectively. Line amplifier definitions of long-haul multichannel systems are given in [ITU-T G.692]. In addition to this, Raman amplification in the transmission fibre or additional fibre segments in the transmission path can be used. The specification of Raman amplification is for further study.

Amplifiers can be used in conjunction with optical receivers and/or transmitters. In these cases, they are hidden in the receiver or transmitter black box and covered by the related specification. It should be noted that receiver side penalties, e.g., jitter penalty, are influenced by the presence of optical amplification.

An exhaustive list of generic amplifier parameters is defined in [ITU-T G.661]. In practical system design, only a part of this set of parameters is of relevance.

6.3.1.1   Power (booster) amplifier

Applications are described in [ITU-T G.663].

6.3.1.2   Preamplifier

Applications are described in [ITU-T G.663].

6.3.1.3   Line amplifier

Applications are described in [ITU-T G.692].

Different technology amplifiers can be used: optical fibre amplifiers (OFAs), semiconductor optical amplifiers (SOAs), as well as Raman fibre amplifiers (RFAs) utilizing the transmission fibre or additional fibre segments in the transmission path. The specification of RFAs is for further study.

6.3.2   Amplifier parameters

6.3.2.1   Multichannel gain variation

This parameter is defined in [IEC 61291-4].

6.3.2.2   Multichannel gain tilt

This parameter is defined in [IEC 61291-4].

6.3.2.3   Multichannel gain-change difference

This parameter is defined in [IEC 61291-4].

6.3.2.4   Total received power

This parameter is the maximum mean input power present at the reference point at the amplifier input.

6.3.2.5   Total launched power

This parameter is the maximum mean output power present at the reference point at the amplifier output.

6.4   Optical path

The optical path consists of all the transmission elements in series between the points 'S' and 'R'. The majority of this is usually optical fibre cable, but other elements (e.g., connectors, optical cross-connects, etc.) between 'S' and 'R' are also part of the optical path, and contribute to the path characteristics. The optical path parameter values listed in the interface ([ITU-T G.957], and [ITU-T G.691], etc.) define the limits of satisfactory operation of the link. Optical paths with values outside these limits may yield link performance that exceeds the required bit error ratio.

The approach used to determine the values of the optical path parameter limits was, in some cases, on the basis of an informed consensus of what could reasonably and practically be expected. The values of the individual parameters of the optical path, and how these combine, were taken into account in the limit determination process (see clause 10 for aspects of statistical design).

6.4.1   Fibre types and parameters

The parameters related to optical fibres and cables are defined in [ITU-T G.650.1], [ITU-T G.650.2], [ITU-T G.652], [ITU-T G.653], [ITU-T G.654] and [ITU-T G.655].

It should be noted that for some high bit-rate, long-distance transmission systems, the given parameters for the different fibre types may not be sufficiently precise to ensure adequate performance.

6.4.2   Optical path effects

Transmission-related aspects of optical fibre transmission systems are given in Appendix II of [ITU-T G.663], where the following effects related to the path are considered:

–   Optical fibre non-linearities:

    •   stimulated Brillouin scattering;

    •   four-wave mixing;

- • modulation instability;
- • self-phase modulation;
- • soliton formation;
- • cross-phase modulation;
- • stimulated Raman scattering.
- – Polarization properties:
  - • polarization mode dispersion;
  - • polarization dependent loss;
  - • polarization hole burning.
- – Fibre dispersion properties.
- – Chromatic dispersion.

6.4.3 Optical path parameters

The optical path from a system perspective is characterized by the following parameters:

6.4.3.1 Maximum attenuation

Definition and values of maximum attenuation for SDH line systems are given in [ITU-T G.691], [ITU-T G.692] and [ITU-T G.957].

For OTN IrDIs, the maximum attenuation definition is given in [ITU-T G.959.1].

The above Recommendations define applications in the O-, C- and L-bands. It should be noted that in other bands, different values of attenuation might apply. In the L-band, it is known that the attenuation coefficient of some fibres may be increased by macrobending and/or microbending loss after cable installation. The actual value of the loss increase is dependent on cable structure, cable installation conditions, and cable installation date. It can be determined by loss measurement at the required wavelengths after cable installation.

The approach used to specify the optical path in the above Recommendations has been to use the assumption of 0.275 dB/km for installed fibre attenuation coefficient including splices and cable margins for 1550-nm systems and 0.55 dB/km for 1310-nm systems. The target distances derived from these values are to be used for classification only and not for specification.

The following path aspects are included:

- – splices;
- – connectors;
- – optical attenuators (if used);
- – other passive optical devices (if used);
- – any additional cable margin to cover allowances for:
  - • future modifications to the cable configuration (additional splices, increased cable lengths, etc.);
  - • fibre cable performance variations due to environmental factors;
  - • degradation of any connectors, optical attenuators or other passive optical devices included in the optical path.

6.4.3.2 Minimum attenuation

The definition and values of the minimum attenuations for SDH line systems are given in [ITU-T G.691], [ITU-T G.692] and [ITU-T G.957].

For OTN and pre-OTN IrDIs, the minimum attenuation definition is given in [ITU-T G.959.1].

6.4.3.3 Dispersion

The maximum and minimum chromatic dispersion normally induced by the optical transmission fibre, to be accommodated by a system is defined for SDH and OTN systems in [ITU-T G.957], [ITU-T G.691], [ITU-T G.692] and [ITU-T G.959.1]. For higher bit rate and longer distance transmission systems, different values may apply due to, e.g., other wavelength range specifications. The values need also to be reconsidered for other bands.

6.4.3.4 Minimum optical return loss

Definitions of minimum optical return loss of the optical paths defined for SDH and OTN systems are given in [ITU-T G.957], [ITU-T G.691], [ITU-T G.692] and [ITU-T G.959.1]. Values for future systems using higher bit rates and transmission over longer distances may be different.

6.4.3.5 Maximum discrete reflectance

The maximum discrete reflectance of SDH and OTN systems are defined in [ITU-T G.957], [ITU-T G.691], [ITU-T G.692] and [ITU-T G.959.1].

6.4.3.6 Maximum differential group delay

The maximum differential group delay due to PMD to be accommodated for SDH and OTN systems is defined in [ITU-T G.691], [ITU-T G.692] and [ITU-T G.959.1]. Higher bit rates and line code systems may offer different specifications.

6.5 Receivers

6.5.1 Receiver types

Amplifiers can be used in conjunction with optical receivers. In this case, the amplifier is hidden in the receiver black box and covered by the related specification. It should be noted that the receiver side penalties, e.g., jitter penalty, are influenced by the presence of optical amplification.

6.5.2 Receiver parameters

These parameters are defined at the receiver reference points R or multi-path interface at the receiver (MPI-R) as given in [ITU-T G.957], [ITU-T G.691], [ITU-T G.692] and [ITU-T G.959.1].

6.5.2.1 Sensitivity

Receiver sensitivities for SDH single-channel systems up to 10 Gbit/s are defined in [ITU-T G.691] and [ITU-T G.957]. Sensitivities for SDH and OTN IrDI receivers are defined in [ITU-T G.959.1].

Receiver sensitivities are defined as end-of-life, worst-case values taking into account ageing and temperature margins as well as worst-case eye mask and extinction ratio penalties as resulting from transmitter imperfections given by the transmitter specification of the particular interface.

Penalties related to path effects, however, are specified separately from the basic sensitivity value.

6.5.2.2 Overload

Receiver overload definition and values for SDH single-channel systems up to 10 Gbit/s are defined in [ITU-T G.691] and [ITU-T G.957]. Overload definition and values for SDH and OTN IrDI receivers up to 40 Gbit/s are defined in [ITU-T G.959.1].

6.5.2.3 Minimum mean channel input power

The minimum mean channel input power of optically multiplexed IrDIs of up to 10 Gbit/s for multichannel receivers is defined in [ITU-T G.959.1].

6.5.2.4   Maximum mean channel input power

The maximum mean channel input power of optically multiplexed IrDIs of up to 10 Gbit/s for multichannel receivers is defined in [ITU-T G.959.1].

6.5.2.5   Optical path penalty

Optical path penalty definition and values for SDH single-channel systems up to 10 Gbit/s are defined in [ITU-T G.691] and [ITU-T G.957]. Path penalty definition and values for both single-channel and multichannel OTN IrDI receivers up to 10 Gbit/s are defined in [ITU-T G.959.1]. Path penalty definitions and values for single-channel SDH and OTN IrDI receivers up to 40 Gbit/s are also defined in [ITU-T G.959.1].

6.5.2.6   Optical path OSNR penalty

The optical path optical signal-to-noise ratio (OSNR) penalty is defined in [ITU-T G.698.2] and is the corresponding parameter to the optical path penalty, but for systems with optical amplifiers between the transmitter and receiver reference points.

6.5.2.7   Maximum channel input power difference

This parameter indicates the maximum difference between channels of an optically multiplexed signal and is defined in [ITU-T G.959.1].

6.5.2.8   Receiver OSNR tolerance

This value defines the minimum optical signal-to-noise ratio that is required for achieving the target bit error ratio (BER) at a receiver reference point at a given power level in OSNR limited (line amplified) systems and is defined in [ITU-T G.698.2]. It should be noted that this is a design parameter.

7   Line coding considerations

Current systems as defined in [ITU-T G.957], [ITU-T G.691], [ITU-T G.692] and [ITU-T G.959.1] are based on non-return to zero (NRZ) transmission. The related parameters (as well as the definition of the logical "0" and logical "1") are defined in the aforementioned Recommendations. For more demanding applications, other line codes can be of advantage.

This clause contains descriptions of more advanced modulation formats than NRZ and examples of specific implementations:

–   Return to zero (RZ)

–   Optical duobinary (ODB)

  •   Phase shaped binary transmission (PSBT)

  •   Return to zero alternate mark inversion (RZ-AMI)

–   Non-return to zero differential phase shift keying (NRZ-DPSK)

  •   Return-to-zero differential phase shift keying (RZ-DPSK)

  •   Partial differential phase shift keying (P-DPSK)

–   Non-return to zero differential quadrature phase shift keying (NRZ-DQPSK)

  •   Return to zero differential quadrature phase shift keying (RZ-DQPSK)

–   Dual polarization quadrature phase shift keying (DP-QPSK)

–   Optical orthogonal frequency division multiplexing (O-OFDM)

  •   Orthogonal polarization frequency division multiplexing differential quadrature phase shifted keying (OPFDM-DQPSK).

The use of line codes different than NRZ will influence the relation between the different parameters defined for the system and, therefore, will be reflected in sets of parameters different to the current parameters and their interdependence used in standardized applications.

7.1 Overview of various line coding schemes

Figure 7-1 provides an overview of some examples of line coding schemes: the conventional on-off keying formats NRZ and RZ (for example, with 50% duty cycle: RZ-50%) and the comparisons with alternative modulation formats such as ODB (PSBT), RZ-AMI, NRZ-DPSK, RZ-DPSK (for example, with 50% duty cycle), NRZ-DQPSK, RZ-50% DQPSK, DP-QPSK, polarization division multiplexed binary phase shift keying (PDM-BPSK) and polarization division multiplexed 16-state quadrature amplitude modulation (PDM-16QAM). All formats are depicted by their transmitter intensity and phase constellation, the optical transmitter spectrum, the intensity eye diagram and block diagram of a transmitter (Tx) generation method and a receiver (Rx) method.

NOTE – For DQPSK, RZ-DQPSK and PDM-BPSK, the symbol-rate is half of the bit-rate B; for DP-QPSK the symbol-rate is one quarter of the bit-rate B; and for PDM-16QAM the symbol-rate is one eighth of the bit-rate B.
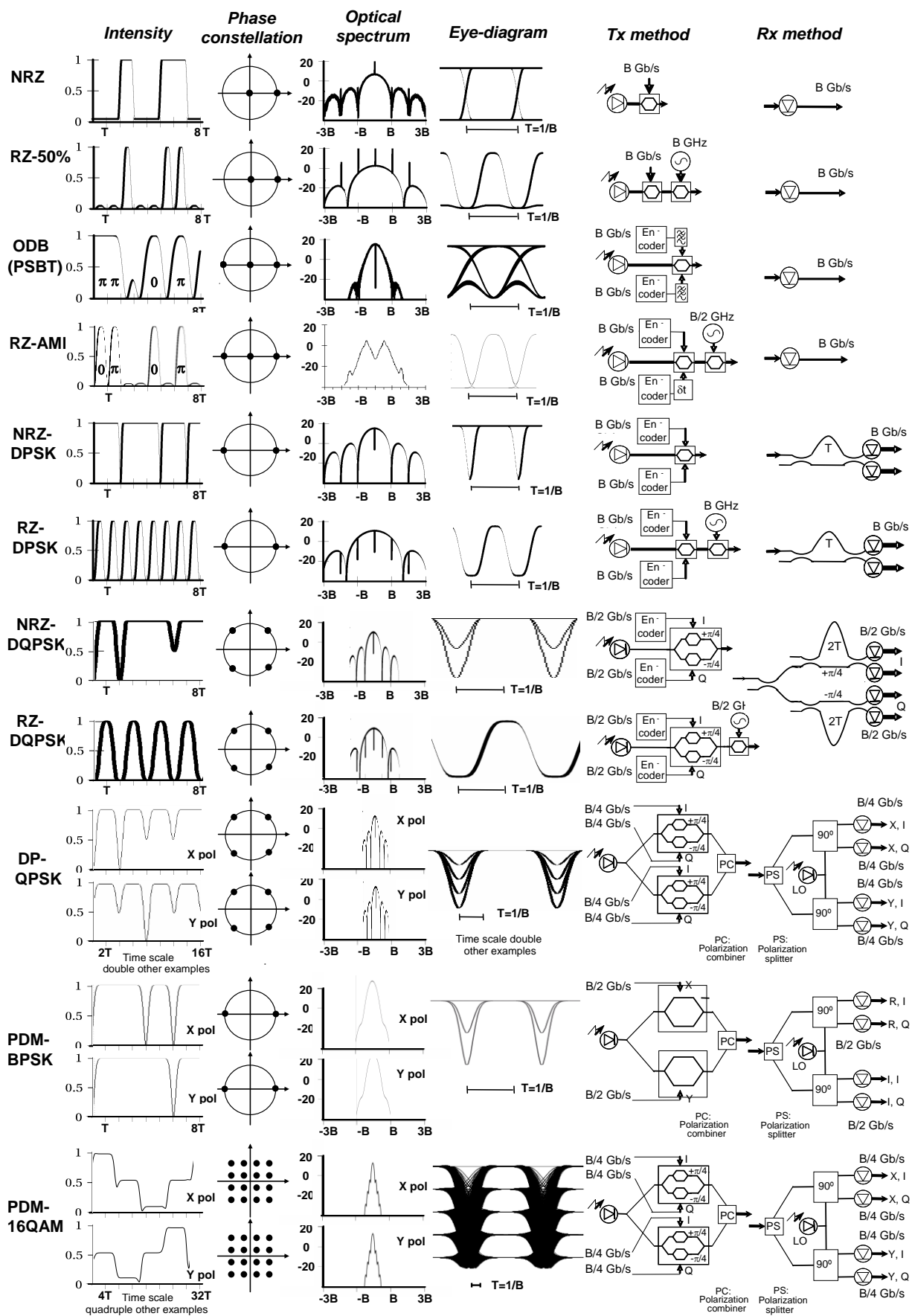
Figure 7-1 – Overview of modulation format examples

More details of the line coding examples are provided in the following clauses.

7.2 Return to zero (RZ) implementation

Return to zero (RZ) line-coded systems are significantly more tolerant to first-order PMD induced differential group delay (DGD) and are, therefore, better suited for ultra-long-haul transmission of high rate signals. However, RZ coding has (due to the broader bandwidth to be used) a potential drawback of being less spectrally efficient compared to NRZ.

There are several methods to generate optical return to zero (RZ) signals, e.g., by directly modulating a semiconductor laser with an RZ data signal, by generating an optical pulse train first and then modulating it with a non-return to zero (NRZ) data signal, or by pulse carving of an optical NRZ signal by a Mach-Zehnder modulator (MZM).

The last option has been practically used because of its simplicity and because various duty cycles can be realized by appropriate combination of the bias voltage and the modulation amplitude of the MZM. The NRZ optical input of the MZM can be generated from a directly modulated laser diode (LD) or a coarse wavelength (CW) laser with either an MZM or an electro-absorption modulator.

Three easily realizable duty cycles of RZ modulation are 1/3, 1/2 and 2/3 (referred as 33%, 50% and 67% in the text below, respectively). Possible implementations corresponding to the MZM implementation are shown in Figure 7-2.

With a driving voltage:

$$V_m(t) = V_{bias} + V_{RF}(t) = V_{bias} + V_{RF} \cos(2\pi f_{mod} t + \phi_m) \tag{7-1}$$

where V_{bias} is the direct current (DC) bias voltage, V_{RF} is the RF modulation amplitude, f_{mod} is the radio frequency (RF) modulation frequency and ϕ_m the phase shift, the optical power transfer function of an MZM can be written as:

$$T(t) \propto \cos^2\left[\frac{\pi V_m(t)}{2V_\pi} + \frac{\theta}{2}\right] = \cos^2\left[\frac{\pi V_{bias}}{2V_\pi} + \frac{\pi V_{RF}(t)}{2V_\pi} + \frac{\theta}{2}\right] \tag{7-2}$$

here, θ is the intrinsic phase shift of the MZM without the driving voltage and V_π is the π phase shift voltage of the MZM. It is defined that if $V_{bias} = V_{max}$, then the MZM is DC biased at its maximum optical transmission; and, if $V_{bias} = V_{min}$, then the MZM is DC biased at its minimum optical transmission. The MZM can also be driven in a balanced manner (push-pull).

Here, NRZ coding is shown using an MZM with a single drive electrode. RZ pulse carving is achieved with push-pull MZM following the NRZ data modulator. Figure 7-2 depicts the basic block diagram for NRZ and RZ format coding.
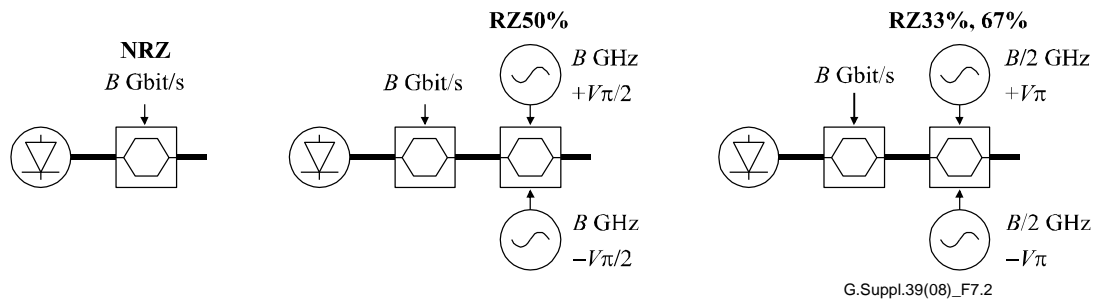
Figure 7-2 – Block diagram of NRZ and RZ format coding with MZM

In the case of chirp-free push-pull modulation of a two-arm z-cut LiNbO₃ MZM, an electrical peak-to-peak modulation of Vπ is split into +Vπ/2 and −Vπ/2 to obtain RZ-50% format, for example, see Figure 7-2. Alternatively, RZ modulation can be realized using a single-arm MZM by applying peak-to-peak modulation of Vπ at the single arm to obtain RZ-50% format.

The generation of the three different RZ duty cycles depends on the RZ modulator frequency, the electrical peak-to-peak modulation voltage and the modulator bias. The driving conditions of RZ formats with 50%, 33% and CS-RZ 67% duty cycle are depicted in Figure 7-3:
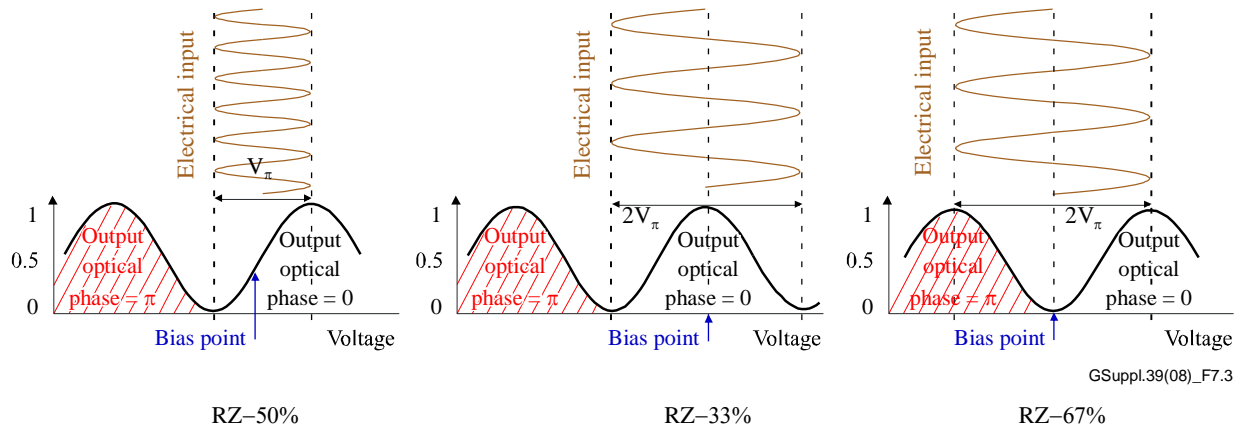
Figure 7-3 – Bias configurations of RZ formats

Table 7-1 summarizes the key figures of the three RZ duty cycles, f_{mod} is the modulation frequency, V_{mod} the peak-to-peak modulation voltage ($2V_{RF}$), V_{bias} describes the bias condition: V_{min} and V_{max} are the bias points at transmission minimum (carrier suppressed) and maximum, respectively, and V_{3dB} is the conventional MZM bias point used also for NRZ data modulation by the NRZ modulator. "Phase shift" describes the phase shift between consecutive RZ pulses and bits.

Table 7-1 – Modulation figures of RZ formats at 43 Gbit/s

RZ-	33%	50%	67% (CS-RZ)
f_{mod} (GHz)	21.5	43	21.5
V_{mod}	$2V_\pi$	V_π	$2V_\pi$
V_{bias}	V_{max}	V_{3dB}	V_{min}
Phase shift	0, 0, 0	0, 0, 0	0, π, 0

Figure 7-4 shows the intensity variation of the RZ pulses following the NRZ data modulation with data sequence of '00100110'. The three different duty cycles are defined by the pulse widths (FWHM/T): 50%, 33% and 67% of the bit period T. The RZ-50% and RZ-33% formats have no phase change, while for CS-RZ-67% consecutive pulses have a phase change of π.
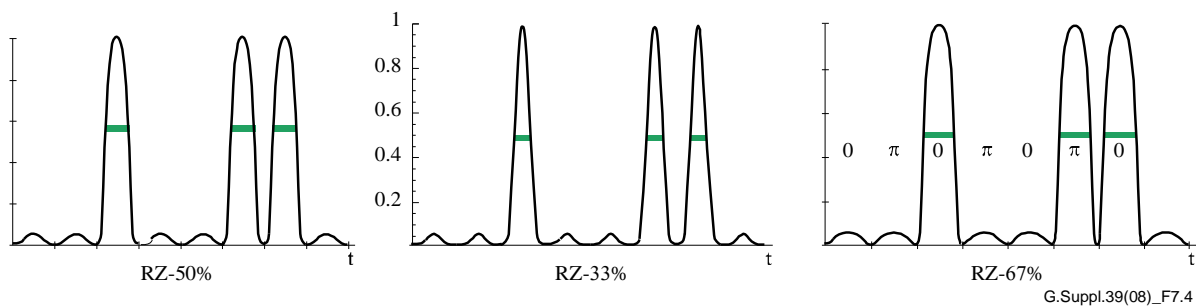
NOTE – The bar indicates FWHM and the duty cycle of the pulses. π and 0 indicate the phase change of RZ pulses at CS-RZ-67%.

Figure 7-4 – RZ pulses of all three duty cycles with data of 00100110

The optical spectra and optical eye pattern of the three RZ formats are depicted in Figures 7-5 and 7-6, respectively. RZ-33% format needs the highest spectral width compared to RZ-50% and CS-RZ-67%, which shows a significantly narrower spectrum, enabling higher spectral efficiency compared to RZ-33% format.
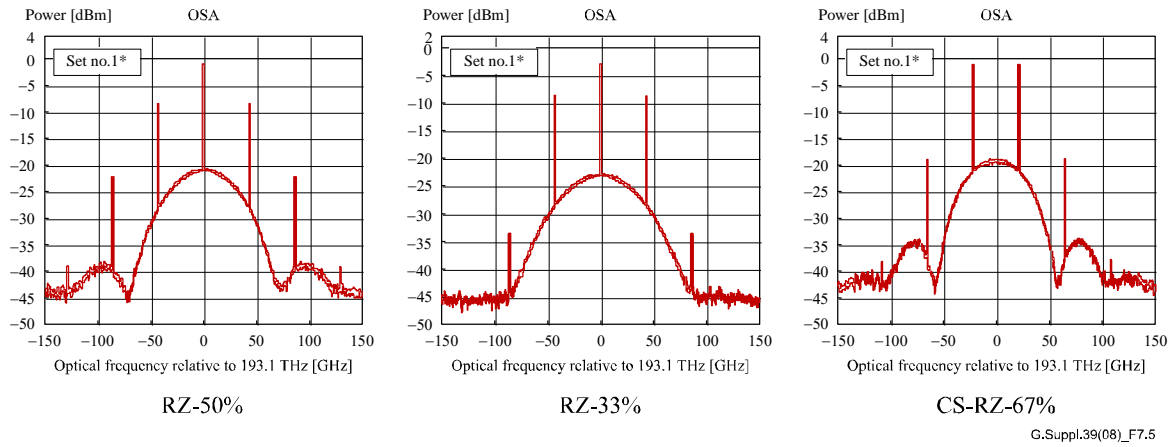
Figure 7-5 – Optical spectra of RZ formats

NOTE – The thin bar indicates the bit period T and the thick bar indicates the pulse width, corresponding to duty cycle.

Figure 7-6 – Optical eye pattern of RZ formats

7.2.1 RZ with 33% duty cycle

In Figure 7-2, the input signal to the MZM is an optical NRZ signal with a bit rate of $1/T_b$ (T_b is the bit duration). The MZM is DC biased at its maximum optical transmission by $V_{bias} = 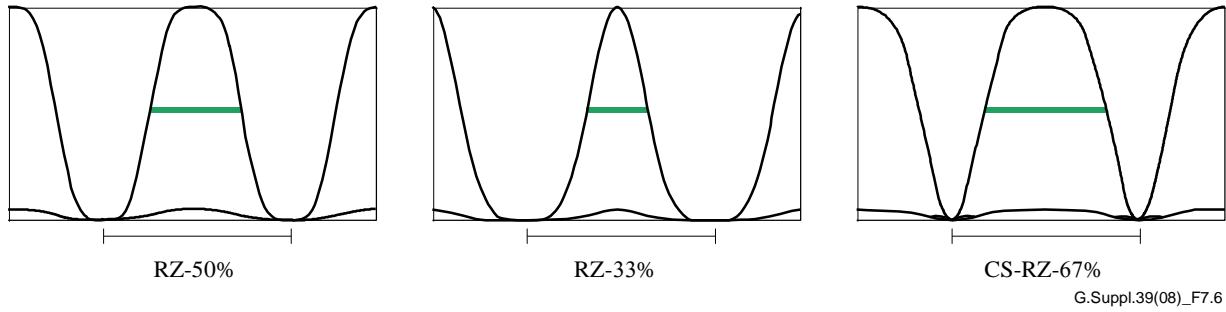V_{max}$, and RF modulated by a sinusoidal signal with a frequency of $f = 1/(2T_b)$ and an amplitude of V_π ($2V_\pi$ peak-to-peak).

Then, the amplitude of the optical field $E_1(t)$ of the MZM output is proportional to:

$$E_1(t) \propto \cos\left[\frac{\pi}{2}\cos\left(\pi\frac{t}{T_b}\right)\right] e_{NRZ}(t) \tag{7-3}$$

where $e_{NRZ}(t)$ is the optical field of the input NRZ signal. The optical output power of the MZM then becomes:

$$P_{out} \propto E_1(t)E_1(t)^* \propto \left[\cos\left[\frac{\pi}{2}\cos\left(\pi\frac{t}{T_b}\right)\right] e_{NRZ}(t)\right]^2 \tag{7-4}$$

7.2.2 CS-RZ with 67% duty cycle

Another modulation scheme is carrier suppressed return to zero (CS-RZ) with a 67% duty cycle. This has better robustness against fibre chromatic dispersion than RZ modulation with 33% duty cycle.

To obtain a CS-RZ format with 67% duty cycle, the MZM is DC biased at its minimum optical transmission by $V_{bias} = V_{min}$ and modulated by a sinusoidal RF signal with a frequency of $f = 1/(2T_b)$ and a phase shift, $\phi_m = \pi/2$; see Figure 7-2. The RF modulation amplitude is V_π ($2V_\pi$ peak-to-peak), corresponding to the half-wave voltage of the MZM. The amplitude of the optical field at the output of the MZM, $E_2(t)$, is proportional to:

$$E_2(t) \propto \sin\left[\frac{\pi}{2}\sin\left(\pi\frac{t}{T_b}\right)\right]e_{NRZ}(t) \tag{7-5}$$

The output power of the MZM is proportional to $E_2(t)E_2(t)^*$, which is:

$$P_{out} \propto E_2(t)E_2(t)^* \propto \left[\sin\left[\frac{\pi}{2}\sin\left(\pi\frac{t}{T_b}\right)\right]e_{NRZ}(t)\right]^2 \tag{7-6}$$

7.2.3 RZ with 50% duty cycle

To obtain an RZ format with 50% duty cycle, the MZM is DC biased at its 3 dB optical transmission by $V_{bias} = V_{3dB}$ and modulated by a sinusoidal RF signal with a frequency of $f = 1/(T_b)$, see Figure 7-2. The RF modulation amplitude is $V_\pi/2$ (V_π peak-to-peak). The amplitude of the optical field at the output of the MZM, $E_3(t)$, is proportional to:

$$E_3(t) \propto \cos\left[\frac{\pi}{4}+\frac{\pi}{4}\cos\left(\frac{2\pi t}{T_b}\right)\right]e_{NRZ}(t) \tag{7-7}$$

The output power of the MZM is proportional to $E_3(t)E_3(t)^*$, which is:

$$P_{out} \propto E_3(t)E_3(t)^* \propto \left[\cos\left[\frac{\pi}{4}+\frac{\pi}{4}\cos\left(\frac{2\pi t}{T_b}\right)\right]e_{NRZ}(t)\right]^2 \tag{7-8}$$

7.3 ODB and RZ-AMI line coding format

Alternative modulation formats have been identified with significantly lower channel bandwidth than standard NRZ format, enabling higher dispersion tolerance and higher spectral density on the transmission fibre. One example is optical duobinary format.

Optical duobinary (ODB) as well as return to zero alternate mark inversion (RZ-AMI) format can be implemented by delay and add operations of two signals D(t) and $\bar{D}$(t-δ) [b-Yonenaga], which could be achieved either in the electrical or optical domain where δ is the delay between the signals.

Common to all of the electrically generated ODB implementations is that a three level duobinary drive signal with polarity of (-,0,+) is used to modulate an MZM biased at the transmission minimum. The optical output signal of such ODB transmitter implementations is an optical binary format, as the drive signal polarity of (-,0,+) is transformed into intensity of (1,0,1) but with phase change (0,0,π), respectively. The difference in the phase evolution between ODB and RZ-AMI is depicted in Figure 7-1.

7.3.1 ODB implementation

ODB can be generated using drive signals in the following examples a) to c) modulating a MZM biased at transmission minimum or with example d) in the optical domain:

a)   D(t) + $\bar{D}$(t-δ) is used to drive MZM and δ = T. The delay corresponds with the bit period T (conventional ODB) [b-Yonenaga].

b)   D(t) and $\bar{D}$(t-δ) on push-pull MZM and δ ≈ 0.7T (fractional bit delay ODB) or T (full bit delay ODB).

c)   D(t) and $\overline{D}$(t) on push-pull MZM while both signals are Bessel low pass filtered (PSBT) [b-Pennickx].

d)   Optically demodulating an NRZ-DPSK signal with a delay and add MZ differential interferometer (DI) to obtain ODB at the DI's constructive port.

7.3.1.1   Phase shaped binary transmission (PSBT) implementation

Phase shaped binary transmission (PSBT) format has been proposed [b-Pennickx] as one specific implementation of the ODB line coding approach. Figure 7-7 illustrates one example of how this format might be implemented. This PSBT generation approach is based on an electrical pre-coder (1-bit delay) and a three-level duobinary electrical drive signal achieved by strong electrical filtering with a high order Bessel filter having a cut-off frequency with 25 to 30% of the bit-rate according to case c) in clause 7.3.1. A Mach-Zehnder modulator (MZM) is modulated with this electrical duobinary signal with $2V_\pi$ driving voltage, as depicted in Figure 7-7. As indicated at the optical output pattern, the phase is changing at bit-changes due to the $2V_\pi$ driving voltage. The output eye-pattern is an NRZ-like eye-pattern as shown in Figure 7-1. The receiver for the PSBT (ODB) implementation is a standard NRZ receiver.
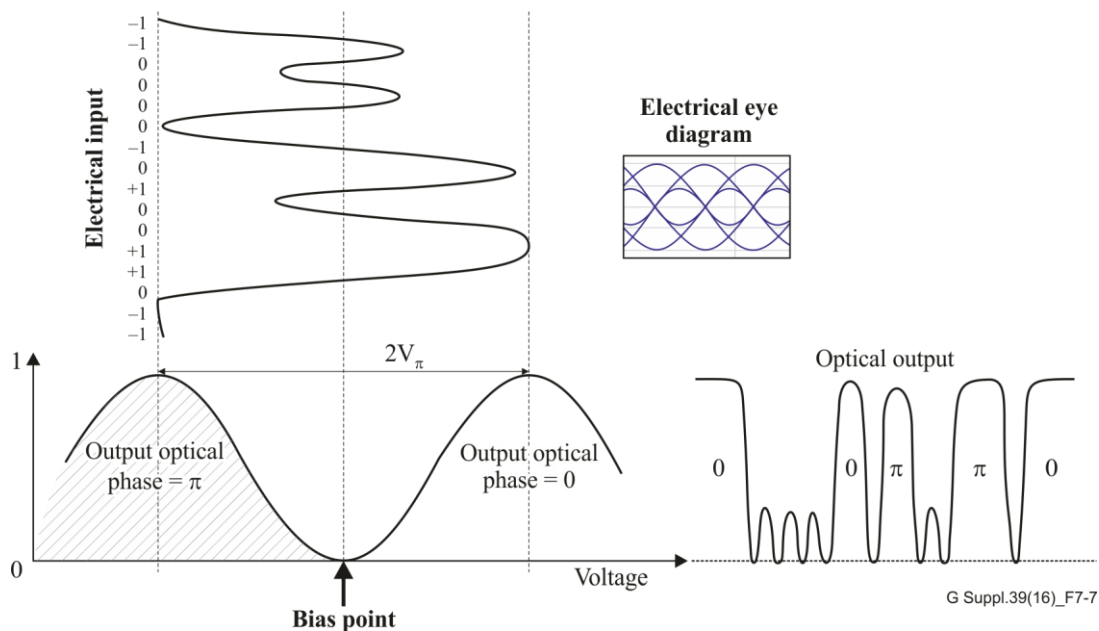
Figure 7-7 – Modulation configuration of ODB (PSBT)

7.3.2   RZ-AMI implementation

RZ-AMI can be realized by at least the following three approaches:

a)   using differential drive signal of D(t) and D(t-δ) with an MZM biased at transmission minimum [b-Winzer];

b)   combining any one of the above ODB implementations with CS-RZ pulse carving;

c)   optically demodulating an NRZ-DPSK signal with a delay and add MZ differential interferometer (DI) to obtain RZ-AMI at the DI's destructive port.

One implementation of RZ-AMI is to combine CS-RZ pulse carving with any of the ODB implementations a) to c) of clause 7.3.1. When either is preceded or followed with CS-RZ pulse carving (as shown in Figure 7-8), the ODB signal is converted into RZ-AMI. Unlike ODB or CS-RZ, RZ-AMI always has a pi phase difference between adjacent "1"s regardless of the number of "0"s in-between.

With an electrical pre-coder, which is done in ODB generation in implementation case b), the receiver for the RZ-AMI implementation is a standard RZ receiver.
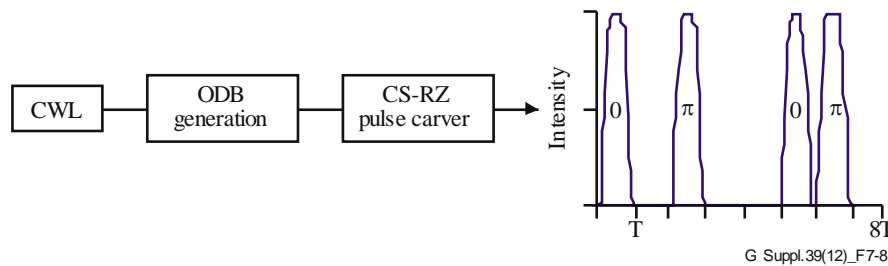

Figure 7-8 – Example of RZ-AMI implementation

7.3.3 Non-orthogonal signalling

For the modulation schemes described in clause 7.7, orthogonal signalling is used because it ensures the absence of inter-symbol interference. In non-orthogonal signalling techniques [b-Rusek], the frequency separation of carriers or sub-carriers is lower than the inverse of the pulse duration and it is possible to recover the inter-symbol interference by signal post-processing at the receiver, in theory introducing no performance degradation with respect to the orthogonal case. These techniques allow an improvement in the spectral efficiency by selecting narrow carrier bandwidths. There are several options for non-orthogonal transmission: experimental examples are provided in [b-Potì] and [b-Cai]. The approach known as Time-Frequency Packing [b-Barbieri] maximizes the spectral efficiency in presence of a receiver with a pre-determined design, in order to deal with practical implementation constraints.
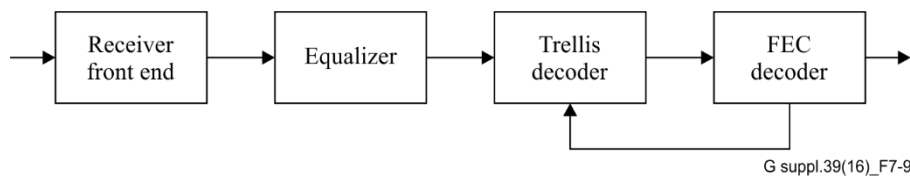
Figure 7-9 – Carrier receiver scheme for non-orthogonal signalling in SCM

The receiver scheme for each carrier (Figure 7-9) consists of an optical front end, including the local oscillator and polarization splitter; an equalizer, typically a feed forward equalizer (FFE) as is common in coherent receivers; a trellis decoder and a forward error correction (FEC) decoder. The trellis and FEC decoders iteratively exchange information until the right code word is detected. Several kinds of FEC codes can be used in the scheme of Figure 7-9 provided that they are suitable for iterative decoding: the choice depends on the design parameters, primarily sub-carrier transmitter bandwidth and, as usual in transmission systems, signal-to-noise ratio at the receiver.

7.4 Differential phase shift keying (DPSK) modulation implementations

7.4.1 Non-return to zero differential phase shift keying (NRZ-DPSK)

Differential phase shift keying (DPSK) line coded systems have been introduced in ultra-long-haul transmission systems as providing 3 dB better OSNR tolerance (due to the balanced detection capability).

For DPSK line coding, in contrast to phase shift keying (PSK) and coherent detection, the bits are encoded by the phase differences between the successive bits and therefore this coding scheme is called differential-PSK. Figure 7-10 shows one example of DPSK modulation implementation with an MZM, depicting the electrical NRZ drive signal and MZM bias condition with $2V_\pi$ driving voltage. Using an MZM rather than a phase modulator, means that the phase modulated optical output signal does not have a perfectly constant amplitude as shown at the optical output pattern. These amplitude

dips between the phase changes from 0 to π, and π to 0 cause negligible impairments as they are positioned at the data crossing points. As indicated in the Tx scheme in Figure 7-1, an electrical data encoder is required, consisting of a simple 1-bit delay encoder.

At the receiver, the differentially phase modulated signal is converted to an amplitude modulated signal using a demodulator consisting, for example, of a 1-bit delay optical interferometer providing constructive and destructive output signals to the balanced receiver. Detecting both of these outputs with two photodiodes and a differential amplifier gives a balanced amplitude modulated eye pattern with twice the eye opening of a standard NRZ receiver, resulting in 3 dB higher sensitivity. The demodulated and balanced received eye diagram of DPSK line coding is shown in Figure 7-11.
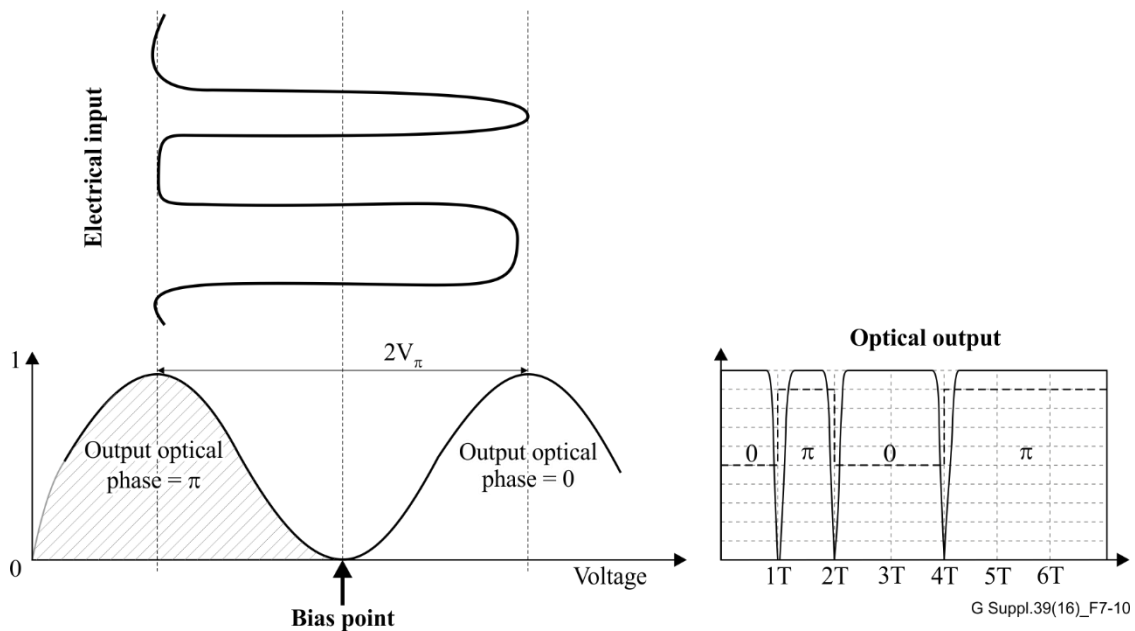
Figure 7-10 – Modulation configuration using MZM modulator for NRZ-DPSK generation
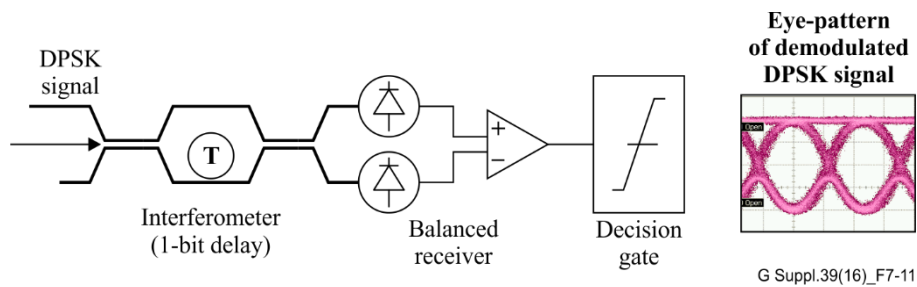
Figure 7-11 – Phase to intensity conversion of a DPSK signal using 1-bit delay interferometer and balanced photoreceiver

7.4.2   Return-to-zero differential phase shift keying (RZ-DPSK)

Similarly to amplitude modulation, RZ-carving can be applied to DPSK using the same duty cycles as described in clause 7.2, to further improve the robustness to noise and non-linear impairments, similarly to the improvement of RZ versus NRZ. Thus, DPSK is also called NRZ-DPSK to differentiate it from RZ-DPSK schemes.

7.4.3   Partial differential phase shift keying (P-DPSK)

To improve robustness of DPSK to filtering, partial differential phase shift keying (P-DPSK) has been proposed [b-Mikkelsen]. The main difference in implementation of P-DPSK versus DPSK is applied at the delayed interferometer in the receiver, using a fractional or partial delay of about 66% of a bit period. Implementation examples of NRZ-DPSK, P-DPSK and RZ-DPSK are depicted in Figure 7-1.

7.5 Differential quadrature phase shift keying (DQPSK) implementation

### 7.5.1 Non-return to zero differential quadrature phase shift keying (NRZ-DQPSK)

A further example of alternative modulation formats having significantly lower channel bandwidth, better robustness to PMD and chromatic dispersion than standard NRZ format is differential quadrature phase shift keying (DQPSK) modulation format. DQPSK has been introduced as a multilevel format coding scheme with two bits per symbol. For better illustration, multilevel formats are usually described using the E-field constellation or phase constellation diagram. Figure 7-1 shows the constellation diagram of DQPSK together with the other formats. For DPSK, the bit is encoded by the phase difference between successive bits as either 0 or π, while for DQPSK, the two data bits are encoded as one of 0, $\pi/2$, π or $3\pi/2$. The two half rate tributaries are denoted as I and Q tributaries with a phase difference of $\pi/2$. Compared to DPSK, a more complex electrical encoder is required.

A Tx generation method and an Rx detection method are shown in Figure 7-1 by applying two parallel $\pi/2$ phase shifted Mach-Zehnder modulators and two parallel $\pi/2$ shifted Mach-Zehnder interferometer based demodulators, respectively, to generate and to demodulate the I and Q tributaries. As the symbol-rate of the tributaries is half of the bit-rate, the optical delays applied for the DQPSK demodulator are 2T compared to T of the DPSK demodulator. Two balanced detectors provide differential I and Q output signals which are superimposed to generate individual I and Q balanced eye-patterns, similar to the eye-pattern shown in Figure 7-10, but with half of the bit-rate.

7.5.2 Return to zero differential quadrature phase shift keying (RZ-DQPSK)

As noted above for DPSK, additional RZ-line coding can also be applied to DQPSK, but using RZ modulation frequencies in relation to the symbol-rate. In case of the example RZ-50%-DQPSK, the RZ-modulation frequency becomes half of the bit-rate while for RZ-50%-DPSK the RZ-modulation frequency corresponds to the bit-rate.

7.6 DP-QPSK (PM-QPSK) implementation

An alternative modulation format has been identified with further lower channel bandwidth than the previously described advanced modulation formats, denoted as dual polarization or polarization multiplexed (DP or PM) quadrature phase shift keying (DP- or PM-QPSK). While DQPSK has been introduced as a coding scheme with two bits per symbol providing further robustness to PMD and chromatic dispersion due to the symbol-rate being half of the bit-rate; DP-QPSK takes this one stage further by generating two QPSK signals on orthogonal polarizations thereby operating with a symbol-rate of one quarter of the bit-rate.

One method of generating this signal is illustrated in Figure 7-1 where the outputs of two independent QPSK modulators (similar to the DQPSK modulator above) are combined in a polarization combiner. Implementations with or without pre-coding are possible. At the receiver in this example, the signal is split into two orthogonal polarizations with a polarization splitter (without making any attempt to track the changes in polarization of the incoming signal) and the resulting signals are passed to two 90° hybrids together with a local oscillator (LO) signal. The output of each 90° hybrid is then an in-phase (I) and quadrature (Q) signal for each of the two received polarizations. Because this is a coherent receiver with a linear transfer function between the optical and electrical domains, impairments that occur during transmission (such as rotation of the signal polarization at the receiver, chromatic dispersion or PMD) and differences between the frequency and phase of the signal and the LO can be compensated for by electronic processing in the receiver.

7.7 Optical orthogonal frequency division multiplexing (O-OFDM)

The concept of OFDM is the division of a high bit rate data stream into several low bit-rate streams by generating several sub-carriers and modulating each low bit-rate stream on to a sub-carrier.

When the spacing between adjacent sub-carriers is higher or equal to the sub-carrier baud rate, O-OFDM is commonly referred to as sub-carrier multiplexing (SCM). In this case, an effective way of generating OFDM signals is by means of analogue radio frequency (RF) electronics, especially when there are a low number of sub-carriers. When there are a large number of sub-carriers, an effective way of generating OFDM signals is by adopting digital signal processing (DSP).

7.7.1 Sub-carrier multiplexing (SCM)

The principle of SCM is outlined in the spectral domain in Figure 7-12.
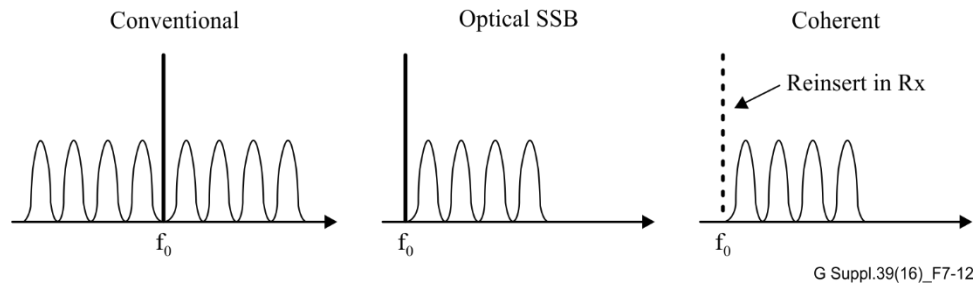
Figure 7-12 – Three approaches to SCM

The information is first encoded on one or more electrical RF carriers using conventional RF IQ-modulation technique and subsequently converted to the optical domain using an intensity modulator. The sub-carriers will appear symmetrically around the laser carrier with spacing equal to the RF carrier frequency and thus the encoded information is present as two replicas on both sides of the laser carrier.

Figure 7-12 outlines three possible approaches to SCM, where the "conventional" and optical single side-band (OSSB) maintain the laser carrier through transmission to allow direct detection of the sub-carriers (self heterodyne detection).

For long-distance transmission, however, it is preferable not to co-transmit the laser carrier and instead re-insert the carrier at the receiver (coherent heterodyne detection), in order to reserve all the available optical power to the sub-carriers that carry the information data.

It is beneficial to remove one side of the spectrum in order to improve spectral efficiency and to allow mitigation of transmission impairments by electrical means, in a DSP. While an optical filter could in principle be used to remove the unwanted sideband, this may be difficult when the guard band between optical carrier and lowest frequency subcarrier is too narrow. In this case, OSSB modulation can be performed by driving I and Q branches of a balanced modulator with the modulating signal and its Hilbert's transform, respectively [b-Hui].

7.7.2 DSP generated modulated sub-carrier based implementation

Orthogonality is realized between the sub-carriers by spacing them by a multiple of the symbol duration. Input data are converted from serial to parallel (S/P) as shown in Figure 7-13. After symbol mapping (coder), sub-carriers with a spacing of multiple symbol duration are generated by an inverse Fourier transform (IFT) function. They are then converted from parallel to serial (P/S) and modulated on to an optical carrier. At the receiver, the OFDM signal is received with either coherent or direct detection and is converted back to the frequency domain using a forward Fourier transform (FFT) [b-Jansen] and [b-Yang].
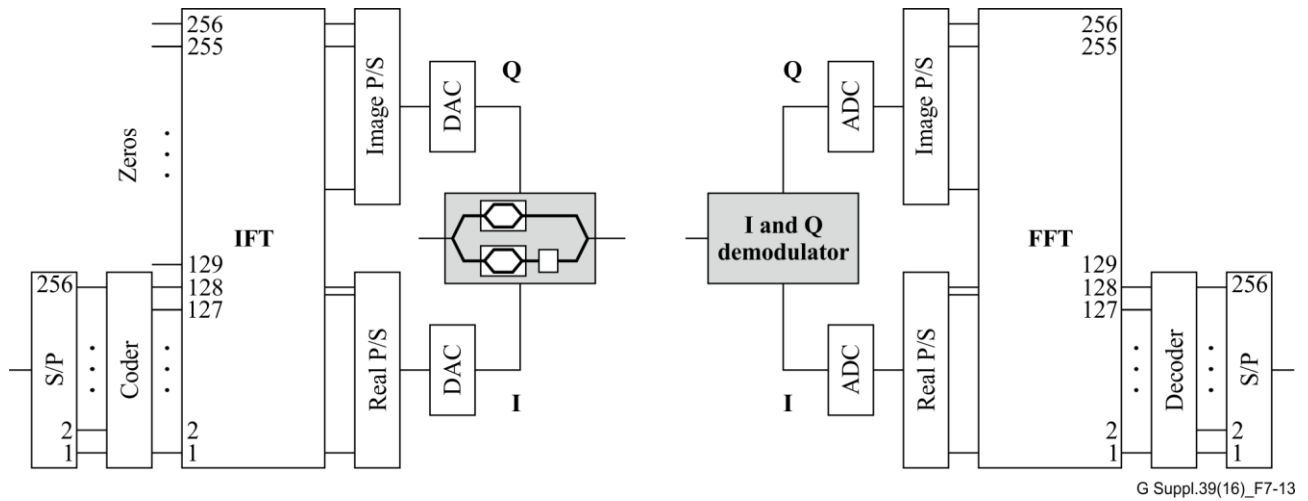
Figure 7-13 – Block diagram of Tx (left) and Rx (right) for O-OFDM

7.7.3 Externally modulated sub-carrier based implementation

Other approaches involve the time domain and therefore do not require the FFT function [b-Kobayashi], [b-Sano] and [b-Yamada]. One implementation for generating two sub-carrier OFDM signals is to use an IQ-modulator as indicated in the transmitter scheme in Figure 7-14. The driving signals $S_I(t)$ and $S_Q(t)$ are given by Equations 7-9 and 7-10, respectively, where $D_1(t)$ and $D_2(t)$ are pre-coded input data signals, and Δf is the frequency spacing between the two sub-carriers. Here, Δf is the symbol duration.

$$S_I(t) = (D_1(t) + D_2(t))\cos(2\pi\frac{\Delta f}{2}t) \tag{7-9}$$

$$S_Q(t) = (D_1(t) - D_2(t))\sin(2\pi\frac{\Delta f}{2}t) \tag{7-10}$$

The modulated output signal $S_{out}(t)$ is given by Equation 7-11, where f_c is the optical carrier frequency. This signal consists of a high frequency sub-carrier $D_1(t)$ and a low frequency sub-carrier $D_2(t)$.

$$S_{out}(t) = D_1(t)\cos 2\pi\left(f_c + \frac{\Delta f}{2}\right)t + D_2(t)\cos 2\pi\left(f_c - \frac{\Delta f}{2}\right)t \tag{7-11}$$
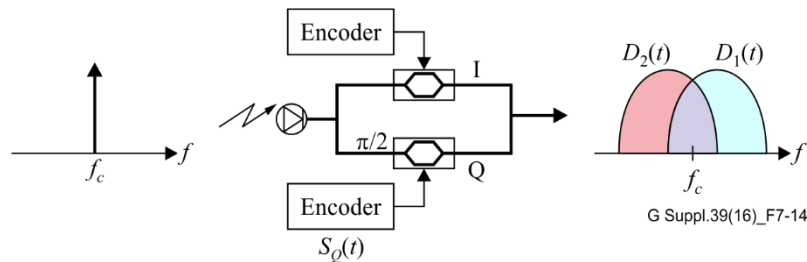
Figure 7-14 – First transmitter scheme for two sub-carrier OFDM generation

Figure 7-15 shows another implementation for generating two sub-carrier OFDM signals. A conventional modulator driven by a $\Delta f/2$ GHz clock signal is used to produce two sub-carriers in the optical domain and each carrier is modulated separately after passing through an optical filter such as an interleaver (IL), and then the two sub-carriers are combined.
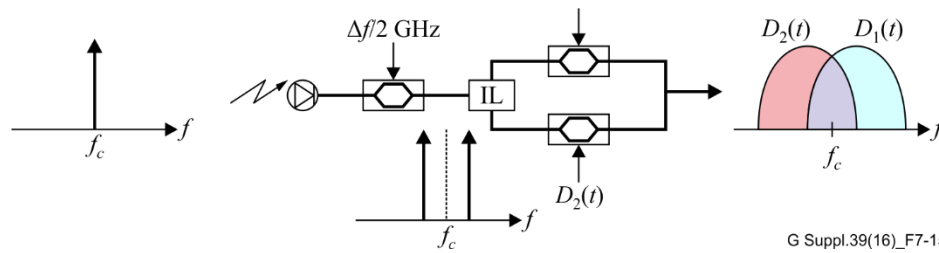
Figure 7-15 – Second transmitter scheme for two sub-carrier OFDM generation

With either approach, the two sub-carrier OFDM signal is demultiplexed (into two sub-carriers) using a Mach-Zehnder interferometer (MZI) with a delay difference of $2\Delta f$ (Δf is the symbol interval) at the receiver. The signal can also be demultiplexed by employing coherent detection aided by time domain digital filters without using FFT processing.

7.7.3.1   Orthogonal polarization optical FDM-DQPSK (OPFDM-DQPSK)

In the case of externally modulated two sub-carrier OFDM implementation, NRZ-DQPSK or RZ-DQPSK modulation scheme can be applied to each sub-carrier after sub-carrier separation. The two sub-carrier DQPSK or RZ-DQPSK tributaries can be then orthogonally polarization-combined (X-pol and Y-pol) to form OPFDM-DQPSK or OPFDM-RZ-DQPSK, as shown in Figure 7-16.

Figure 7-16 – OPFDM-DQPSK generation and detection scheme

For detection, an optical filter is applied first to an OPFDM-DQPSK or OPFDM-RZ-DQPSK signal to separate the two sub-carrier DQPSK trib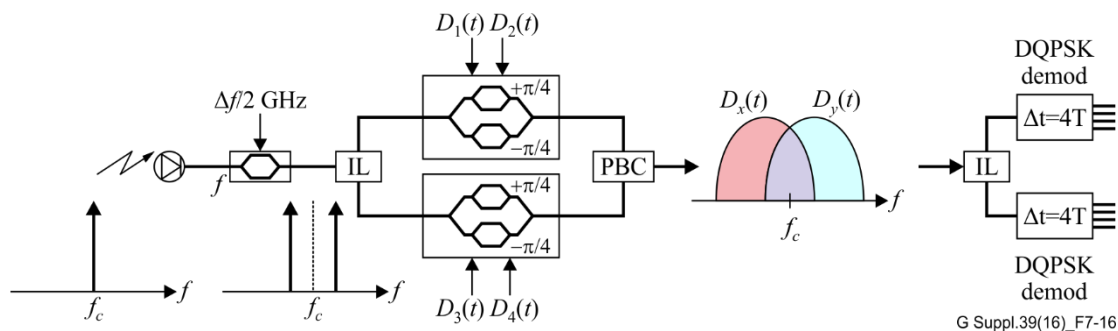utaries in the frequency domain. Suitable optical filters can be an MZI-based optical demodulator or simply an interleaver (IL). After being spectrally separated, each sub-carrier DQPSK or RZ-DQPSK can be detected using common DQPSK detection schemes as described in clause 7.5.1.

Each sub-carrier DQPSK tributary in OPFDM-DQPSK carries half of the bit-rate and has a symbol-rate at 1/4 of the bit-rate. The optical delays applied in each sub-carrier DQPSK demodulator are 4T compared to 2T of a single carrier DQPSK demodulator.

The OPFDM-DQPSK modulation scheme is, in principle, not limited to two sub-carriers. However, there will be a limitation from practical implementation consideration to the number of sub-carriers that can be externally modulated cost-effectively.

7.7.4   Orthogonal-band-multiplexed (OBM) OFDM

OBM-OFDM seeks to improve spectral efficiency over conventional OFDM by arranging multiple orthogonal bands into a complete OFDM spectrum [b-Yang]. The conventional OFDM per optical band/channel is shown on the left side of Figure 7-17. The right part of Figure 7-16 shows the entire OBM-OFDM spectrum, which consists of multiple orthogonal OFDM bands. In OBM-OFDM, a multi-tone generator is required to provide the multiple orthogonal optical carriers. The signal is generated in an arrangement similar to Figure 7-13 and the orthogonality is satisfied for the whole

band-multiplexed OFDM signal when the spacing of the optical sub-carriers is an integer multiple of the subcarrier spacing of RF OFDM signal in each sub-band.
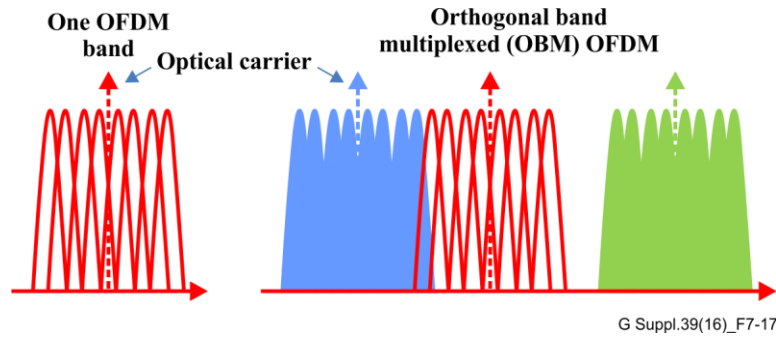
Figure 7-17 – Principle of OBM-OFDM

7.8 Nyquist WDM

Another alternative sub-carrier multiplexing approach to increase the spectral efficiency without sacrificing optical reach is Nyquist WDM. The basic concept of Nyquist WDM is that the subcarriers are spectrally shaped either in the optical or electrical domain at the transmitter so that their occupancy is close or equal to the baud rate, also known as Nyquist spacing, for high tolerance of both interchannel interference (ICI or crosstalk) and intersymbol interference (ISI) impairments.

7.8.1 Digital Nyquist shaping/filtering

The Nyquist criterion is a basic principle related to spectral efficiency in Nyquist WDM. According to the Nyquist first criterion, ISI can be eliminated if the spectrum of a signal satisfies a certain condition. The necessary and sufficient condition for $h(t)$ to satisfy Equation 7-12 is that its Fourier transform $H(f)$ satisfies Equation 7-13.

$$h(nT) = \begin{cases} 1, n = 0 \\ 0, n \neq 0 \end{cases} \tag{7-12}$$

$$\sum_{m=-\infty}^{\infty} H(f + m/T) = T \tag{7-13}$$

Here T is the duration of a symbol. The smallest bandwidth with non-ISI is 1/2T. For this value, $h(t)$ has to be a sinc function and its spectrum is rectangular, given as Equation 7-14.

$$h(t) = \frac{\sin(\pi t/T)}{\pi t/T} = \sin c(\frac{\pi t}{T}) \tag{7-14}$$

7.8.2 Implementations

One possible implementation is based on Nyquist pulse generation in the electrical domain using a digital-to-analogue converter (DAC) at the transmitter as shown in Figure 7-18(a). In-phase and quadrature components of an optical carrier are modulated in a single IQ modulator driven by two electrical sinc signals which have ideally rectangular spectrum and the spacing between channels is equal to the signal baud rate [b-Cigliutti]. A conventional optical multiplexer is used to combine the multiple channels into a WDM signal. A conventional optical coherent receiver is employed in Figure 7-18(b). This configuration makes no special demands on the receiver, but requires a high sampling rate and high accuracy DAC at the transmitter.

Another possible implementation is based on spectral shaping via a standard optical filter, such as a wavelength-selective switch (WSS), as shown in Figure 7-19(a). The optical filter also performs the

optical multiplexing functions and the filtered spectrum width can be equal to or even smaller than the original signal symbol rate. The enhanced high-frequency noise after the digital equalization algorithm can be significantly suppressed by the addition of a simple linear delay-and-add filter[b-Jia] in the digital domain, while the introduced ISI is compensated via simplified independent-lane multi-symbol detection, such as maximum likelihood sequence detection (MLSD) or maximum a posteriori probability (MAP), in the digital signal processing (DSP) module shown in Figure 7-19(b). Compared with the scheme of Figure 7-18, the advantage of this scheme is that there is no need of a high-resolution DAC and specific optical filter shape at the transmitter and it is still compatible with conventional DSP algorithms in the coherent optical receiver.
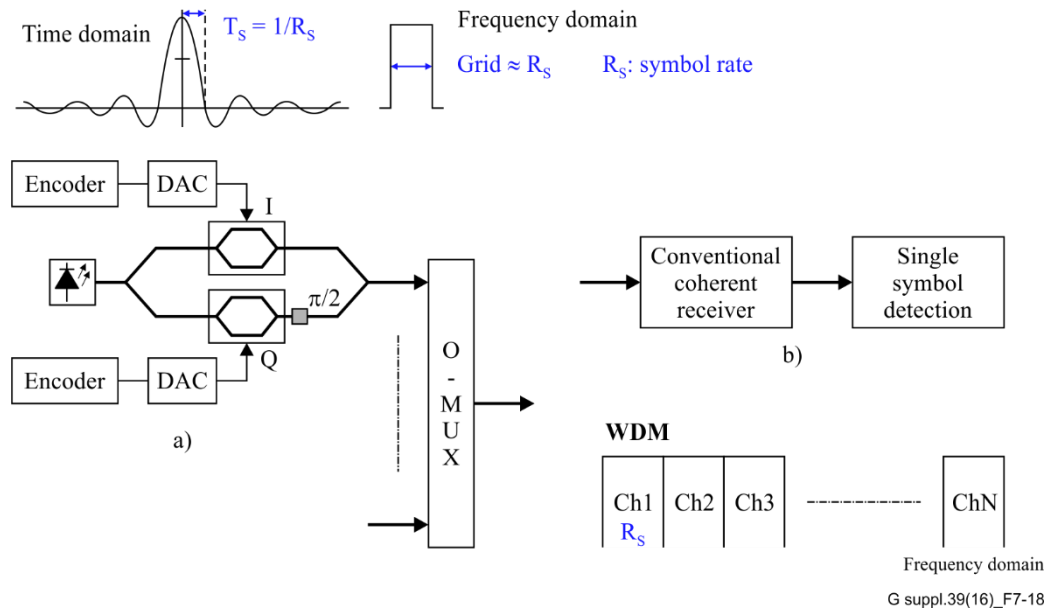
Figure 7-18 – Electrical-domain Nyquist WDM generation and detection
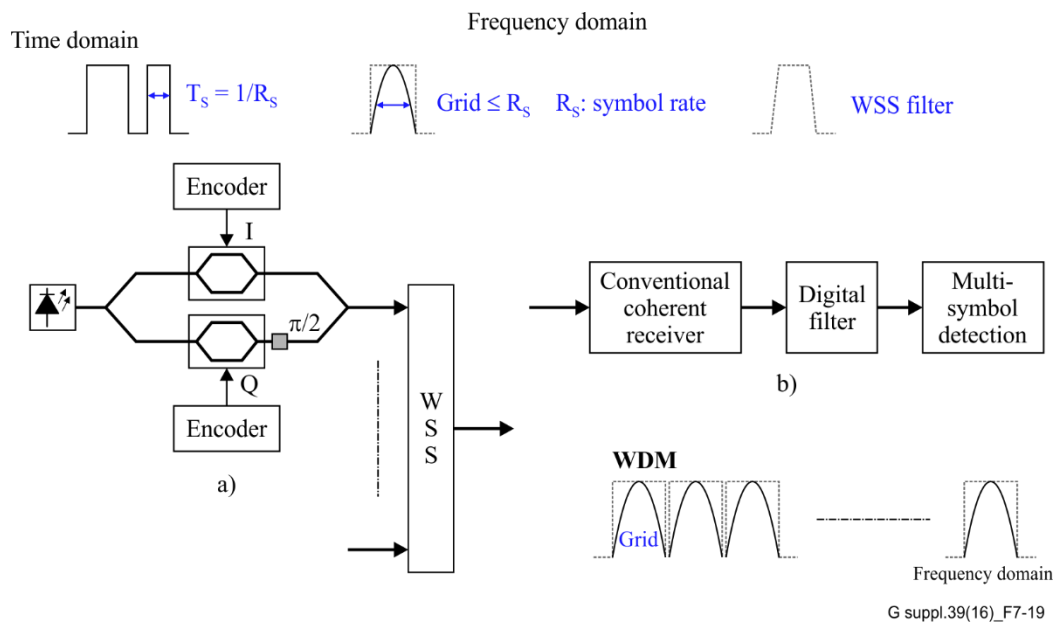
Figure 7-19 – Optical-domain Nyquist WDM generation and detection

7.9 Polarization division multiplexing binary phase shift keying (PDM-BPSK) implementation

7.9.1 Non-return to zero polarization division multiplexed binary phase shift keying

For NRZ-PDM-BPSK modulation format generation, a continuous wave laser output is separated and modulated by two MZM (Mach-Zehnder modulators), both biased at maximum-attenuation, driven in push-pull with transmission data. Then one output of the MZM passes through a polarization rotator which rotates the polarization states of the original signal to make it orthogonal to the other. The two BPSK signals are then combined using a polarization beam combiner to form NRZ-PDM-BPSK.

For detection, a local oscillator laser after a PBS: Polarization beam splitter (PBS) and a hybrid is applied to an incoming NRZ-PDM-BPSK signal to separate two BPSK signals in different polarization states. Each one is detected using two balanced photo-detector pairs followed by digital signal processing, which offers superior tolerance to PMD, chromatic dispersion (CD) and fibre non-linear effects.

7.9.2 Return to zero polarization division multiplexed binary phase shift keying

As noted above for DPSK and DQPSK, additional RZ-line coding can also be applied to PDM-BPSK, but using RZ modulation frequencies in relation to the symbol-rate. In case of the example RZ-50%-PDM-BPSK, the RZ-modulation frequency becomes half of the bit-rate while for RZ-50%-DPSK the RZ-modulation frequency corresponds to the bit-rate.

7.10 Quadrature amplitude modulation (QAM) implementation

QAM carries information using both the amplitude and phase of the carrier signal, which has two components with a phase separation of 90 degrees (in-phase and quadrature-phase). One 2^m QAM signal can transmit m bits in a single time slot, where m is an integer [b-Sano2].

There are several approaches for generating an optical QAM signal. One is based on multi-level signal generation in an electric field using a digital-to-analogue converter (DAC) as shown in Figure 7-20. In-phase and quadrature-phase components of an optical carrier are modulated in a single IQ modulator driven by two electric multi-level signals. This configuration is simple and offers flexibility for various QAM formats, but the symbol-rate is restricted by the operating speed and accuracy of the DAC. A constellation diagram is also shown in Figure 7-20 as an example of 16 QAM, although many other possibilities such as 8-QAM and 32-QAM are also used.

Another approach is based on an optical synthesis technique. In this case, several IQ modulators with a parallel configuration are used, and each modulator is driven by a binary electrical signal. The generation of a 16 QAM signal is shown in Figure 7-21, where two QPSK signals are coupled each with an amplitude ratio of 2:1. This scheme is suitable for high-speed operation. By using n parallel IQ modulators, 2^{2n} QAM signals (n is an integer) can be generated, while the complexity of the configuration increases as the number of modulators increases.

A further approach is based on cascading multiple optical modulators. Also in this case, each modulator is driven by a binary electrical signal. The generation of a 16 QAM signal is shown in Figures 7-22 [b-Secondini] and 7-23 [b-Lu]. As in the optical synthesis technique, just two-level driving signals are required per each modulator, so avoiding DAC accuracy limitations at high operation speed. Due to the serial configuration, there is no penalty due to synchronization issues between parallel bit streams. Moreover, it can be demonstrated [b-Secondini] that the scheme allows to easily perform quadrant differential encoding to solve 90 degree phase ambiguity of the recovered signal, without requiring dedicated additional bits.

The signal can be received with a coherent receiver, where the input optical signal is converted to an electrical signal through a 90° hybrid and a balanced receiver. An analogue-to-digital converter (ADC) and a digital signal processor can be used to demodulate the signal. In the receiver,

impairments such as chromatic dispersion and PMD can be compensated for by digital signal processing.

It is also possible to create polarization division multiplexed QAM signals by using a polarization multiplexing technique to increase the bit rate (or reduce the symbol-rate). Moreover RZ-carving can be applied to QAM signals to improve the robustness to noise and non-linear impairments.
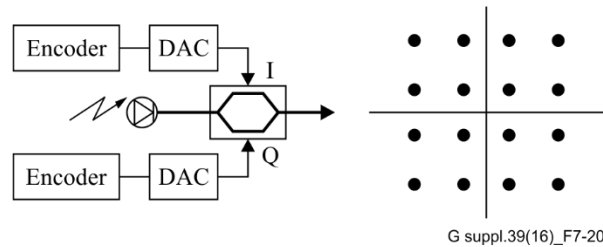
Figure 7-20 – First transmitter scheme for 16 QAM generation [b-Winzer2]
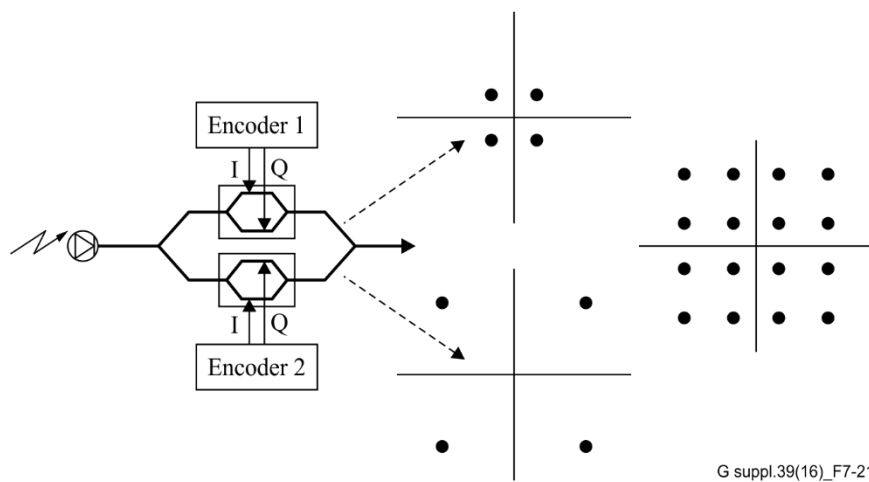
Figure 7-21 – Second transmitter scheme for 16 QAM generation [b-Sano2]
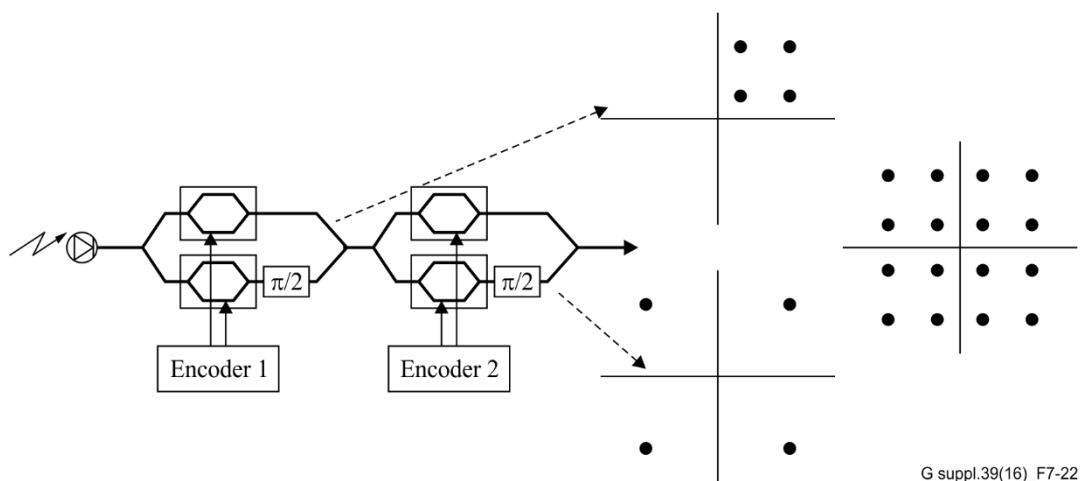
Figure 7-22 – Third transmitter scheme for 16 QAM generation [b-Secondini]
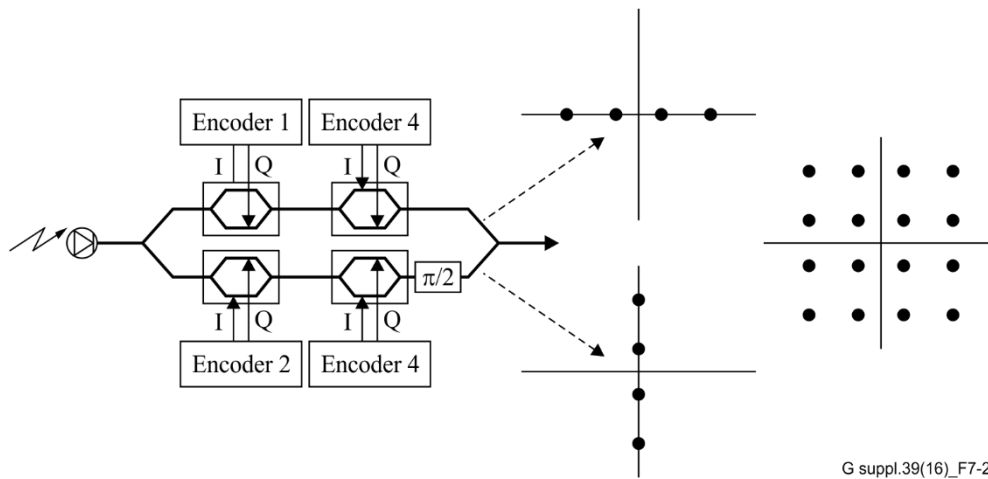
Figure 7-23 – Fourth transmitter scheme for 16 QAM generation [b-Lu]

7.11 System impairment considerations

7.11.1 Fibre attribute-induced impairments

7.11.1.1 Chromatic dispersion (CD) and pulse broadening

In the case of free space transmission or for very low fibre chromatic dispersion, the RZ format with a duty cycle of 33% has a better receiver sensitivity compared to the RZ formats with larger duty cycle or NRZ format [b-Pauer]. However, after propagation through an optical fibre, the overlapping of adjacent pulses produces ghost pulses [b-Böckl], since all logical '1's have the same optical phase.

In the CS-RZ case, adjacent pulses have opposite phases. The optical fields of two adjacent logical '1' bits add up destructively. There is no ghost pulse generated between two logical '1's. Moreover, due to the narrower spectrum, pulse broadening caused by CD is smaller than that with the conventional RZ format. Therefore, CS-RZ is a very robust modulation format for optical fibre links with significant residual chromatic dispersion.

Figures 7-24a and 7-24b show pulse shapes of the two RZ modulation formats with a bit rate of 40 Gbit/s at an accumulated chromatic dispersion of $D = 20$ ps/nm. To assess the chromatic dispersion penalty, the system model was simplified by neglecting any influence of PMD and fibre non-linearity, i.e., assuming that the CD impairment is isolated from the PMD and fibre non-linearity impairments. The model showed that, as the pulses propagate along the fibre, ghost pulses were generated between two adjacent '1's for RZ-33% in Figure 7-24a, while no ghost pulse can be observed in the CS-RZ case; see Figure 7-24b.
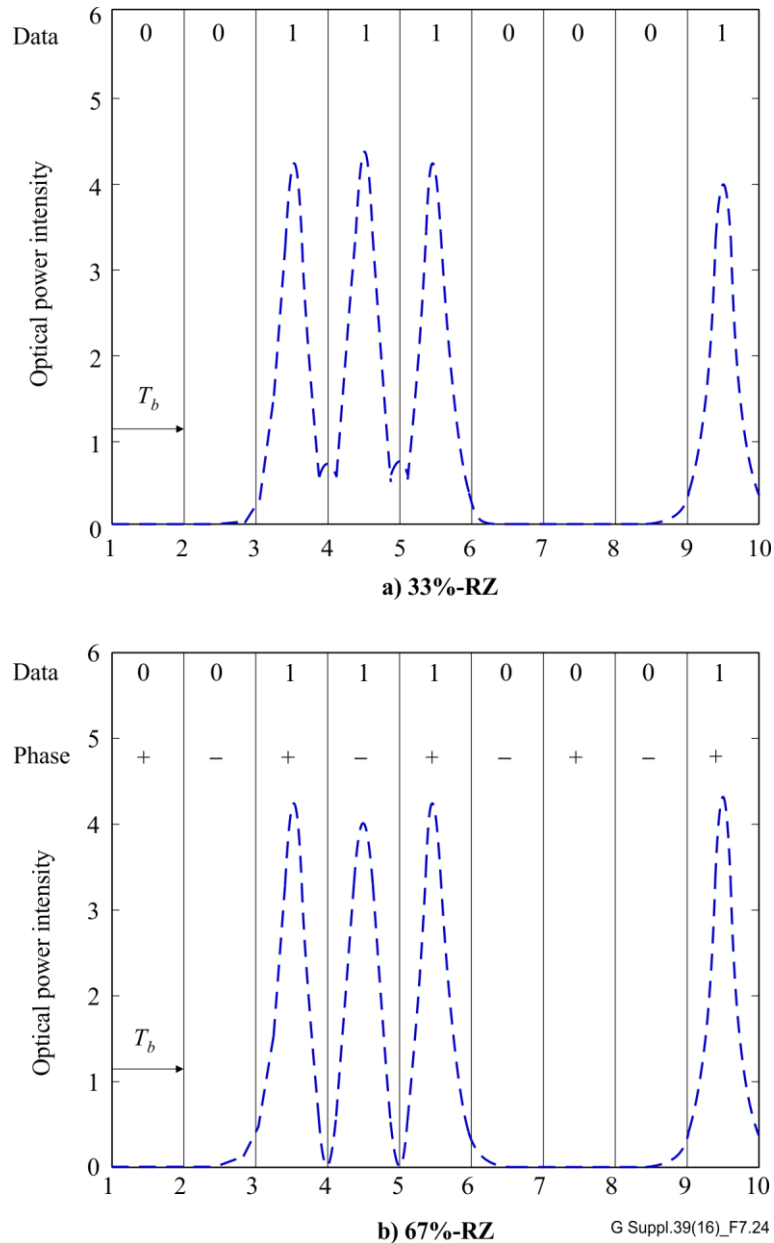
Figure 7-24 – 40-Gbit/s pulse form after accumulated dispersion of 20 ps/nm

7.11.1.2   Polarization mode dispersion (PMD)

Polarization mode dispersion (PMD) of transmission fibres degrades transmission performance by waveform distortion, especially in 40-Gbit/s transmission systems. Therefore, PMD tolerance is one of the key parameters to specify in 40-Gbit/s applications. First-order PMD is differential group delay (DGD). (An explicit definition of DGD can be found in [ITU-T G.671]). Tolerance of 40-Gbit/s systems against deterministic DGD strongly depends on the electrical bandwidth of the receiver.

Figures 7-25 and 7-26 show power penalty contour maps for RZ line-coding with duty ratios of 33% and 50%, as a function of receiver bandwidth and DGD obtained by numerical simulation. It was found that the DGD tolerance depended on both DGD and the receiver bandwidth [b-PMD]. In the conventional receiver bandwidth range as shown in the figure, PMD tolerance showed some deviation. For example, the maximum allowable DGD was 11.5 ps (for a 1 dB penalty) over a very narrow range of receiver bandwidth centred on 0.8 in RZ-33%. In contrast, in a conventional receiver bandwidth range, a penalty of more than 1 dB is inevitable.
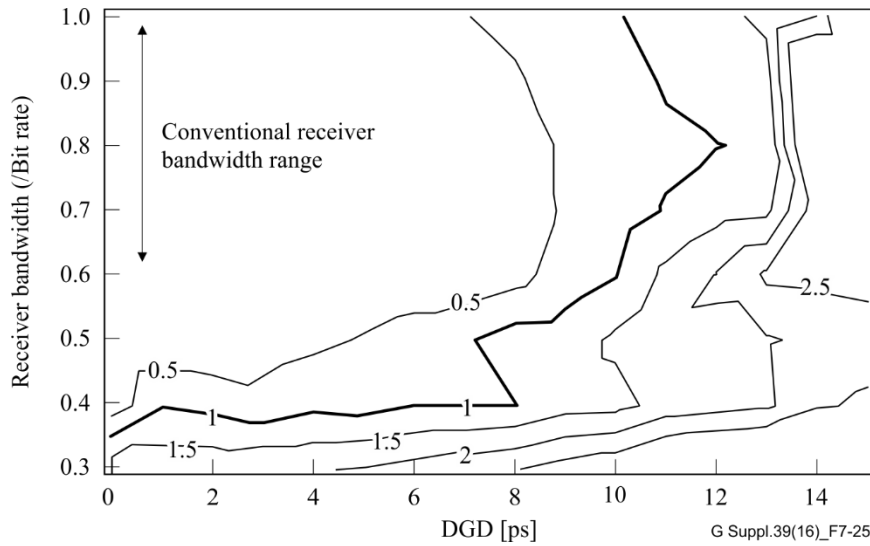
Figure 7-25 – Contour map for DGD tolerance (RZ-33%)
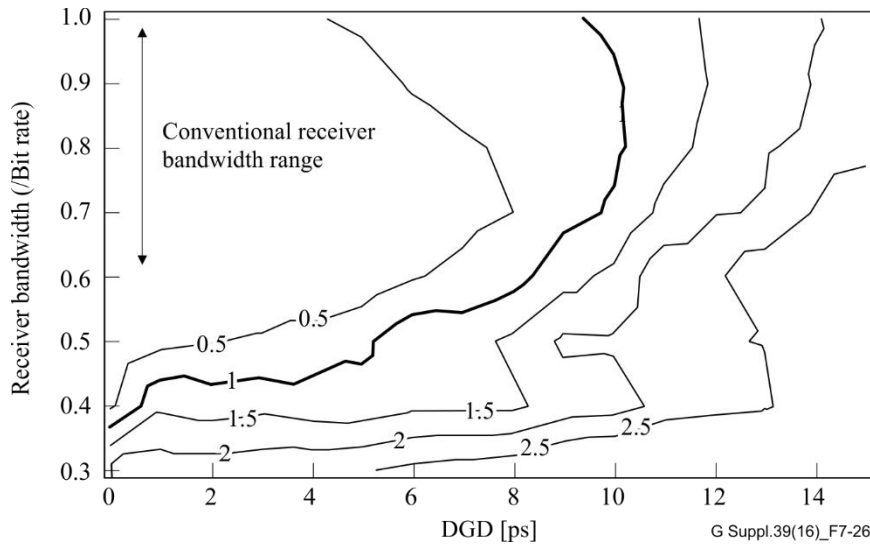
Figure 7-26 – Contour map for DGD tolerance (RZ-50%)

The power penalty showed strong dependence on receiver bandwidth. Thus, careful consideration for receiver bandwidth is required to design 40-Gbit/s RZ systems with sufficient DGD tolerance.

For 40-Gbit/s class interfaces, use of NRZ and RZ line coding has been proposed for the single-channel application codes. The RZ code has been proposed to use 33% duty cycle. This code will, due to its nature, be slightly more tolerant to PMD than the CS-RZ code of duty cycle 66% (which is another alternative). Measurements have been carried out to verify the validity of the proposed DGD tolerance values.

A PMD emulator generating first-order PMD has been used in this experiment. The OSNR penalty as a function of DGD is shown in Figure 7-27.
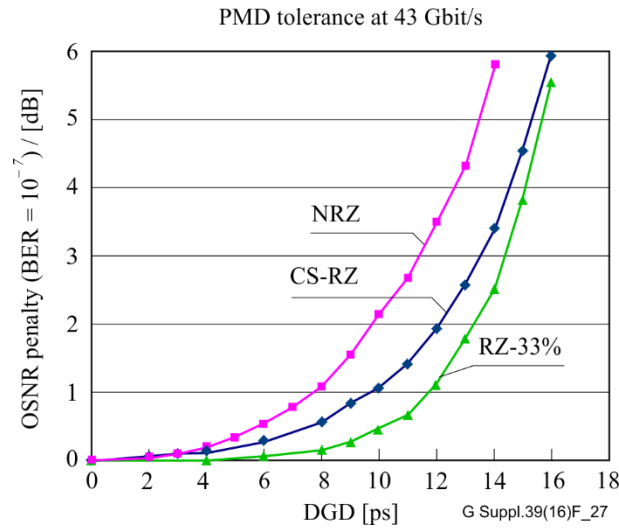
Figure 7-27 – OSNR penalty versus DGD for different line codes

The DGD for generating a 1 dB OSNR penalty was independent of the actual underlying OSNR BER down to low error ratio levels in this experiment. As the receiver was optimized for CS-RZ, the DGD tolerance that can be expected for the other line codes of 7.5 ps for 1 dB penalty in NRZ and 11.5 ps for 1 dB penalty for RZ-33% should be achievable. It can, however, be seen that RZ-66% (the other driving point of a MZ-Modulator implementation) does not support 11.5 ps for 1 dB maximum penalty at 43 Gbit/s (G.709/Y.1331 rate) so RZ-33% would have to be used for that application.

The OSNR penalty at BER of 10^{-4} as a function of DGD for various modulation formats (NRZ, ODB, DPSK, RZ-DPSK, DQPSK, RZ-DQPSK, OPFDM-DQPSK) is shown in Figure 7-28. The bit rate is 43 Gbit/s and the duty ratio of the RZ line-coding is 50%. The 3 dB-down bandwidth of the optical filter is 70 GHz and the electrical bandwidth of the receiver is 0.7B, where B is the baud rate.

The PMD tolerance of the DP-QPSK format is not included here since, with a coherent receiver followed by electronic processing, PMD may be compensated for electronically and hence the achievable PMD tolerance is a function of the complexity of the electronics.
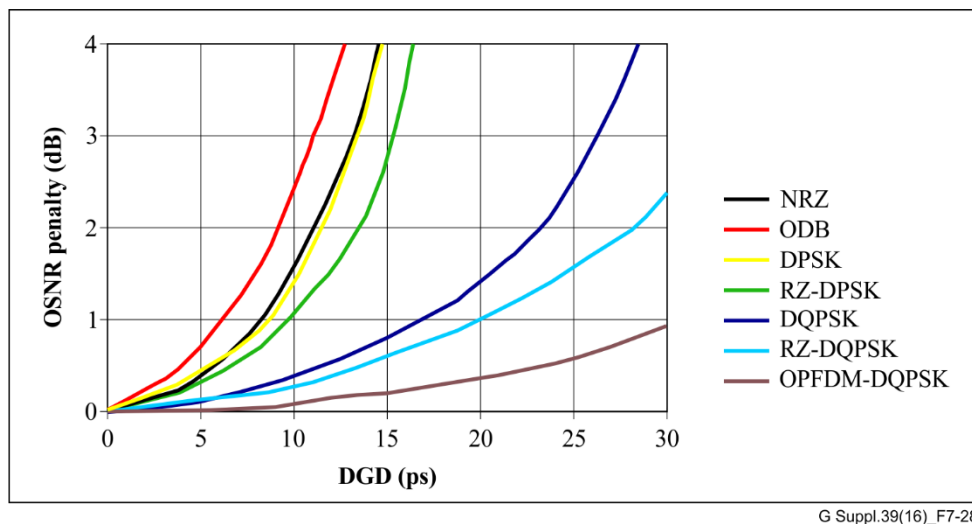
Figure 7-28 – OSNR penalty versus DGD for various modulation formats

7.12 Multi-dimensional modulation formats

In polarization multiplexed modulation formats, such as DP-QPSK (clause 7.6), OPFDM-DQPSK (clause 7.7.3.1), PDM-BPSK (clause 7.9) and PDM-16QAM (clause 7.1), independent information

is modulated onto orthogonal polarizations of the optical carrier. For these modulation formats it is usual that the change of a single data bit changes the constellation point value in only a single polarization. However, a better noise tolerance can be achieved if both polarizations (and both in-phase and quadrature components in each polarization) are changed together. While this might result in fewer combinations of constellation points, the effective noise tolerance is increased. Three examples of these formats (described as multi-dimensional modulation formats) are Polarization-switched QPSK (PS-QPSK), 6-polarization shift keying QPSK (6PolSK-QPSK) and 3-dimensional simplex (3D-Simplex). Other multi-dimensional formats can be derived by set-partitioning from higher order dual polarization QAM (DP-QAM) formats.

Other improved noise tolerance multi-dimensional modulation formats can be defined. By combining multiple symbols and selecting a subset of the possible constellation combinations, multi-symbol multi-dimensional modulation formats can be defined. For a baseline modulation format, each symbol is IQ modulated, a combination of N symbols results in a 2N-dimensional modulation format. The subset of valid constellation combinations is selected such that the 2N-dimensional Euclidean distance between closest neighbours is larger than for the full set of constellation combinations. Examples of multi-symbol multi-dimensional modulation formats are discussed in clause 7.12.4.

G Suppl.39(16)_F7-29
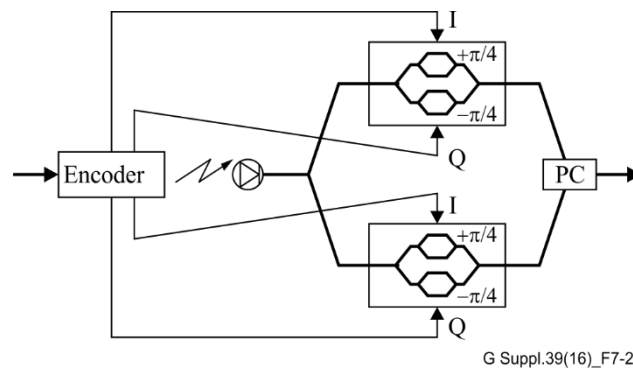
Figure 7-29 – Transmitter schematic for multi-dimensional modulation formats

All of the multi-dimensional formats described here can be generated using a dual-polarization IQ-modulator as shown in Figure 7-29. The drive signals for each modulation branch are derived in an encoder stage from the set of data bits. The signals are received in a coherent receiver and post-processed to obtain the transmitted information. If the information bit rate is Rb coded in the four dimensional [Ix, Qx, Iy, Qy] space and the number of allowed points within this space is Nc, the symbol rate of the modulated signal is Rs=Rb/log2(Nc). For multi-symbol, multi-dimensional modulation formats with Nc allowed constellation combinations, the symbol rate of the modulated signal is Rs=Rb $\times$ N/log2(Nc).

7.12.1 Polarization-switched QPSK (PS-QPSK)

The constellation of PS-QPSK, as introduced by [b-Agrell], can be considered as a subset of DP-QPSK. As only Nc=8 points are used for data encoding (out of 16 for DP-QPSK) only 3 bits are encoded per symbol. Using this subset, the minimum Euclidean distance can be increased by a factor of $\sqrt{2}$, thus increasing the effective noise power tolerance of the modulation format, although a higher baud rate is required to compensate for the smaller information content per symbol. Table 7-2 shows a possible realization for a list of allowed 4-dimensional points. These points can be represented as projections onto the x- and y- polarization planes, as shown in Figure 7-30.

Table 7-2 – PS-QPSK coordinates

Point number	Ix	Qx	Iy	Qy
1	1	1	1	1
2	1	1	−1	−1
3	1	−1	1	−1
4	1	−1	−1	1
5	−1	1	1	−1
6	−1	1	−1	1
7	−1	−1	1	1
8	−1	−1	−1	−1

Figure 7-30 – Representation of PS-QPSK constellation in x- and y-polarization planes with point numbers from Table 7-1

7.12.2 6-polarization shift keying QPSK (6PolSK-QPSK)

With the 6PolSK-QPSK modulation format [b-Buelow], Nc=24 constellation points are used to encode data, yielding log2(24)=4.58 bits/symbol. Therefore, 9 data bits can be encoded in a combination of 2 symbols. The 4-dimensional coordinates are shown in Table 7-3. 16 of the points (points 1 to 16 in Table 7-3) correspond to the points in DP-QPSK. Eight points (points 17 to 24) are added to the constellation with the same average power and the same minimum Euclidean distance. While the noise tolerance is therefore the same as for DP-QPSK, the increased information content can be used to reduce the symbol rate.

Table 7-3 – 6PolSK-QPSK coordinates

Point number	Ix	Qx	Iy	Qy
1	1	1	1	1
2	1	1	1	−1
3	1	1	−1	1
4	1	1	−1	−1
5	1	−1	1	1
6	1	−1	1	−1
7	1	−1	−1	1
8	1	−1	−1	−1
9	−1	1	1	1
10	−1	1	1	−1
11	−1	1	−1	1

Table 7-3 – 6PolSK-QPSK coordinates

Point number	Ix	Qx	Iy	Qy
12	−1	1	−1	−1
13	−1	−1	1	1
14	−1	−1	1	−1
15	−1	−1	−1	1
16	−1	−1	−1	−1
17	2	0	0	0
18	−2	0	0	0
19	0	2	0	0
20	0	−2	0	0
21	0	0	2	0
22	0	0	−2	0
23	0	0	0	2
24	0	0	0	−2

The representation of the 6PolSK-QPSK constellation points in the x- and y-polarization planes are shown in Figure 7-31. The solid dots represent the DP-QPSK points 1-16, the hollow dots and the hollow diamonds represent the additional points 17-20 and 21-24, respectively.

G Suppl.39(16)_F7-31
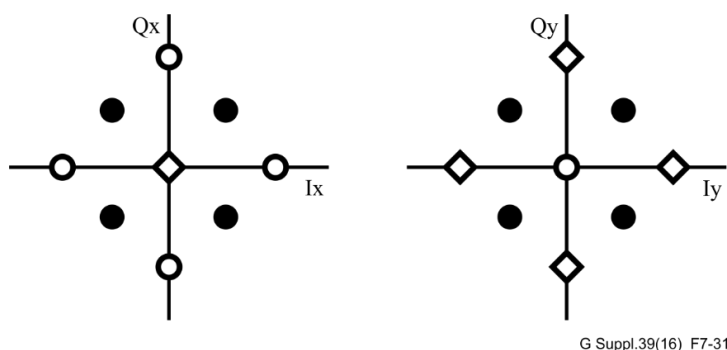
Figure 7-31 – Representation of 6PolSK-QPSK in x- and y-polarization planes

7.12.3 3-dimensional simplex (3D-Simplex)

The 3-dimensional simplex (3D-Simplex) constellation [b-Dochhan] can be arranged to only use three of the four dimensions in quadrature and polarization space. The fourth dimension is set to zero. A possible realization for a set of points is shown in Table 7-4. While two data bits are encoded per symbol, as is the case for PDM-BPSK, the noise tolerance is improved by up to 1.76 dB.

Table 7-4 – 3D-Simplex coordinates

Point number	Ix	Qx	Iy	Qy
1	1	1	1	0
2	1	−1	−1	0
3	−1	1	−1	0
4	−1	−1	1	0

The representation of the 3D-Simplex points as projections onto the x- and y-polarization planes are shown in Figure 7-32. The numbers correspond to the points in Table 7-4.

G Suppl.39(16)_F7-32
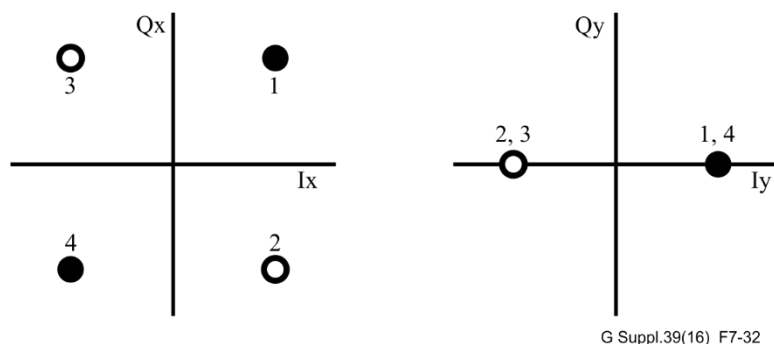
Figure 7-32 – Representation of 3D-Simple in x- and y-polarization planes

7.12.4   Multi-symbol multi-dimensional modulation formats

To realize multi-symbol multi-dimensional modulation formats, multiple symbols are grouped by single-parity-check bit and a subset of the possible combinations is chosen as valid constellation points. For example, two symbols of single-polarization QPSK can be combined into a 4-dimensional modulation format, when a subset of eight constellation points is chosen. Possible I- and Q-coordinates of the two symbols are shown in Table 7-5 for the eight constellation points. These coordinates correspond to those shown in Table 7-2 for the PS-QPSK format with the two orthogonal polarizations replaced by two consecutive symbols. Polarization multiplexing can be used for the multi-symbol multi-dimensional modulation formats.

Table 7-5 – 2-symbol QPSK coordinates

Point number	I(symbol1)	Q(symbol2)	I(symbol2)	Single-parity-check bit: Q(symbol2) $= I(symbol1) \oplus Q(symbol1) \oplus I(symbol2)$
1	1	1	1	1
2	1	1	−1	−1
3	1	−1	1	−1
4	1	−1	−1	1
5	−1	1	1	−1
6	−1	1	−1	1
7	−1	−1	1	1
8	−1	−1	−1	−1

Similarly, a subset of 128 ($16 \times 16/2$) constellation points out of the combination of two symbols of single-polarization 16-QAM represents a 4-dimensional modulation format. 3-symbol 16-QAM includes a subset of 2048 ($16 \times 16 \times 16/2$) points for a 6-dimensional modulation format, and a 128- point ($4 \times 4 \times 4 \times 4/2$) subset of 4-symbol QPSK, is an 8-dimensional modulation format. The performance of 2-symbol single-polarization QPSK is the same as that of PS-QPSK, and the performance of 2-symbol single-polarization 16-QAM is the same as that of 128-SP-QAM [b-Sjodin]. All of these formats only use half of the available point combinations between the symbols, such that a quasi parity-check bit is introduced to increase the Euclidean distance between valid constellation points.

8 Optical network topology

[ITU-T G.692] and [ITU-T G.959.1] currently concern point-to-point transmission systems, while leaving more complex arrangements (e.g., those involving optical add/drop) for further study. This clause discusses both point-to-point topologies as well as those containing optical add/drop.

8.1 Topological structures

Two types of networks are distinguished according to the properties of the optical network elements (ONEs) that the signal traverses: firstly, networks with 1R regeneration and secondly, networks where some in-line ONEs do provide 2R and/or 3R regeneration. The latter case does not exclude that some or all of the in-line ONEs may have 1R regeneration as well.

Following Annex A of [ITU-T G.872], 1R regeneration comprises optical amplification and dispersion compensation, i.e., analogue mechanisms without bit processing are captured by 1R regeneration. On the other hand, 2R and 3R regeneration apply digital processes (e.g., digital reshaping and digital pulse regeneration).

Different topological classes are defined including point-to-point links, bus structures, ring and meshed networks. Each class is introduced by a generic approach. Thus, particular implementation schemes are neither presumed nor excluded. Additionally, the number of topological classes is minimized by this approach, and a huge manifold of different implementation schemes are arranged in just a few groups. The absence of a generic representation would yield a huge number of diagrams for each individual minor topological modification.

Finally, the generic description is illustrated by a small number of typical examples for the purpose of clarification.

8.1.1 Networks with 1R regeneration

Networks with 1R regeneration include point-to-point links, bus structures, ring and meshed networks.

8.1.1.1 Point-to-point links

The generic representation of a point-to-point (ptp) link is shown in Figure 8-1. Light of n WDM channels is carried by one output fibre of a multichannel transmitter equipment (M-Tx). This optical signal passes transmission sections with alternating fibre pieces and 1R regenerators before entering a multichannel receiver equipment (M-Rx). The double-lined boxes and triangles in Figure 8-1 indicate the possibility of different realization schemes (with respect to the detailed topology and implementation **within** the doubled-lined boxes).

G.Suppl.39(08)_F8.1
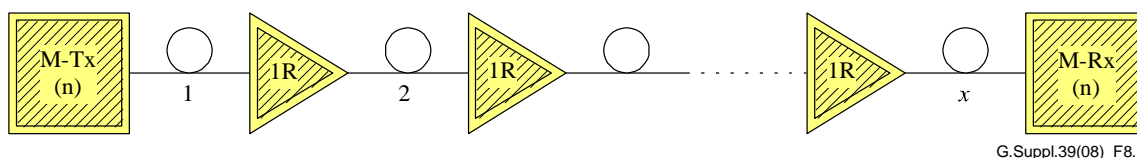
Figure 8-1 – Generic representation of a point-to-point link with 1R regenerators

Figure 8-2 shows a typical realization scheme of a multichannel transmitter equipment with a number of n WDM channels operating at central wavelengths λ_1, λ_2, ... λ_n. Examples of 1R regenerators are presented in Figure 8-3 including an optical amplifier (OA) – left-hand side – and a line amplifier with integrated passive dispersion compensator (PDC) – right-hand side. It should be noted that many other 1R regenerator realization schemes with PDC capabilities are possible.

An example of a typical WDM ptp link is shown in Figure 8-4. This is **only one particular** WDM ptp realization scheme.

G.Suppl.39(08)_F8-2
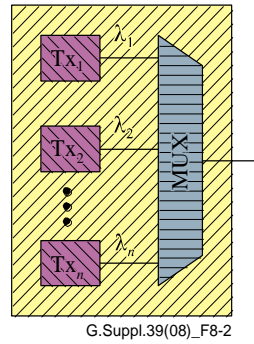
Figure 8-2 – Example of a multichannel transmitter realization scheme

G.Suppl.39(08)_F8.3
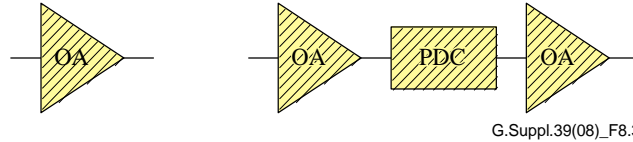
Figure 8-3 – Examples of 1R regenerator realization schemes

G Suppl.39(12)_F8-4
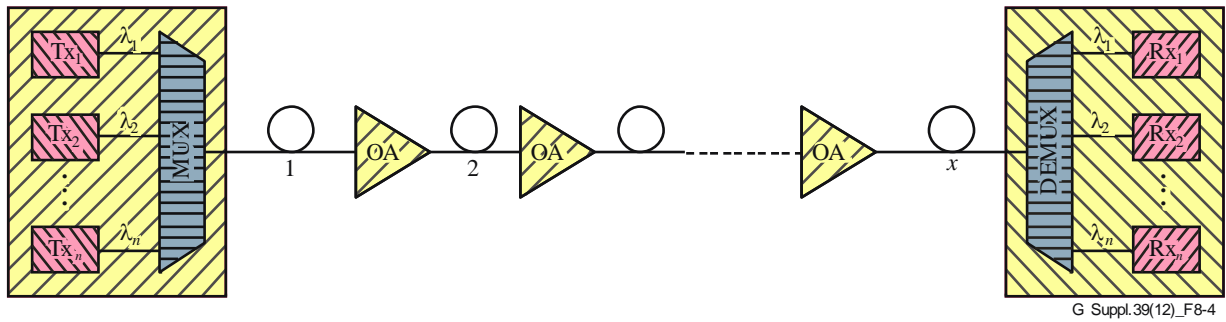
Figure 8-4 – Example of a WDM point-to-point link

8.1.1.2   Bus structures

The generic representation of a bus structure is shown in Figure 8-5. A number (n) of WDM channels emitted by the M-Tx enters the first optical network element (ONE) ONE_1. A subset (n_1) of WDM channels is dropped and added by ONE_1 and detected by receiver and transmitter equipment (denoted by "Rx (n_1)" and "Tx (n_1)") for those n_1 channels. The same procedure is continued at the subsequent optical network elements ONE_2 ... ONE_k where k denotes the total number of ONEs ($k \geq 1$). The number of dropped and added channels may range from:

$$0 \leq n_j \leq n, \quad (1 \leq j \leq k)$$

G.Suppl.39(08)_F8-5
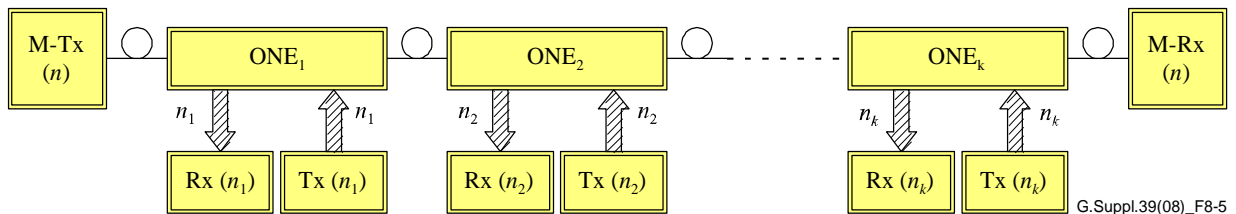
Figure 8-5 – Generic representation of a bus structure

In case of $n_j = n$, all WDM channels are dropped and added. If $n_j = 0$ holds, then no channel is added or dropped, i.e., ONE_j is just a 1R regenerator in this case. Thus, a hybrid topological scheme

incorporating a sequence of optical amplifiers and optical add/drop multiplexers (OADMs) are also captured by this generic approach.

The hatched arrows at the tributary ports of each optical network element ONE_j ($j = 1 ... k$) indicate that up to n_j fibres may be used.

Some particular realization schemes of bus structures are shown below. Figure 8-6 represents a bus with two OADMs and one fibre for each added and dropped WDM channel at the tributary ports. Figure 8-7 is an example of a bus structure with a chain of OAs plus just one additional OADM adding and dropping a number ($n*$) of WDM channels. In contrast to Figure 8-6, only one fibre (carrying the light of all $n*$ WDM channels) is used at the tributary ports of this particular OADM.
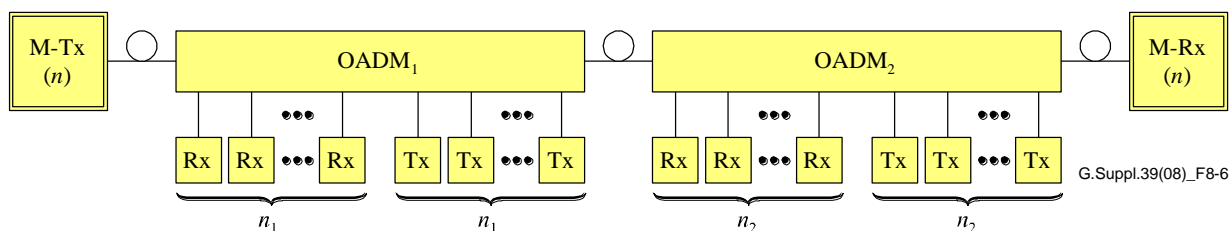
Figure 8-6 – Example of a bus structure with two OADMs and one fibre for each added/dropped WDM channel
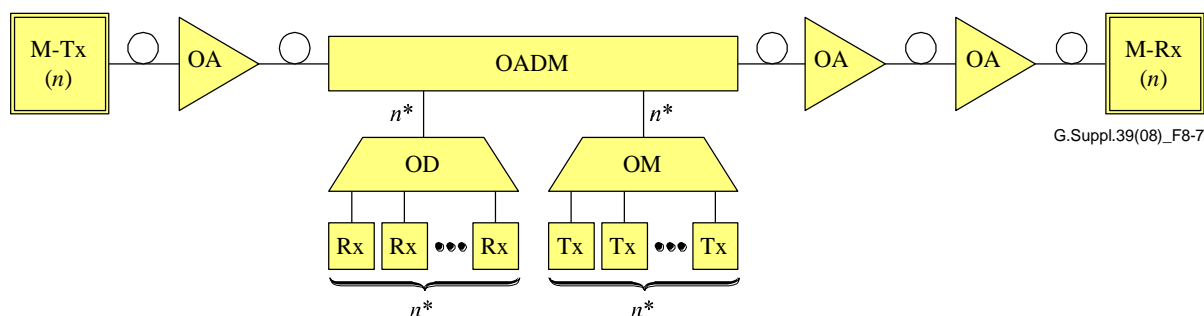
Figure 8-7 – Example of a bus structure with optical amplifiers and one OADM

9 "Worst-case" system design

For "worst-case" system design, optical systems in client networks (PDH, SDH, OTN) are specified by optical and electrical system parameters with maximum and minimum values at the end-of-life ([ITU-T G.955], [ITU-T G.957], [ITU-T G.691], [ITU-T G.692] and [ITU-T G.959.1]).

9.1 Power budget concatenation

Power budgets of single-channel (TDM in [ITU-T G.957] and [ITU-T G.691]) and multichannel (WDM in [ITU-T G.959.1]) optical systems have been given with the following optical parameters in a "worst-case" approach:

–   maximum mean (channel) output power;

–   minimum mean (channel) output power;

–   maximum mean total output power (for multichannel applications);

–   maximum attenuation;

–   minimum attenuation;

–   maximum chromatic dispersion;

–   minimum chromatic dispersion;

–   maximum differential group delay (DGD);

–   maximum mean (channel) input power;

–   maximum mean total input power (for multichannel applications);

–   minimum receiver sensitivity (or minimum equivalent sensitivity);

–   maximum optical path penalty.

When the optical path includes one or more optical amplifiers (e.g., [ITU-T G.698.2]), the system budgets employ the following optical parameters in place of the last two parameters in the above list:

–   minimum receiver OSNR tolerance;

–   maximum optical path OSNR penalty.

9.1.1   Minimum receiver sensitivity

The receiver sensitivity is defined (for the worst-case and end-of-life) as the minimum acceptable value of mean received optical power at point MPI-R to achieve a BER of 1×10^{-12}. Worst-case transmitter extinction ratio, optical return loss at point MPI-S, receiver connector degradation, measurement tolerances and ageing effect cause the worst-case condition.

Optical systems that would otherwise be limited in transmission length by optical fibre attenuation can be operated with the use of optical (booster-, line- or/and pre-) amplifiers ([ITU-T G.661], [ITU-T G.662] and [ITU-T G.663]).

9.1.2   Maximum optical path penalty

Power penalties associated with the optical path (such as chromatic fibre dispersion or polarization-mode dispersion, jitter, reflections) are contained in the maximum optical path penalty, but not in the minimum receiver sensitivity. Note, however, that the minimum average optical power at the receiver must be greater than the minimum receiver sensitivity by the value of the optical path penalty.

Optical systems that would otherwise be limited in transmission length by chromatic fibre dispersion require certain dispersion accommodation (DA) processes [ITU-T G.691] to overcome fibre length limitation, as considered in clause 9.2.1.

9.1.3   Minimum receiver OSNR tolerance

This value defines the minimum optical signal-to-noise ratio that is required for achieving the target BER of 1×10^{-12} at a receiver reference point at a given power level in OSNR limited (line amplified) systems. Worst case transmitter extinction ratio, optical return loss at point MPI-S, receiver connector degradation, measurement tolerances and ageing effect cause the worst-case condition. The receiver OSNR tolerance does not have to be met in the presence of chromatic dispersion, non-linear effects, reflections from the optical path, PMD, polarization dependent loss (PDL) or optical crosstalk; these effects are specified separately in the allocation of maximum optical path OSNR penalty.

9.1.4   Maximum optical path OSNR penalty

OSNR penalties associated with the optical path (such as non-linear effects, reflections from the optical path, PMD, PDL or optical crosstalk) are contained in the maximum optical path OSNR penalty, but not in the minimum receiver OSNR tolerance. Note, however, that the minimum average OSNR at the receiver must be greater than the minimum OSNR tolerance by the value of the optical path OSNR penalty.

9.2 Chromatic dispersion

9.2.1 Chromatic dispersion – Analytical approach

Chromatic dispersion in a single-mode fibre is a combination of material dispersion and waveguide dispersion, and it contributes to pulse broadening and distortion in a digital signal. From the point of view of the transmitter, this is due to two causes.

One cause is the presence of different wavelengths in the optical spectrum of the source. Each wavelength has a different phase delay and group delay along the fibre, so the output pulse is distorted in time. (This is the cause considered in [ITU-T G.957].)

The other cause is the modulation of the source, which itself has two effects:

One effect is that of the Fourier frequency content of the modulated signal. As bit rates increase, the modulation frequency width of the signal also increases and can be comparable to or can exceed the optical frequency width of the source. (A formula for a zero-frequency width source is quoted in [ITU-T G.663].)

Another effect is that of chirp, which occurs when the source wavelength spectrum varies during the pulse. By convention, positive chirp at the transmitter occurs when the spectrum during the rise/fall of the pulse shifts towards shorter/longer wavelengths respectively. For a positive fibre dispersion coefficient, longer wavelengths are delayed relative to shorter wavelengths. Hence, if the sign of the product of chirp and dispersion is positive, the two processes combine to produce pulse expansion. If the product is negative, pulse compression can occur over an initial length of fibre until the pulse reaches a minimum width and then expands again with increasing dispersion.

9.2.1.1 Bit-rate limitations due to chromatic dispersion

This clause generalizes the "epsilon-model" of [ITU-T G.957] to account for the dispersion effects of the widths of both the source spectrum and the transmitter modulation, in the case where chirp and any side modes are negligible by comparison. In many practical cases, chirp may dominate, and the theoretical dispersion limits indicated in this clause will be higher or lower than are experienced.

The theory is given in Appendix I. It also assumes that the rms-width theory of Gaussian shapes for the source and modulation spectra can be applied to general shapes, and that second-order dispersion is small compared to the first-order dispersion. As in [ITU-T G.957], it considers the allowed pulse spreading as a fraction of the bit period to be limited to a maximum value, called the "epsilon"-value (ε-value), that is determined below by the allowable power penalty.

Dispersion formulae

These formulae follow from clause I.7 where they are given in general form before conversion to particular numerical units used below. The duty cycle is f; for RZ, $f < 1$ and for NRZ, $f = 1$. For a bit-rate B in Gbit/s along a fibre of length L in km with a dispersion coefficient D in ps/km·nm at the source mean wavelength λ in μm (not nm), the maximum allowed link chromatic dispersion in ps/nm is:

$$DL = \frac{1819.650\,\varepsilon}{\lambda^2 B \left[\left(\frac{1.932\,B}{f} \right)^2 + \Gamma_v^2 \right]^{0.5}} \tag{9-1}$$

Here Γ_v in GHz is the –20 dB width of the source spectrum in optical frequency. It corresponds to a –20 dB width of the wavelength spectrum Γ_λ in nm given by:

$$\Gamma_\lambda \approx \frac{\lambda^2}{299.792} \Gamma_v \tag{9-2}$$

Comparing the left-hand side result with Equation 9-1 shows that the "effective" 20 dB spectral width of the modulated source is $\left[\left(\dfrac{1.932\,B}{f}\right)^2 + \Gamma_\nu^{\,2}\right]^{0.5}$, a combination of the modulation and optical frequency spectra.

For the limiting case of a broad spectrum/low bit rate, Equations 9-1 and 9-2 give:

$$D\,L\,B\,\lambda^2\,\Gamma_\nu \approx 1819.650\,\varepsilon \quad \text{or} \quad D\,L\,B\,\Gamma_\lambda \approx 6.0697\,\varepsilon \qquad (9\text{-}3)$$

These approximations are accurate to within 1% of Equation 9-1 whenever $\Gamma_\nu > \dfrac{14B}{f}$. The equivalent of the right-hand side result of Equation 9-3 was used in [ITU-T G.957] (for a 1 dB penalty and $BER = 10^{-10}$) to derive the source requirements for target distances in the tables there.

For the opposite limit of a narrow spectrum/high bit rate, one has:

$$D\,L\,B^2\,\lambda^2 \approx 941.826\,\varepsilon\,f \qquad (9\text{-}4)$$

The approximation is accurate to within 1% of Equation 9-1 whenever $\Gamma_\nu > \dfrac{B}{4f}$, defining a "narrow linewidth" source. For a 1 dB penalty and NRZ, Equation 9-4 gives:

$$D\,L\,B^2\,\lambda^2 \approx 282.548 \qquad (9\text{-}5)$$

The result quoted in [ITU-T G.663] is close to this for 1550 nm.

NOTE – The number of significant figures shown in the formulae above, and used in the results below, are a result of the numerical manipulations. They do not imply that the formulae and results have the displayed degree of accuracy.

Time-slot fraction related to power penalty

For [ITU-T G.957], the equation relating the fractional pulse spreading to the power penalty P_{ISI} (in dB) for NRZ pulses and SLM lasers was [b-Agrawal2]:

$$P_{ISI} = 5\log_{10}\left(1 + 2\pi\varepsilon^2\right) \quad \text{or} \quad \varepsilon = \left(\frac{10^{\frac{P_{ISI}}{5}} - 1}{2\pi}\right)^{0.5} \qquad (9\text{-}6)$$

The result is independent of BER, taken to be 10^{-10} in [ITU-T G.957]. In reality, there is a very slight penalty increase in going to 10^{-12}, thereby decreasing ε by perhaps a few per cent at a particular dB penalty level.

Table 9-1 gives values at several power penalties of interest, incorporating approximately 1½-2% rounding-down.

Table 9-1 – Power penalty for several epsilon values

Power penalty [dB]	Epsilon value
0.5	$0.203 \approx 0.2$
1	$0.305 \approx 0.3$
2	$0.491 \approx 0.48$

For MLM lasers, the power penalty for mode partition noise (MPN) was modelled as [b-Agrawal2]:

$$P_{MPN} = 2\left(-5\log_{10}\left\{1 - \frac{1}{2}\left[kQ\left(1 - e^{-\pi^2\varepsilon^2}\right)\right]^2\right\}\right) \tag{9-7}$$

where k is the MPN factor and the Q factor is the effective signal-to-noise ratio at a particular BER. A BER of 10^{-12} corresponds to $Q \approx 7.03$. The total power penalty is the sum of P_{ISI} and P_{MPN}.

The extra factor of 2 in Equation 9-7 compared to that found in [b-Agrawal2] is due to evidence that the equation in [b-Agrawal2] under-predicted the mode partition noise penalty by a factor of two.

In deciding the value of ε associated with MLM lasers in [ITU-T G.957], a total power penalty of 1 dB was allowed, with $Q = 6.36$, corresponding to 10^{-10} BER, and a value of $k = 0.7$ for the MPN factor. The maximum value of $\varepsilon = 0.115$ in [ITU-T G.957] is slightly less than the value which would be consistent with Equation 9-7, as a result of engineering judgment which determined that a more conservative value should be adopted.

For BER of 10^{-12}, use an epsilon value of 0.109, which is derived from Equation 9-7 with $Q = 7.03$ and $k = 0.76$.

The examples consider only SLM lasers in which the MPN is zero.

Examples

Here the synchronous transport module (STM) bit rates used are for NRZ 10 Gbit/s: 9.95328 Gbit/s, and for NRZ 40 Gbit/s: 39.81312 Gbit/s as in [ITU-T G.707]. From Table 9-1, $\varepsilon = 0.3$ or 0.48 is used for a power penalty of 1 or 2 dB, respectively.

Example 1: Consider the maximum allowable chromatic dispersion at several unchirped NRZ bit rates with non-zero width sources (with negligible chirp or side modes) for a 1 dB penalty. Then for 1550 nm, Equation 9-1 gives Figure 9-1 (from Equation 9-2 at this wavelength, a frequency spread of 100 GHz corresponds to a wavelength spread of about 0.8 nm). These are the required dispersion values independent of fibre type.

Note that as the source spectral width increases, the maximum allowed chromatic dispersion decreases. This is less pronounced at higher bit rates, where the modulation spectrum makes up a greater fraction of the total spectral width.

The dispersion-limited length is obtained by dividing the chromatic dispersion by the fibre chromatic dispersion coefficient. For the example of an ITU-T G.652 fibre with $D(1550) = 17$ ps/nm·km, a plot similar to Figure 9-1 results with the vertical axis scale divided by 17 to display the length in km.
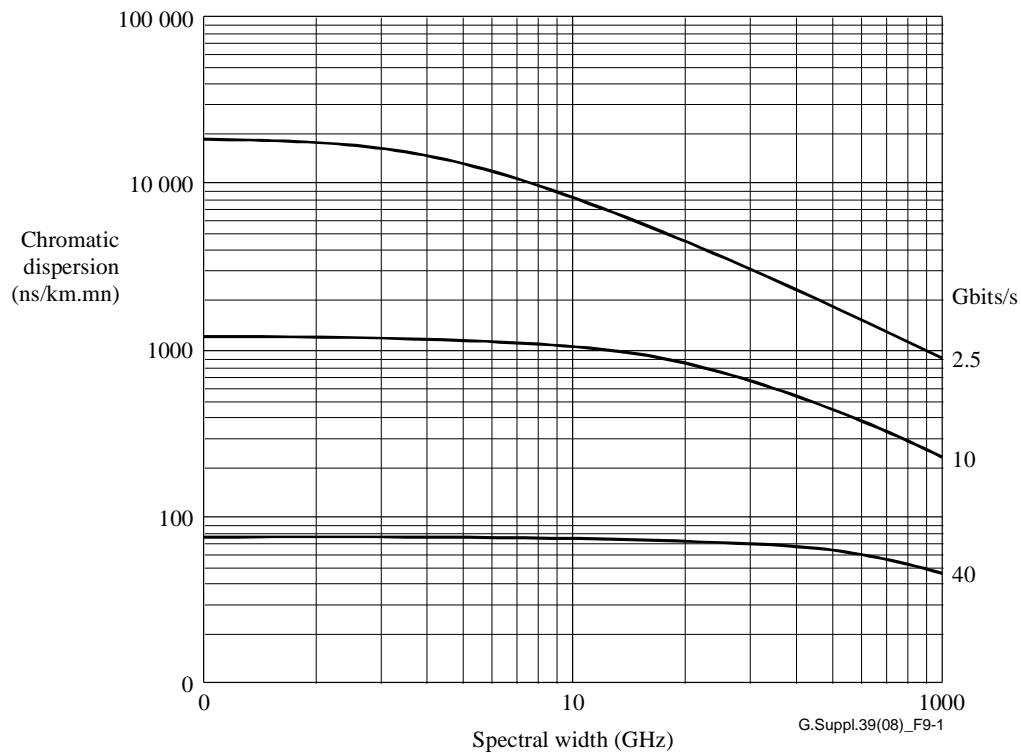
Figure 9-1 – Maximum allowed chromatic dispersion versus source spectral width at 1550 nm for several unchirped NRZ bit rates at a power penalty of 1 dB

Example 2: Consider the limiting case in Example 1 of a high bit-rate and narrow-linewidth spectrum transmitter (the values on the ordinate of the above graphs). The allowed chromatic dispersion is given by Equation 9-4 as:

$$DL \approx \frac{117.606 \text{ or } 188.169}{B^2} \qquad (9\text{-}8)$$

for a 1 or 2 dB penalty, respectively. Table 9-2 shows the corresponding values. (The 1 dB numbers correspond to the vertical intercepts of Figure 9-1.)

Table 9-2 – Maximum theoretical allowable chromatic dispersion for a chirp-free narrow-linewidth source at 1550 nm for several unchirped NRZ bit rates and power penalties

Unchirped NRZ bit rate [Gbit/s]	Maximum chromatic dispersion [ps/nm]	
	1 dB penalty	2 dB penalty
2.5	18 820	30 110
10	1 175	1 880
40	73.5	118

Example 3: Consider the narrow-linewidth source at the upper range of the C-band at 1565 nm and a 1 dB penalty. Then Equation 9-5 gives the dispersion-limited length as:

$$L = \frac{115.362}{B^2 D} \qquad (9\text{-}9)$$

Table 9-3 shows some examples.

Table 9-3 – Theoretical length limitations for a chirp-free narrow-linewidth source at 1565 nm with 3 fibre types and 2 unchirped NRZ bit rates for a 1 dB penalty

Fibre type		ITU-T G.652	ITU-T G.653	ITU-T G.655
Dispersion coefficient at 1565 nm in ps/(nm·km)		19	3.5	10
Dispersion-limited length in km	NRZ 10 Gbit/s	61	333	116
	NRZ 40 Gbit/s	3.8	20.8	7.3

Considering that in the system application codes there are: intra-office, I (≤ 25 km), short-haul, S (≤ 40 km), long-haul, L (≤ 80 km) and very long-haul, V (≤ 120 km), for the 1565 nm examples in Table 9-3:

– NRZ 10 Gbit/s systems with ITU-T G.653 fibre for I, S, L and V applications or with ITU-T G.655 fibre for I, S and L applications usually require no chromatic dispersion accommodation.

– NRZ 10 Gbit/s systems with ITU-T G.652 fibre for L and V applications require chromatic dispersion accommodation.

– NRZ 40 Gbit/s systems require dispersion accommodation for all fibre types and for I, S, L and V applications. For ITU-T G.652 fibre, the NRZ 40 Gbit/s length limitation starts at a few km.

Active and/or passive dispersion accommodation techniques, as given in [ITU-T G.691], and in clauses 9.2.1.2 and 9.2.1.3, can be applied to overcome fibre length limitations due to chromatic dispersion.

Example 4: As a final example, consider Equation 9-4 applied to several formats at 40 Gbit/s.

Table 9-4 – Maximum theoretical allowable chromatic dispersion for a chirp-free narrow-linewidth source at 1550 nm for several unchirped 40 Gbit/s formats and a 2 dB power penalty

Format (unchirped)	Maximum chromatic dispersion [ps/nm]
NRZ	118
RZ(⅔)	78
RZ(½)	59
RZ(⅓)	39
NOTE – The value given above for RZ(⅔) is for conventional RZ modulation and not for carrier-suppressed RZ.	

9.2.1.2 Penalty due to chromatic dispersion

[ITU-T G.959.1] indicates that a maximum path penalty of 1 dB for low-dispersion systems, and of 2 dB for high-dispersion systems, is allowed. The path penalties are not made proportional to the target distance to avoid operating systems with high penalties.

[ITU-T G.698.2] defines "maximum transmitter (residual) dispersion OSNR penalty" parameter of 2 dB to describe OSNR penalty due to dispersion alone.

In the future, systems employing DA techniques based on pre-distortion (e.g., prechirping) of the optical signal at the transmitter may be introduced. In this case, the path penalty in the above sense can be defined only between points with undistorted signals. These points, however, do not coincide with the main path interfaces, and may thus not even be accessible. The definition of path penalty for this use is for further study.

9.2.1.3   Chromatic dispersion accommodation

The following active dispersion accommodation techniques are reported in [ITU-T G.691]:

–   A prechirp is applied in the optical transmitter to obtain pulse compression and to get an increase in the transmission distance.

–   Self-phase modulation (SPM) uses the non-linear Kerr effect in the ITU-T G.652 fibre for obtaining pulse compression and a longer transmission distance, but requires an optical signal power above the non-linearity threshold.

–   Dispersion-supported transmission (DST) uses an optical frequency shift keying/amplitude shift keying (FSK/ASK) (or a pure optical FSK) modulation and utilizes the dispersive transmission fibre to convert the FSK signal parts at the transmitter into an ASK signal at the receiver. The optical FSK modulation interacts with the chromatic dispersion of the fibre in a high-pass-like transfer function. Using a low-pass filter (DST-filter) in the electrical domain of the receiver, the response signal can be equalized.

Because all active DA techniques are additional techniques in the electrical to optical conversion (E/O) transmitter and optical to electrical conversion (O/E) receiver (also for equalization in the electrical domain), this process has been introduced into [ITU-T G.798] as channel dispersion accommodation (DAc) process.

The passive chromatic dispersion accommodation technique (DA), defined in [ITU-T G.691], can be used in a long-haul or multi-span high data rate transmission system. A passive dispersion compensator (PDC, ITU-T G.671) can be dispersion-compensating fibres (DCF) or fibre gratings. It can be applied in an optical transmitter with booster amplifier and/or an optical receiver with preamplifier as well as in an optical line-amplifier. To compensate for the additional loss of the PDC modules, line amplifiers can be designed with dual stage configuration and these devices may be sandwiched between line amplifiers to meet the OSNR requirement at the receiver. This amplifier-aided dispersion accommodation (DAa) process has been introduced into [ITU-T G.798].

Another active dispersion accommodation method is to use a coherent receiver followed by an electrical DSP process to compensate CD at the receiver.

In a multi-wavelength system, the PDC can exactly compensate for the chromatic dispersion of one wavelength; it might not be able to exactly compensate at the other wavelengths. The difference in residual dispersion between channels can be minimized by applying dispersion compensation and dispersion slope compensation together. Since the chromatic dispersion in a fibre may vary with time/temperature, a high-speed system may need to be compensated partly by PDC, and partly by dynamically adjusted adaptive compensation.

9.2.2   Chromatic dispersion – Computational approach

9.2.2.1   Introduction

In the following, system tolerances on residual chromatic dispersion are evaluated and suggestions for single-channel (SC) and multichannel (MC) systems that deal with return to zero (RZ) transmission format are provided.

In the case of SC 40-Gbit/s transmission, a maximum value is suggested for the residual chromatic dispersion that depends on the input average power. In the case of MC transmission (within the wavelength range of ITU-T G.959.1 applications), the effects of fibre dispersion slope and its compensation have been considered.

9.2.2.2 System assumptions and calculation tool description

The results reported below are based on the following assumptions:

– $N \times 40$ Gbit/s system on typical terrestrial lengths (500-1000 km), with quite long amplifier spacing (for example, 100 km).

–   RZ transmission format with Gaussian pulses ($T_{FWHM} = 5$ ps). Since aim is the analysis of dispersion effects, an "ideal" transmitter is considered.

–   Periodic dispersion compensation with the same period as the amplifier spacing. Several schemes for dispersion compensation have been proposed in the literature (post-compensation, pre-compensation, post-compensation with prechirp) [b-Zitelli]. Here, the post-compensation is dealt with.

–   Ideal receiver is made up of: optical filter with bandwidth 160 GHz, ideal photodiode and electrical filter (4th order Bessel-Thomson with bandwidth 32 GHz).

–   Propagation of a pseudo-random bit sequence of 32 bits. In the case of MC systems, the bit sequences on the different channels are uncorrelated.

A simplified scheme of the system is shown in Figure 9-2.

G.Suppl.39(16)_F9-2
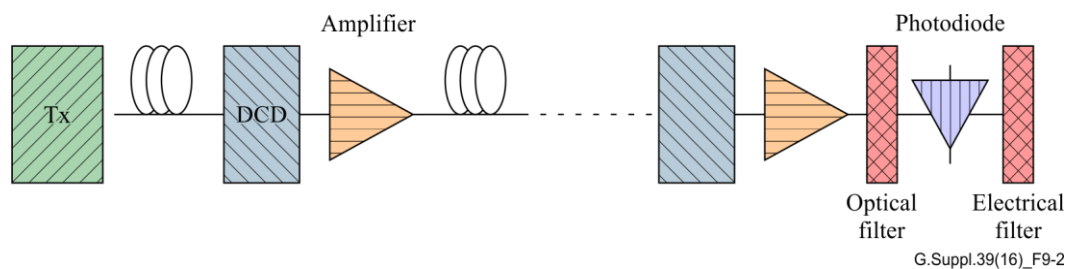
Figure 9-2 – Scheme of the system with periodic post-compensation

Concerning the simulations, the Split-Step Fourier method, also called beam propagation method (BPM), has been implemented. For a detailed description of the BPM, see [b-Agrawal] and [b-Iannone]; a very short description is given here. The BPM allows solving numerically non-linear Schrödinger equation that describes the propagation of an optical pulse in a fibre, considering chromatic dispersion, non-linear effects (self-phase modulation, cross-phase modulation and four-wave mixing), effect of dispersion slope, fibre losses and lumped amplification.

The BPM is the basis of nearly all commercial simulation tools. The adopted code was tested by several researchers and its results compared with those of other commercial tools before its use.

System performance has been evaluated both in terms of penalty on the eye diagram and BER (or Q factor).

9.2.2.3 Tolerances towards residual chromatic dispersion on 1×40 Gbit/s SC systems

It is quite difficult to give a general guideline for the maximum tolerable residual chromatic dispersion in a 1×40 Gbit/s system because several aspects should be considered.

A first aspect is the transmission modulation format: in this case the RZ transmission format ($T_{FWHM} = 5$ ps) has been examined. A second point is the optical input power; in fact, low input powers allow operation in the linear regime but cannot guarantee a sufficient optical signal-to-noise ratio (OSNR). On the other hand, higher input powers, in spite of a good OSNR, cause consistent non-linear effects (see also clauses 9.5 and 9.7).

Simulations have been made with 100-km amplifier spacing over 500 km, varying the input optical power between 0 and 10 dBm, and the residual dispersion between –30 and +30 ps/nm. Figure 9-3 reports the penalty on the eye diagram expressed in dB versus the residual dispersion for two optical input powers: 5 dBm (solid line) and 10 dBm (dashed line).

It can be observed that, setting an upper limit of 1 dB in the penalty on the eye closure with respect to the exact compensation case, the resulting maximum residual dispersion is about 17 ps/nm. This residual dispersion value corresponds to a tolerance of about only 1 km on the total link length when dealing with ITU-T G.652 fibres, and about 4 km with ITU-T G.655 fibres.

In conclusion, 40-Gbit/s systems are characterized by a very small tolerance towards chromatic dispersion, especially with ITU-T G.652 fibres. Experimental results [b-Matera] put in evidence that it is a crucial point to realize exact dispersion compensation in correspondence of each amplifier.

The above considerations do not depend on the kind of dispersion compensation device adopted, though obviously the availability of tunable devices would allow one to solve this kind of problem. When dealing with dispersion-compensating fibres (DCFs), the system should be modified to include double stage amplifiers. Results of Figure 9-3 are only valid for launching in the DCF optical powers lower than 3 dBm to reduce their strong non-linear effects.
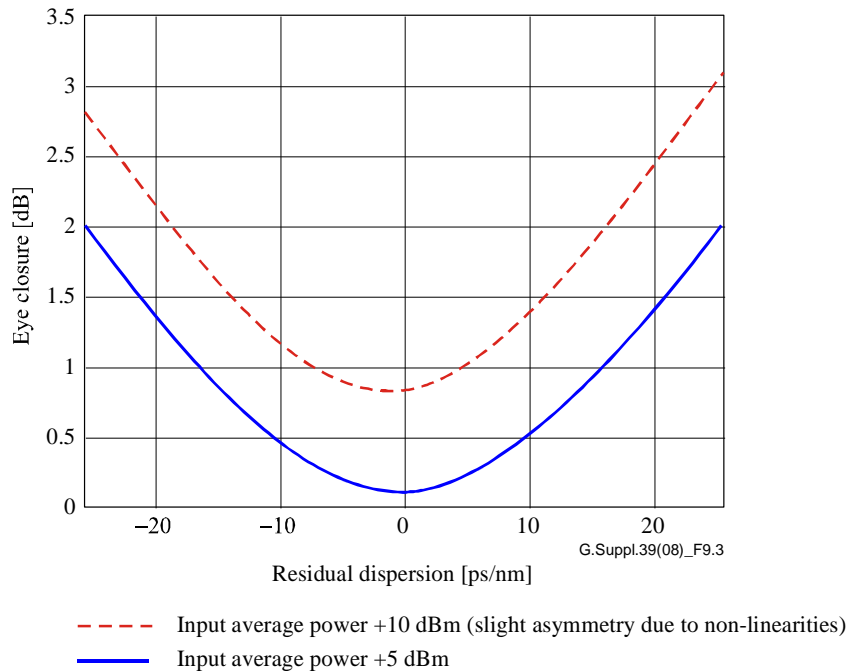
Figure 9-3 – Eye penalty as function of the residual dispersion obtained by varying the length of the last span

9.2.2.4 Tolerances towards residual chromatic dispersion on N × 40 Gbit/s MC systems

In the case of wavelength division multiplexed (WDM) systems, it is also necessary to take into consideration the fibre dispersion slope. Due to the dispersion slope, each WDM channel is characterized by a different value of dispersion coefficient. This can be approximated in the 1550 nm region as:

$$D(\lambda) = D(1550) + S_0(\lambda - 1550) \tag{9-10}$$

where D is the dispersion coefficient, S is the dispersion slope coefficient, and λ is the channel wavelength.

So far, it is still quite difficult to find dispersion-compensation devices able to compensate exactly for the dispersion slope. As a consequence, when dealing with WDM systems, the dispersion-

compensating device is chosen to obtain exact compensation for the central channel while the lateral ones experience a residual dispersion. At this point, the maximum tolerable residual dispersion for each channel can be evaluated looking again at Figure 9-3. Such a value gives the limit at the same time to three quantities: number of channels (N), channel spacing and system length.

When some channels are characterized by a larger residual dispersion, it is still possible to obtain acceptable performances by means of an additional compensation placed after the demultiplexer and with the optimum value for each channel.

9.2.2.5   An example: 4×40 Gbit/s on ITU-T G.652 fibres with DCF

In this clause, a practical example of the previous discussion is provided.

A 4×40 Gbit/s WDM transmission system on ITU-T G.652 fibres using DCF has been considered with the following parameters:

–   Four WDM channels spaced at 200 GHz, at the wavelengths:
  •   Channel 1: $\lambda_1 = 1554.13$ nm;
  •   Channel 2: $\lambda_2 = 1555.75$ nm;
  •   Channel 3: $\lambda_3 = 1557.36$ nm;
  •   Channel 4: $\lambda_4 = 1558.98$ nm;

–   Demultiplexer with bandwidth $B = 160$ GHz;

–   ITU-T G.652 fibres with $D = 17$ ps/nm·km and $S_0 = 0.0677$ ps/nm^2·km;

–   Dispersion compensation by means of DCF with $D = -80$ ps/nm·km and $S_0 = -0.2$ ps/nm^2 · km;

–   The other parameters are the same as those considered in clause 9.2.2.2.

As the fibre dispersion slopes are different from that of the DCF, different channels experience different dispersions and so they are not equally compensated.

The DCF is chosen to obtain exact compensation on the third channel ($\lambda_3 = 1557.36$ nm). After the electrical filter, the system performances is evaluated by means of the eye closure expressed in dB.

Figure 9-4 shows, for each channel, the difference between its cumulative dispersion with respect to that of the third channel. In this way, the residual dispersions at the amplifier locations can be evaluated.
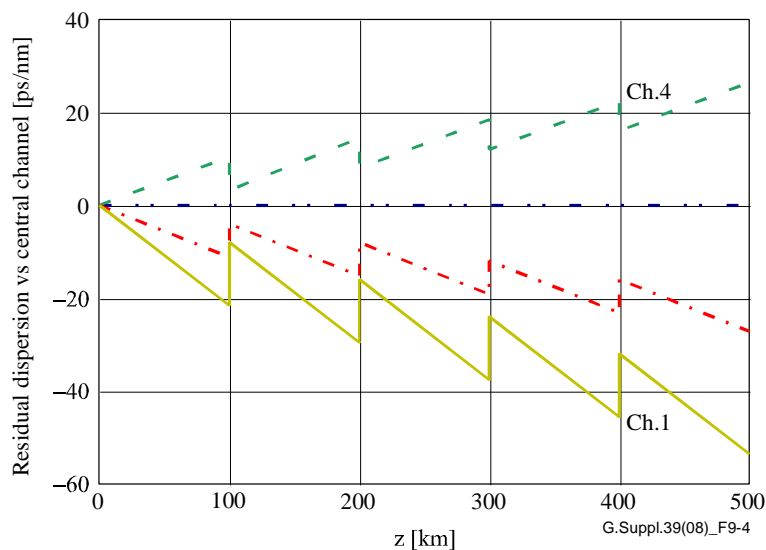
Figure 9-4 – Difference between the cumulative dispersion of each channel and that of the third channel (which is exactly compensated)

Table 9-5 indicates CD values obtained after 500 km.

Table 9-5 – Obtained values of chromatic dispersion [ps/nm]

CD(λ_1)	CD(λ_2)	CD(λ_3)	CD(λ_4)
–40.9	–20.9	–1	19.1

According to the curve of Figure 9-5, it is possible to affirm that the residual dispersion on the first channel is too high. Moreover, Figure 9-5 confirms that it is not possible to obtain acceptable performance on that channel. In fact, while the DCF exactly compensates for chromatic dispersion at a fixed wavelength, its dispersion is not optimized in order to compensate also the dispersion slope. The eye penalties reported in the figures correspond to an input average power of +5 dBm. Simulations were carried out also for higher powers showing even stronger penalties due to the non-linear effect.

a) Channel 1

b) Channel 2

c) Channel 3
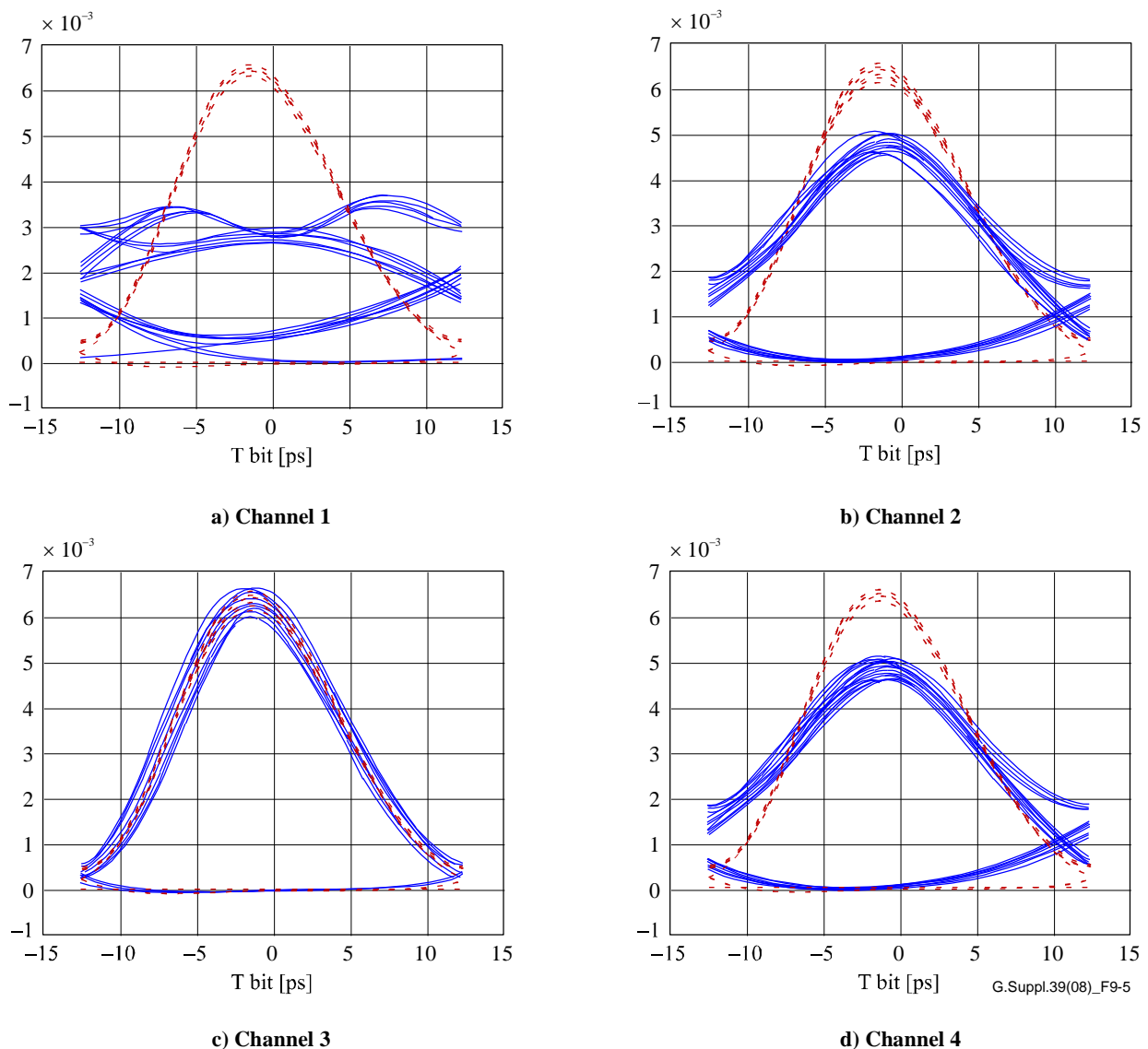
d) Channel 4

Figure 9-5 – Eye diagrams for several channels at the end of a 500-km non-linear system

9.2.2.6   Conclusions

It has been shown that fibre dispersion slope seriously limits the maximum length of WDM systems. Since it is a deterministic effect, it is possible to compensate residual dispersion on side channels by

means of optimized dispersion-compensating devices for each channel placed after the optical demultiplexer. On the other hand, it can be underlined that high bit-rate systems present a very small tolerance towards chromatic dispersion and so the fibre lengths should be selected with a high precision.

9.3 Polarization mode dispersion

For NRZ transmission up to 40 Gbit/s, the maximum DGD is set to 30% of the bit period, corresponding to a maximum of 1 dB path penalty. Second-order PMD and its interaction with chromatic dispersion as well as tolerance for RZ is under study.

9.3.1 PMD compensation

Existing link element specifications include statistical aspects to support system requirements. Further discussion of this can be found in clause 10.4.

PMD compensation techniques may be used for links with excessive PMD. To establish the extent to which PMD compensation is required, a careful investigation of the outside plant may be needed.

9.3.2 PMD penalty

The power or OSNR penalty induced by DGD at the receive point R is a function of the relative power of the two orthogonal polarization modes. This varies as the relative alignment of the principle states of polarization of the optical fibre cable, and the polarization of the source, varies. The maximum link DGD is set to allow no more than a given power penalty due to the first order PMD in the worst-case power splitting ratio (equal power in both modes). The worst-case power penalty is also affected by the transmission format, NRZ or RZ.

For 10 Gbit/s NRZ applications in [ITU-T G.691] and [ITU-T G.959.1], a 1 dB power penalty allowance corresponds to a 30 ps limit on the DGD at point R. (This corresponds to the same epsilon value as for chromatic dispersion, and 20 ps is expected to be the 0.5 dB value.) As with chromatic dispersion, the RZ case is for further study.

For 10 Gbit/s NRZ applications in [ITU-T G.698.2], a 2 dB OSNR penalty allowance corresponds to a 30 ps limit on the DGD at point Rs. For a well-designed receiver, this corresponds to an OSNR penalty of 0.2 to 0.4 dB for a DGD of 0.1 bit period.

Other line coding format cases are for further study.

9.4 BER and Q factor

Applications in [ITU-T G.691], [ITU-T G.692] and [ITU-T G.959.1] have an optical section design objective of an end-of-life bit error ratio (BER) not worse than 10^{-12}. The requirement for SDH applications is derived from [ITU-T G.826] (and more recently [ITU-T G.828]), while corresponding requirements for OTN applications are given in [ITU-T G.8201].

Applications in [ITU-T G.957], however, have an end-of-life BER requirement of 10^{-10} due to less stringent requirements being in place at the time of their development.

In order to "migrate" applications from a BER of 10^{-10} to 10^{-12}, a convention has been adopted where application codes with a maximum attenuation range of 12 dB at a BER of 10^{-10} were reduced to 11 dB at a BER of 10^{-12}, and application codes with a maximum attenuation range of 24 dB at a BER of 10^{-10} were reduced to 22 dB at a BER of 10^{-12}.

In general, the lower the value of the reference BER, the more difficult it is to actually verify the receiver performance due to the extended measurement time required. This is particularly valid for STM-1 and STM-4 receiver sensitivities at a BER of 10^{-12}. Two approaches have been proposed to address this problem. The first is to use a particular length of error-free operation to establish a certain probability of the error rate being below the required level. The required number of error free bits (n) can be found as:

$$n = \frac{\log(1-C)}{\log(1-P_E)} \tag{9-11}$$

where C is the required confidence level (e.g., 0.95 for 95% confidence) and P_E is the BER requirement (e.g., 10^{-12}). Therefore, if a confidence level of 95% for the BER to be less than 10^{-12} is required, 3×10^{12} error free bits are needed (20 minutes at STM-16 rate).

Since this still requires long measurement times at lower rates, an alternative method is to measure the Q factor. The Q factor is the signal-to-noise ratio at the decision circuit in voltage or current units, and is typically expressed by:

$$Q = \frac{(\mu_1 - \mu_0)}{(\sigma_1 + \sigma_0)} \tag{9-12}$$

where $\mu_{1,0}$ is the mean value of the marks/spaces voltages or currents, and $\sigma_{1,0}$ is the standard deviation. A BER of 10^{-12} corresponds to $Q \approx 7.03$.

Since practical Q measurement techniques make measurements in the upper and the lower regions of the received "eye" in order to infer the quality of the signal at the optimum decision level, Q can be considered as only a qualitative indicator of the actual BER.

The mathematical relations to BER (in case of non-FEC operation) when the threshold is set to the optimum value are:

$$BER = \frac{1}{2} \text{erfc}\left(\frac{Q}{\sqrt{2}}\right) \tag{9-13}$$

where:

$$\text{erfc}(x) = \frac{1}{\sqrt{2\pi}} \int_x^\infty e^{-\frac{\beta^2}{2}} \, d\beta \tag{9-14}$$

A commonly used approximation for this function is:

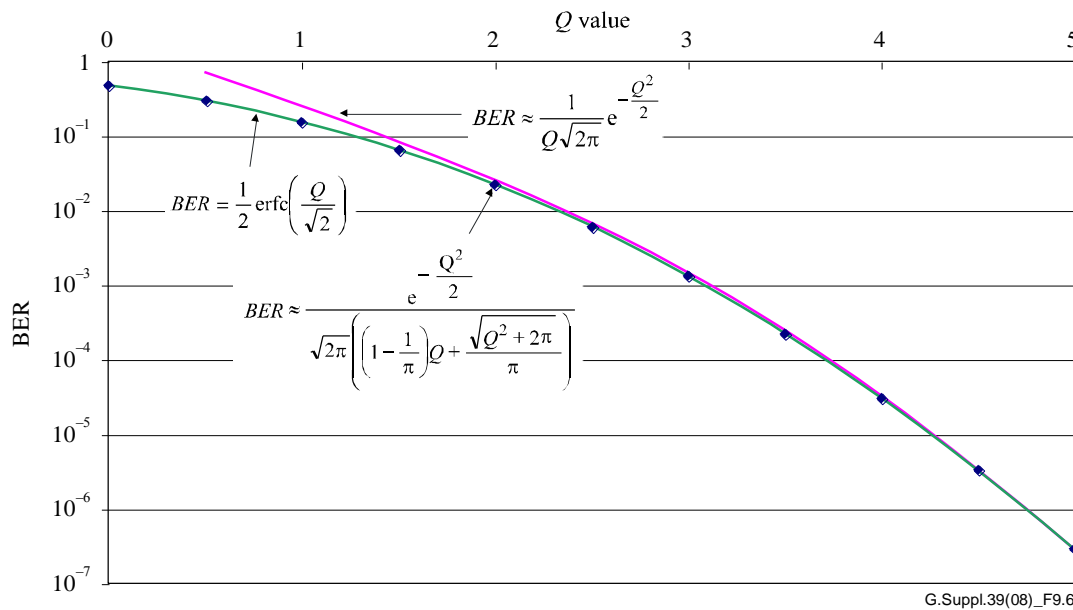$$BER \approx \frac{1}{Q\sqrt{2\pi}} e^{-\frac{Q^2}{2}} \tag{9-15}$$

for $Q > 3$.

An alternative expression that gives accurate answers over the whole range of Q [b-Spirit] is given in:

$$BER \approx \frac{e^{-\frac{Q^2}{2}}}{\sqrt{2\pi}\left(\left(1 - \frac{1}{\pi}\right)Q + \frac{\sqrt{Q^2 + 2\pi}}{\pi}\right)} \tag{9-16}$$

A graph comparing these two approximations for Q-values less than 5 is given in Figure 9-6.

Figure 9-6 – Approximations relating BER and Q

9.4.1 BER in FEC-enabled applications

In [ITU-T G.693], [ITU-T G.959.1] and [ITU-T G.698.1], several application codes with optical interface parameter sets have been defined or proposed at the OTUk rates requiring the transmission of FEC bytes as specified in [ITU-T G.709]. In these application codes, the system BER is required to be met only "after the correction (if used) has been applied". In these specific cases, the optical parameters are specified at a bit error ratio (BER) not worse than 10^{-12} at the FEC decoder output. This is illustrated in Figure 9-7. As shown in Table 11-2, the theoretical BER at the receiver output (point A in Figure 9-7) is 1.8×10^{-4} for 10^{-12} BER at the FEC decoder output (point B).
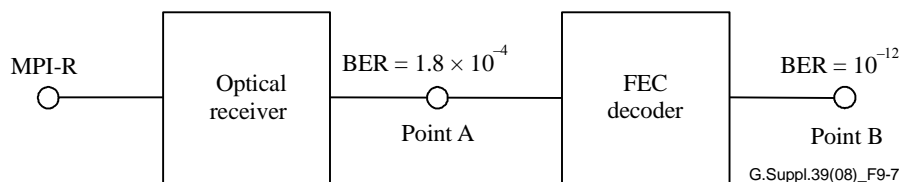
Figure 9-7 – Effect of usage of FEC on receiver performance in relation to the bit error ratio

In cases where it is not easy to apply FEC techniques to component verification, it may be much more practical and cost-effective to verify the performance of optical transmitter and receiver devices (intended for use in FEC-enabled applications) at bit error ratios appropriate to a FEC decoder input, rather than at 10^{-12} which would, in most cases, pose test criteria much more stringent than necessary for the application.

The appropriate BER to use for this purpose depends to some extent on the application because variations in the error statistics (away from the random error distribution assumed by the theory) will require the average BER at point A to be lower than 1.8×10^{-4} for an average BER of 10^{-12} at point B. For most practical purposes, however, a value in the range of 10^{-5} to 10^{-6} is considered appropriate.

Using this methodology, the values for receiver sensitivity and optical path penalty measured at the receiver output (point A) at a BER of 10^{-6} will normally be conservative estimates of the values for receiver sensitivity and path penalty at the BER of 10^{-12} after the FEC decoder (point B).

9.4.2 BER estimation from constellation

Digital signal processing (DSP) together with coherent detection is an increasingly popular technique for long-haul optical transmission systems. Coherent detection obtains full information of the optical field in both polarizations. Constellation diagrams before decision can reflect system performance. Pre-FEC BER estimation can use tail extrapolation which is based on a statistic analysis of the probability density function (pdf) from the constellation diagrams. With reference to [b-Jeruchim], the tail extrapolation technique is based on the assumption that the pdf in the tail region of the decision device input waveform is described by some member of a family of distributions that shall be referred to as the generalized exponential function (GEF) class, namely

$$f_v(x) = \frac{v}{2\sqrt{2}\sigma\Gamma(1/v)} \exp\left(-\left|\frac{x-\mu}{\sqrt{2}\sigma}\right|^v\right), \forall x \in R \tag{9-17}$$

where $\Gamma(\cdot)$ is the gamma function and μ is the mean value of the distribution, v is related to the distribution's variance V_v by $V_v = 2\sigma^2\Gamma(3/v)/\Gamma(1/v)$.

μ, v and σ can be derived from the constellation diagram data by a maximum likelihood estimation algorithm mathematically, then the pdf based on GEF is known from the following calculation:

The probability of error for one point in the constellation diagram is the pdf integration in the tail, and given by:

$$P_E = \int_S f(x)dx. \tag{9-17b}$$

Where t is referred to as the threshold and is the difference between the actual threshold and the mean value.

The symbol error ratio in the I/Q directions (for square mQAM modulation formats) or angle (for mPSK modulation formats) can be calculated for all points in the constellation diagram by the above equations. Then the symbol error ratio of mQAM modulation formats is calculated by $P_T = 1 - (1 - P_I)(1 - P_Q)$, where P_I and P_Q are the symbol error ratios for the I and Q directions respectively.

Considering the differential encoding penalty, bit error ratio can be calculated from symbol error ratio. Differential encoding may be used for phase ambiguity mitigation, but if so, two consecutive bits will be wrong if one bit is detected wrongly, so partial differential encoding may be preferred. For a detailed description of differential encoding penalty, see [b-Weber].

An example of BER estimation from a constellation is given in Figure 9-8. It is a result of coherent PM-QPSK after 16×80 km transmission. It shows the X polarization constellation diagram before symbol decision and its corresponding level -1 and level $+1$'s pdf for the I direction, Pre-FEC BER is estimated as 4.5×10^{-4}.
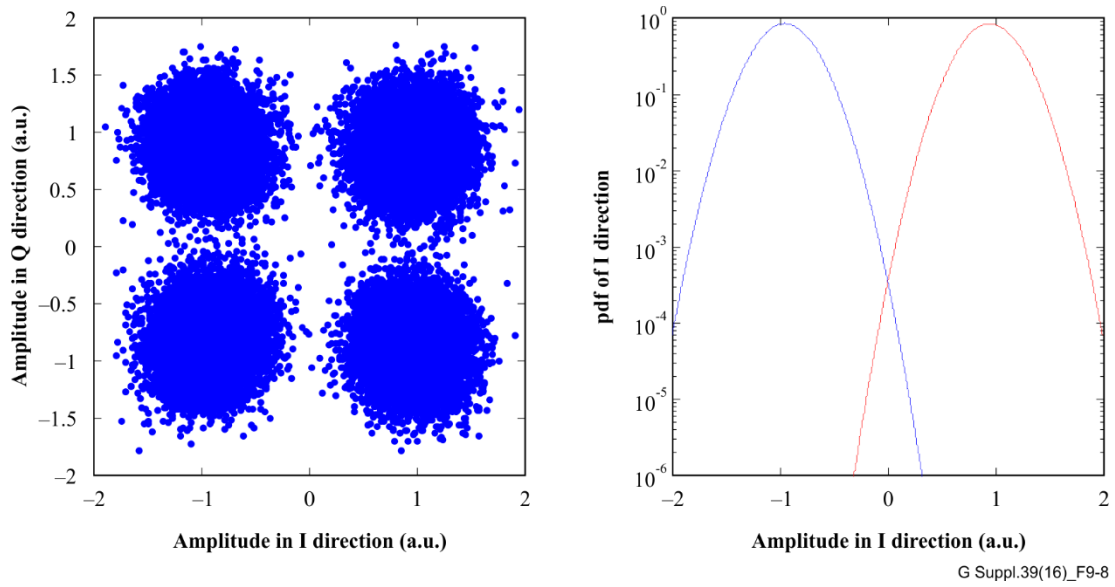
Figure 9-8 – An example constellation diagram and its pdf in the I direction

9.5 Noise concatenation

In a system with a cascaded optical amplifier chain, amplified spontaneous emission (ASE) noise accumulates from the contributions of all optical amplifiers. Therefore, the OSNR degrades after each optical amplifier. OSNR is useful for monitoring and characterizing optical amplifier performance. The equation of the worst-case OSNR estimation and the text are proposed as follows:

Figure 9-9 depicts a multichannel N span reference system with a booster amplifier, N−1 line amplifiers and a preamplifier. For this reference system, the following main assumptions are made:

– All optical amplifiers in the chain including booster and preamplifier have the same noise figure.

– The losses (per channel) of all spans are equal.

– The output powers (per channel) of the booster and line amps are the same.
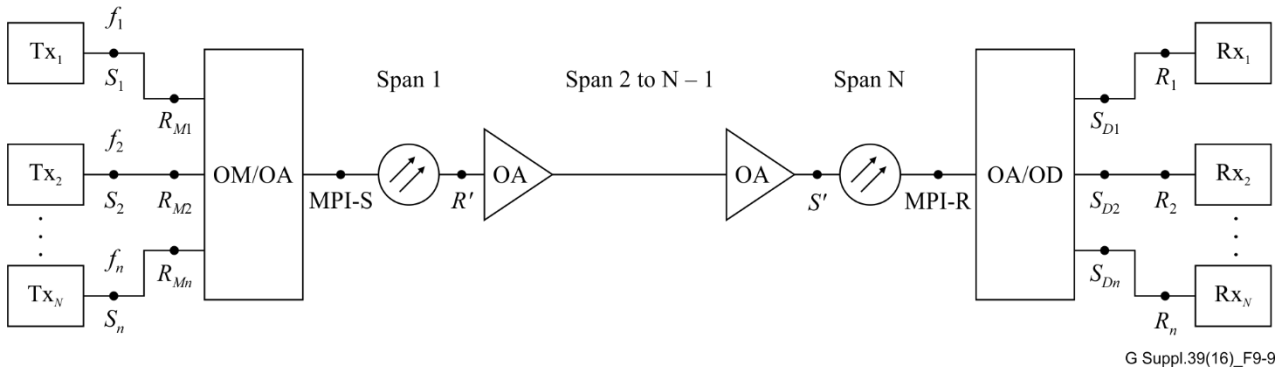
Figure 9-9 – Representation of optical line system interfaces (a multichannel N-span system)

In this case, the OSNR at the input of the receivers (point R_i in Figure 9-9, $i = 1, ... n$) can be approximated as:

$$OSNR = P_{out} - L - NF - 10\log\left(N + \frac{10^{\frac{G_{BA}}{10}}}{10^{\frac{L}{10}}}\right) - 10\log(h\nu\nu_r) \tag{9-18}$$

P_{out} is the output power (per channel) of the booster and line amplifiers in dBm, L is the span loss in dB (which is assumed to be equal to the gain of the line amplifiers), G_{BA} is the gain of the optical booster amplifier in dB, NF is the signal-spontaneous noise figure of the optical amplifier in dB, h is Planck's constant (in mJ·s to be consistent with P_{out} in dBm), v is the optical frequency in Hz, v_r is the reference bandwidth in Hz (corresponding to c/Br in clause 9.5.1), $N–1$ is the total number of line amplifiers.

Equation 9-18 indicates that the ASE noise is accumulated from all $N + 1$ amplifiers. It can be simplified in the following cases:

1)   If the gain of the booster amplifier is approximately the same as that of the line amplifiers, i.e., $G_{BA} \approx L$, Equation 9-18 can be simplified to:

$$OSNR = P_{out} - L - NF - 10\log(N+1) - 10\log(hvv_r)$$ (9-19)

2)   The ASE noise from the booster amplifier can be ignored only if the span loss L (resp. the gain of the line amplifier) is much greater than the booster gain G_{BA}. In this case Equation 9-19 can be simplified to:

$$OSNR = P_{out} - L - NF - 10\log(N) - 10\log(hvv_r)$$ (9-20)

NOTE – Equation I-3 of [ITU-T G.692] describes only a particular case.

3)   Equation 9-19 is also valid in the case of a single span with only a booster amplifier, e.g., short-haul multichannel IrDI in Figure 5-5 of [ITU-T G.959.1], in which case it can be modified to:

$$OSNR = P_{out} - G_{BA} - NF - 10\log(hvv_r)$$ (9-21)

4)   In case of a single span with only a preamplifier, Equation 9-19 can be modified to:

$$OSNR = P_{out} - L - NF - 10\log(hvv_r)$$ (9-22)

9.5.1   OSNR measurement

OSNR is usually expressed in a reference optical bandwidth of 0.1 nm and defined as shown in Equation 9-23:

$$OSNR = 10\log\frac{P_i}{N_i} + 10\log\frac{B_m}{B_r}$$ (9-23)

where:

P_i is the optical signal power in watts at the i-th channel

N_i is the amplified spontaneous emission (ASE) noise power in watts measured in noise equivalent bandwidth, B_m, at the i-th channel

B_r is the reference optical bandwidth. (The units for B_m and B_r may be in frequency or wavelength but must be consistent.) Typically, the reference optical bandwidth is 0.1 nm

If the interpolation method is used to measure the OSNR the noise power is determined as:

$$N_i = \left(\frac{N(v_i - \Delta v) + N(v_i + \Delta v)}{2} \right)$$

where Δv is the interpolation offset equal to one-half the channel spacing (for the case of 200 GHz channel spacing, $\Delta v = 100$ GHz). The commonly agreed evaluation procedure of OSNR from measurement data is shown in Figure 9-10. In order to achieve an accurate result, care must be taken to use a resolution bandwidth that is appropriate for the bit rate of the signals being measured, e.g., at 40 Gbit/s a minimum measurement resolution bandwidth of 1 nm is recommended.
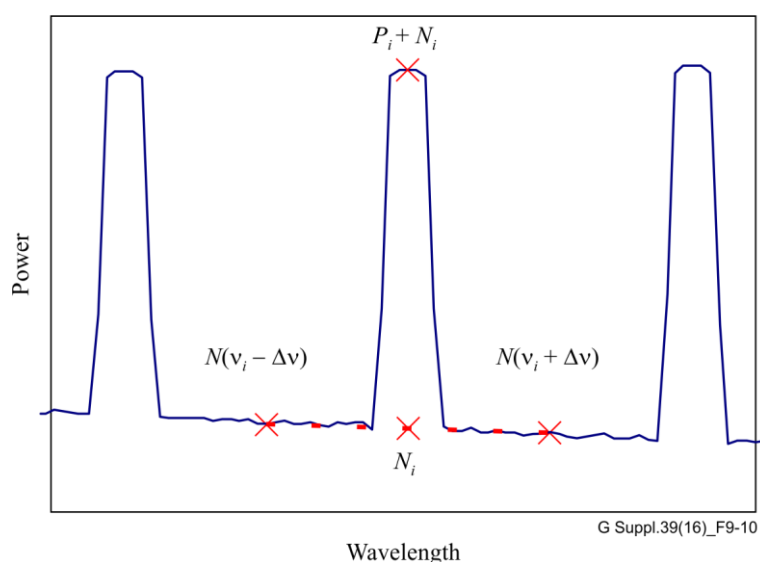
Figure 9-10 – OSNR measurement from the optical spectrum

It should also be noted that this method of evaluating OSNR can give inaccurate results in some circumstances. Figure 9-11 shows the case where the noise in between the channels has undergone filtering due to the presence of an OADM part-way along a link. Here, the interpolation of noise measurements in the gaps between channels does not give a valid estimate of the noise at the signal wavelength.
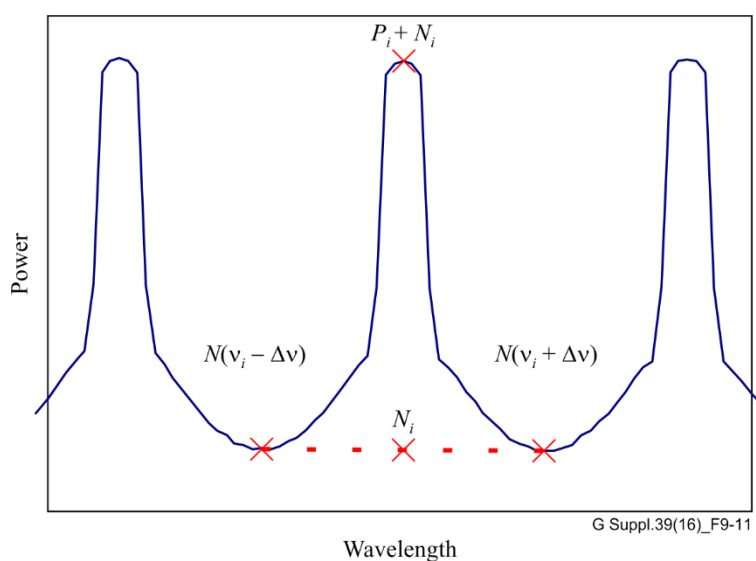
Figure 9-11 – Inaccurate OSNR measurement due to noise shaping

For an accurate OSNR measurement in the presence of noise shaping, it is essential to measure the filtered noise value in the passband of the optical filters in a system (often called 'in-band' OSNR measurement). Three in-band OSNR measurement methods for use in the presence of noise shaping are discussed in [ITU-T G.697].

A similar problem can occur in systems with high bit-rate channels on a close channel spacing where the skirts of the signal peaks do not reach the true noise level at the midpoint between the channels as shown in Figure 9-12. The in-band OSNR measurement method for use in the presence of close channel signal overlap is for further study.

P + N_i

N_i(ν − Δν)   N_i(ν + Δν)
            N_i

G Suppl.39(16)_F9-12

Power

Wavelength
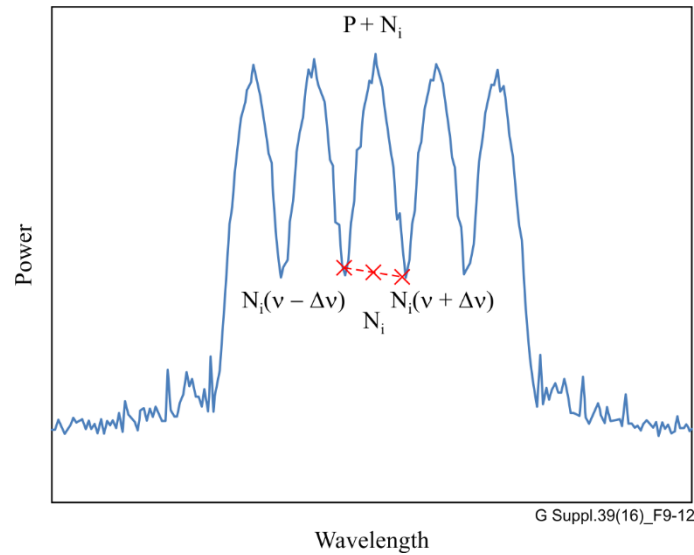
Figure 9-12 – Inaccurate OSNR measurement due to close channel overlapping

9.5.2 OSNR and received optical power for single span preamplified systems

The OSNR degradation by ASE of a system with one span and one optical preamplifier is described by Equation 9-24:

$$OSNR = P_{out} - L - NF - 10\log(h\nu\nu_r) \tag{9-24}$$

applying: $P_{received} = P_{out} - L$ and $-10\log(h\nu\nu_r) = +58$ dB at 0.1-nm resolution bandwidth and at wavelength of 1550 nm, Equation 9-24 has the form:

$$OSNR = P_{received} - NF + 58 \text{ dB} \tag{9-25}$$

Equation 9-25 is valid for 1 span and for back-to-back measurements with an optical preamplifier. The signal input power ($P_{received}$) at the input of the preamplifier and the OSNR at the output of the preamplifier are in strong linear correlation via the noise figure NF of the preamplifier.

As depicted in Figure 9-13, the OSNR can be varied by attenuating the signal input power ($P_{received}$) to the optical preamplifier (EDFA), using a high OSNR (> 40 dB) signal source. The OSNR is measured directly after the EDFA. A linear correlation with respect to received optical power is expected according to Equation 9-23.

Signal → | Attenuator | → | EDFA | → | Channel filter | → Signal + noise

$P_{received}$ $OSNR$ G Supp.39(16)_F9-13
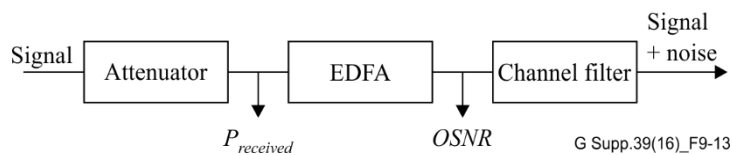
Figure 9-13 – Set-up for OSNR measurement

Figure 9-14 shows an example of OSNR versus received optical power over a wide range using a 43 Gbit/s NRZ modulated channel at 1550 nm, using 1-nm resolution bandwidth on the optical spectrum analyser. If the measured power at the channel wavelength is P_m ($P_m = P_i + N_i$), then it can be estimated that the value of OSNR by calculating $OSNR = 10\log\dfrac{P_m}{N_i} + 10\log\dfrac{B_m}{B_r}$. For OSNR values below about 20 dB, however, this leads to an overestimate as shown on the curve "n_uncor" in Figure 9-13, so a better procedure is to calculate $OSNR = 10\log\dfrac{P_m - N_i}{N_i} + 10\log\dfrac{B_m}{B_r}$, which gives the linear relationship labelled "n_cor" as expected from Equation 9-24. This linear relationship relies

on the noise figure of the amplifier being constant, so it will no longer be valid if the input power becomes high enough to cause saturation.
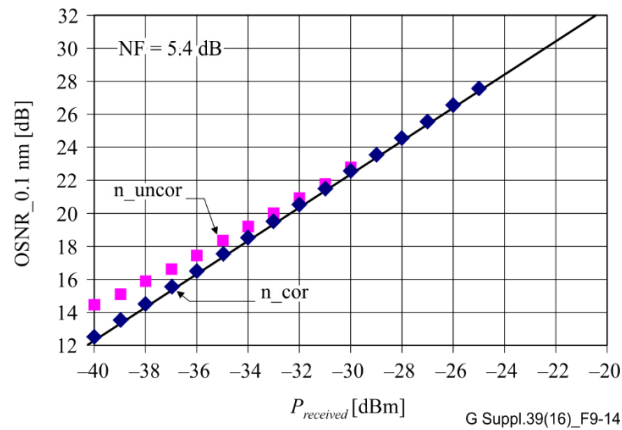
Figure 9-14 – OSNR versus received optical power measurement: with noise correction (n_cor) and without noise correction (n_uncor) at the signal channel wavelength

In summary, for the case of single span transmission and back-to-back system tests with an optical preamplifier, a linear correlation of OSNR and received optical power is obtained. Thus, any path penalty due to eye-closure is directly related to the OSNR penalty in a preamplified receiver.

NOTE 1 – Power penalty and OSNR penalty are different for long-haul multiple span (OSNR limited) transmission systems.

NOTE 2 – As shown in Figure 9-15, power penalties are different for preamplified and non-preamplified receivers as the slope of the BER versus received optical power is different. A 1 dB penalty in a non-preamplified receiver is equivalent to a 2 dB OSNR penalty in a preamplified receiver.
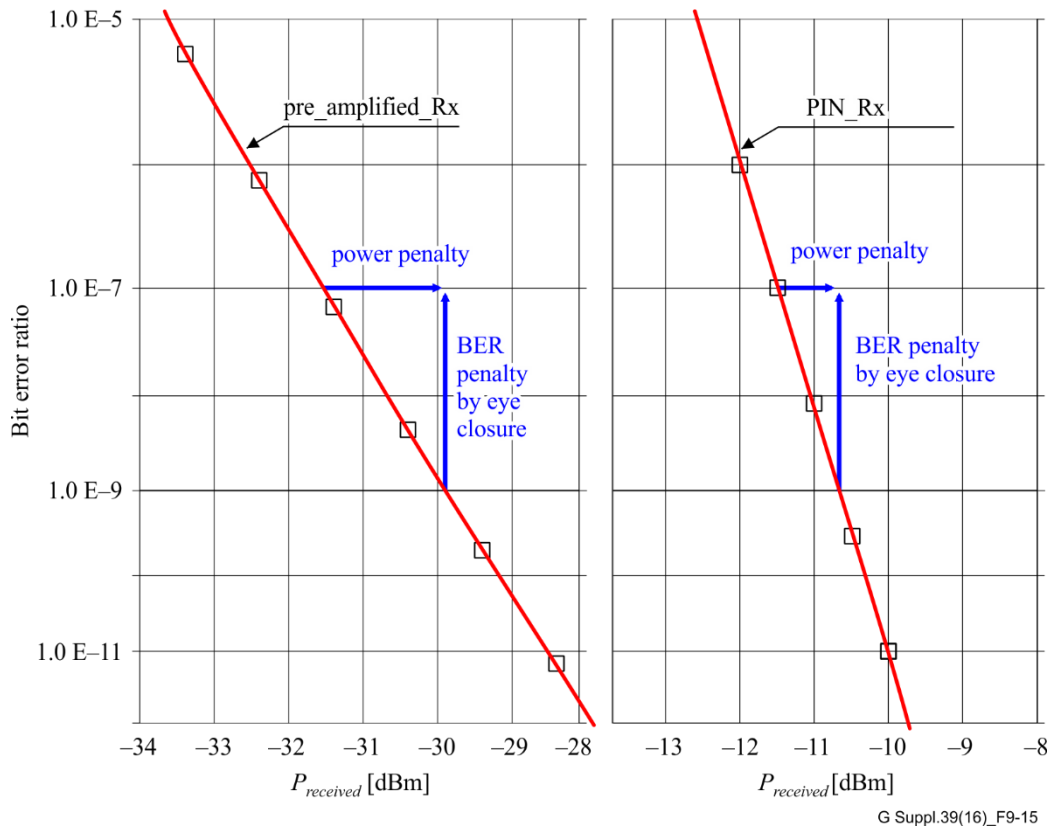
Figure 9-15 – BER versus received power with and without an optical preamplifier

9.6 Optical crosstalk

9.6.1 Definition of terms

Since the terms used to describe optical crosstalk and its effects are not entirely consistent across the industry, it is useful to briefly define them here (see Table 9-6). Within ITU-T Study Group 15, there is a convention that the term "crosstalk" is reserved for the description of system effects and that the properties of components use the term "isolation".

Table 9-6 – Terms used

Parameter [unit]	Symbol	Defined in Rec. ITU-T	Definition
System parameters			
Inter-channel crosstalk [dB]	C_C	G.698.1	Ratio of total power in the disturbing channels to that in the wanted channel. (Wanted and disturbing channels at different wavelengths (k total))
Interferometric crosstalk [dB]	C_I	G.698.1	Ratio of the disturbing power (not including ASE) to the wanted power within a single channel (wavelength). This parameter is also known as "Intra-channel crosstalk"
Inter-channel crosstalk penalty [dB]	P_C	–	Penalty assigned in the system budget to account for inter-channel crosstalk
Interferometric crosstalk penalty [dB]	P_I	–	Penalty assigned in the system budget to account for interferometric crosstalk
Channel power difference [dB]	d	G.959.1	The maximum allowable power difference between channels entering a device
Extinction ratio (linear used here)	r	G.691	Ratio of power at the centre of a logical "1" to the power at the centre of a logical "0"
Eye-closure penalty [dB]	E		Receiver sensitivity penalty due to all eye-closure effects. This includes transmitter eye-closure and chromatic dispersion penalty
Component parameters			
Insertion loss [dB]	IL	G.671	The reduction in power from input to output port at the wanted channel wavelength
Unidirectional isolation [dB]	I	G.671	The difference between the device loss at a disturbing channel wavelength and the loss at the wanted channel wavelength
Adjacent channel isolation [dB]	I_A	G.671	The isolation of the device at the wavelengths one channel above and below the wanted channel
Non-adjacent channel isolation [dB]	I_{NA}	G.671	The isolation of the device at the wavelengths of all disturbing channels except for the adjacent channels

The consideration of crosstalk effects is divided into two categories: inter-channel and interferometric.

9.6.2 Inter-channel crosstalk

The most commonly considered cause of this effect is imperfect demultiplexing of a multichannel transmission signal into its individual channels prior to a set of single-channel receivers. This situation is depicted in Figure 9-16.
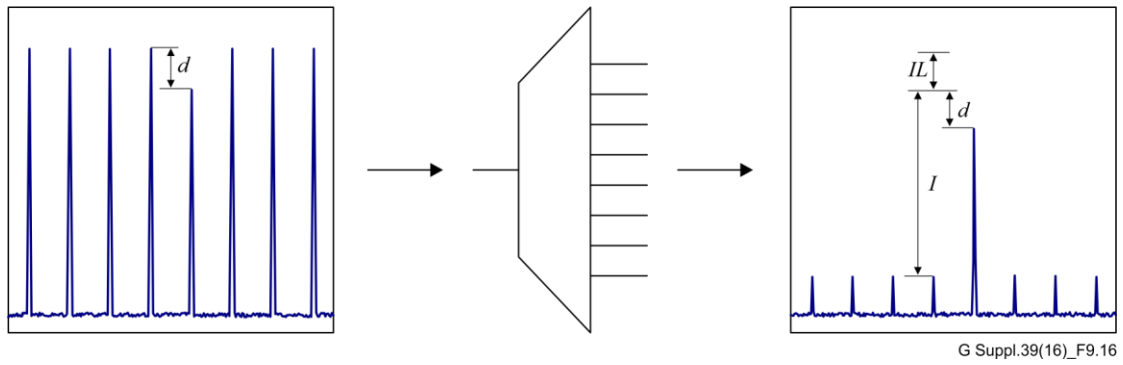
Figure 9-16 – Simple demultiplexer example

Here, a number of DWDM channels enter the common port of a demultiplexer. The worst case for any particular channel is for its power to be at the minimum and that of all of the other channels to be at the maximum. The maximum allowable difference between channels has been denoted as d (dB). When the channels emerge from the individual output ports, the disturbing channels have been attenuated with respect to the wanted channel by an amount equal to the unidirectional isolation I (dB).

The main parameter that governs the maximum level of optical crosstalk that can be tolerated in any given optical system is the inter-channel crosstalk penalty P_C. From this, and a small number of other parameters, it is necessary to be able to obtain the required isolation parameters of the demultiplexer.

In the situation shown by Figure 9-16, an equation can be written for the inter-channel crosstalk of a k channel system C_C:

$$C_C = d - I + 10\log_{10}(k-1) \qquad \text{dB} \qquad (9\text{-}26)$$

It is desirable to be able to derive the required value of C_C from the value of the inter-channel crosstalk penalty. If one assumes a very large number of equal amplitude interfering signals as above, then relatively simple models can be generated to do this. In practical demultiplexers, the isolation value given for the channels immediately adjacent to the wanted channel I_A is smaller than the isolation of the non-adjacent disturbing channels I_{NA}. Taking account of this, the situation changes to that illustrated in Figure 9-17.
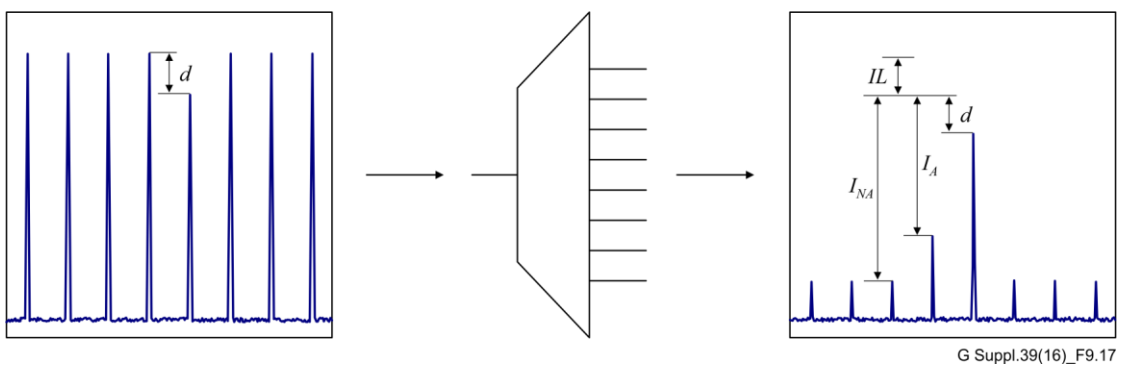
Figure 9-17 – More realistic demultiplexer example

The equation for the inter-channel crosstalk C_C then becomes:

$$C_C = d + 10\log_{10}\left(2 \times 10^{\frac{-I_A}{10}} + (k-3)10^{\frac{-I_{NA}}{10}} \right) \qquad \text{dB} \qquad (9\text{-}27)$$

In this situation, however, different values of I_A and I_{NA} can give systems with different inter-channel crosstalk penalties P_C that have the same total C_C value.

The equations for the two limiting cases are given below.

For a single disturbing channel:

$$P_C = 10\log_{10}\left(1 - 10^{\frac{C_C}{10}}\frac{r+1}{r-1}\right) \qquad \text{dB} \qquad (9\text{-}28)$$

where r is the linear extinction ratio.

NOTE 1 – This equation does not directly include the effect of any reduction in eye opening due to transmitter eye closure or path penalty. These effects can, however, be included by calculating an effective value of r (denoted r') that takes both extinction ratio and eye closure into account.

$$r' = \frac{(r+1) + 10^{\frac{-E}{10}}(r-1)}{(r+1) - 10^{\frac{-E}{10}}(r-1)} \qquad (9\text{-}29)$$

where E is the eye closure penalty in dB. As an example, if the extinction ratio is 6 dB, then $r = 3.98$. To account for eye closure penalty of a further 3 dB set $r' = 1.86$.

For a very large number of equal amplitude disturbing channels (with uncorrelated data), the inter-channel crosstalk becomes noise-like and a Gaussian approximation can be assumed. In this case, the noise-like crosstalk must be convolved with the noise distribution of the receiver (or ASE) to produce an effective penalty. By following the methods in [b-Takahashi] and [b-Liu] and using a Gaussian approximation to the binomial distribution, the equation becomes:

$$P_C = -5\log_{10}\left(1 - \frac{10^{\frac{2C_C}{10}}}{k-1}Q^2\left(\frac{r+1}{r-1}\right)^2\right) \qquad (9\text{-}30)$$

where $Q = \sqrt{2}\,\text{erfc}^{-1}(2 \times BER)$. For a BER of 10^{-12}, $Q \approx 7.03$.

The induced optical penalty is plotted against inter-channel crosstalk for a variety of assumptions in Figure 9-18. The actual penalty incurred in a practical system lies somewhere below the highest curve.

NOTE 2 – The crosstalk penalty may also be dependent on the line code (RZ or NRZ) and the relative bit rates of the wanted and interfering signals.
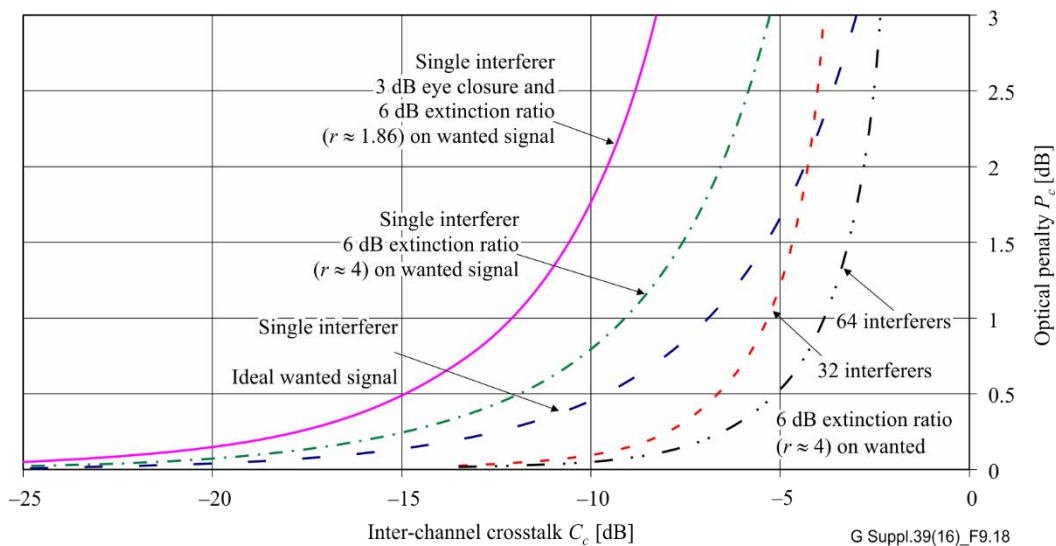
Figure 9-18 – Graph of optical penalty versus inter-channel crosstalk

The procedure for determining the required isolation might then be:

–   From system parameters, establish a value for P_C which may be different for different systems. A short reach system might assign a higher crosstalk penalty than a long reach one, for example. For the purposes of illustration, choose 0.5 dB.

–   Derive a value for C_C from P_C. The model required is somewhere between that of two interfering signals when there is a very large difference between I_A and I_{NA} through to a Gaussian model when I_A equals I_{NA} and k is large. Choosing the worst example curve on Figure 9-18 gives a value of -15 dB.

–   From system parameters, establish a value for d, which again will be different from system to system. In [ITU-T G.959.1], for example, the application code P16S1-1D2 has $d = 6$ dB while P16S1-2C2 has $d = 2$ dB. (This leads to a 4 dB difference in required isolation between these applications.) So for P16S1-1D2, set $d = 6$ dB. (Also, for this application, $k = 16$.)

–   Substituting these values into the simple equation $C_C = d - I + 10 \log_{10}(k - 1)$ gives $-15 = 6 - I + 10\log_{10}(15)$ which leads to a value of $I = 32.8$ dB for this example.

9.6.3   Interferometric crosstalk

Interferometric crosstalk occurs when the disturbing channel and the wanted channel are at the same nominal wavelengths. Four examples of this are:

–   in an optical add-drop multiplexer where the wavelength in question is incompletely dropped before the new signal is added;

–   in an optical multiplexer where one transmitter may be emitting power at the wavelength of another channel (e.g., due to inadequate sidemode suppression ratio), this is termed transmit-side crosstalk in [ITU-T G.692];

–   in an optical cross-connect where lack of sufficient switch isolation causes light from more than one source fibre to reach the receiver;

–   in any component or group of components where there is more than one path that the light can take to reach the receiver. This is called multi-path interference (MPI).

Interferometric crosstalk behaves differently from inter-channel crosstalk when the two optical signals are sufficiently close together that their beat frequency is within the electrical bandwidth of the receiver. In this case, it is the optical fields which interact to produce the crosstalk instead of the

optical powers and, consequently, the levels of crosstalk required to produce a particular penalty are much smaller.

For a single interferer, the crosstalk can be modelled as having a bounded probability density function (pdf). The crosstalk penalty from [b-Legg] (and including the effect of imperfect extinction ratio) for an average power decision threshold is:

$$P_I = 10 \log_{10} \left(\frac{\dfrac{r-1}{r+1}}{\dfrac{r-1}{r+1} + 10^{\frac{C_I}{10}} - 4\sqrt{\dfrac{r}{r+1}} \, 10^{\frac{C_I}{10}}} \right) \quad \text{dB} \tag{9-31}$$

and for an optimized decision threshold is:

$$P_I = -10 \log_{10} \left(1 - 2 \left(\frac{(1+\sqrt{r})\sqrt{10^{\frac{C_I}{10}}(r+1)}}{r-1} \right) \right) \quad \text{dB} \tag{9-32}$$

The interferometric crosstalk penalty for a wanted signal with 6 dB extinction ratio is plotted in Figure 9-18.
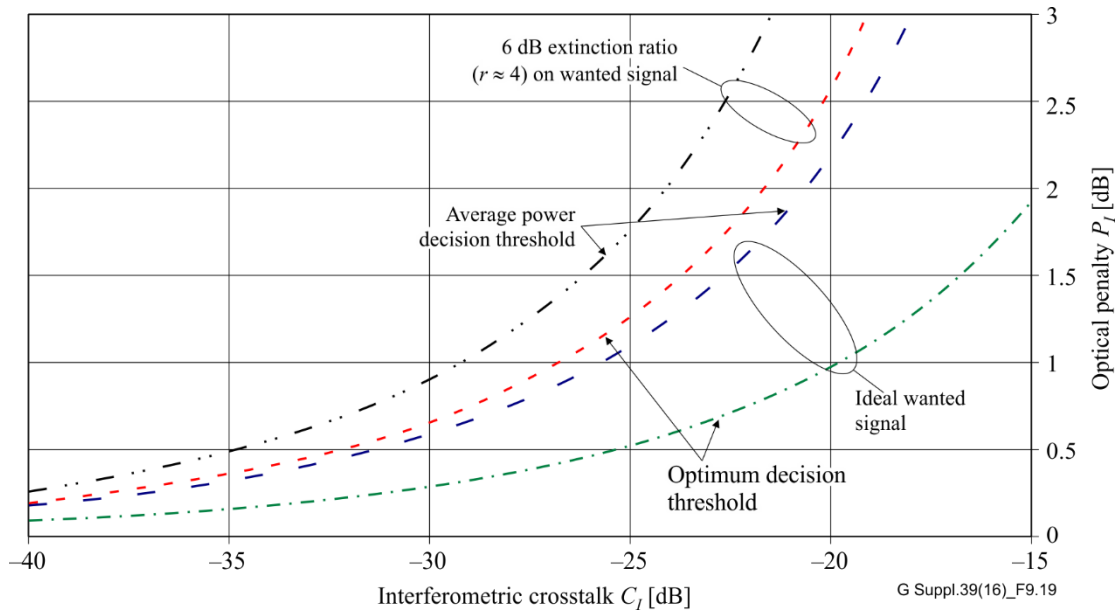
Figure 9-19 – Graph of optical penalty versus interferometric crosstalk for a single interferer (bounded model)

For multiple interferers, the pdf becomes approximately Gaussian and for a P type-intrinsic-n type (PIN) receiver the optical crosstalk penalty from [b-Liu] is:

$$P_I = -5 \log_{10} \left(1 - 4 \times 10^{\frac{C_I}{10}} Q'^2 \frac{1+\dfrac{1}{r}}{\left(1-\dfrac{1}{r}\right)^2} \right) \quad \text{dB} \tag{9-33}$$

for an average power decision threshold:

$$P_I = -5\log_{10}\left(1 - 2\times10^{\frac{C_I}{10}}Q'^2\left(\frac{r+1}{r-1}\right)^2 + \left(10^{\frac{C_I}{10}}\right)^2 Q'^4\left(\frac{r+1}{r-1}\right)^2\right) \qquad \text{dB} \qquad (9\text{-}34)$$

for an optimized decision threshold, where $Q' = \sqrt{2}\,\text{erfc}^{-1}(4 \times BER)$ and $Q = \sqrt{2}\,\text{erfc}^{-1}(2 \times BER)$. For a BER of 10^{-12}, $Q' \approx 6.94$ and $Q \approx 7.03$.

These functions are plotted in Figure 9-20 for an ideal wanted signal and also for a signal with 6 dB extinction ratio.
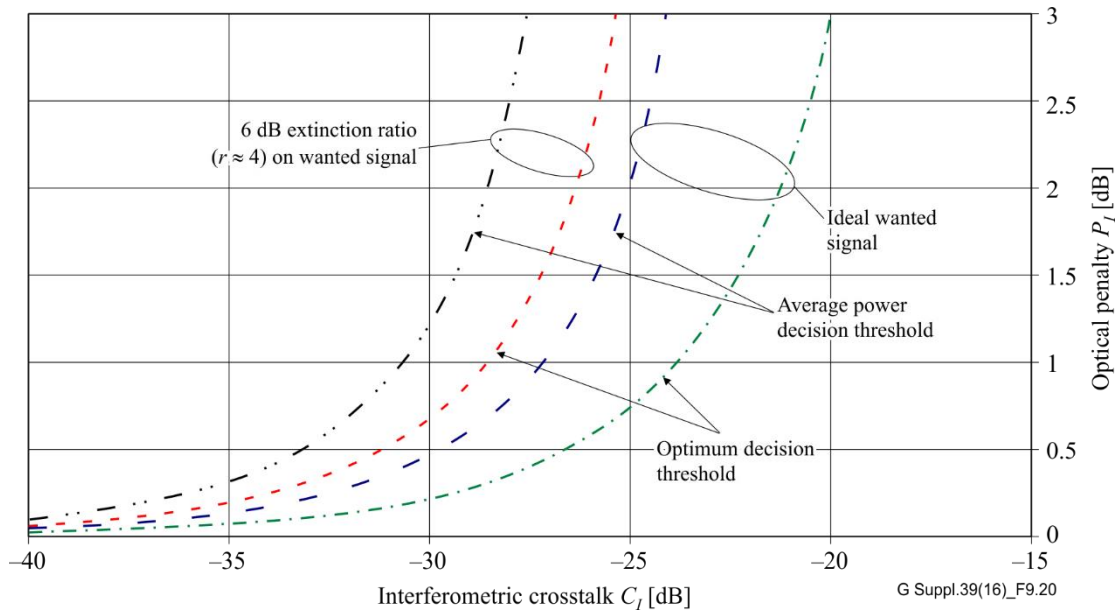
Figure 9-20 – Graph of optical penalty versus interferometric crosstalk for multiple interferers (Gaussian model)

9.7 Concatenation of non-linear effects – Computational approach

9.7.1 Influence of non-linear effects

A multi-span high-speed transmission system with complete dispersion compensation is affected by non-linear optical phenomena, particularly SPM in single-channel systems, cross-phase modulation (XPM) and four-wave mixing (FWM) in multichannel systems. These non-linear phenomena are due to the fibre Kerr effect and their influence increases with the optical input power. As a consequence, the system performance can be strongly degraded by such non-linear effects, if the fibre input optical power is very high.

The system performance is also degraded at low fibre optical input power due to the low optical signal-to-noise ratio at the receiver. Therefore, there exist a maximum and a minimum input power threshold corresponding to a certain system performance (Q factor, BER, etc.) penalty. Suggestions on the minimum input power threshold can be found in clause 9.5 (Noise concatenation).

9.7.2 Dispersion management

With the implementation of long-haul DWDM transmission system, the consideration of non-linear effects in the transmission fibre has been a major issue at the optimization of transmission distances and margins of DWDM systems. The performance of DWDM long-haul transmission systems is ensured by thoroughly performed system design usually called dispersion management. By deliberate choice of pre-, in-line, post-dispersion compensation and path average dispersion, non-linear effects, e.g., self-phase modulation (SPM) and cross-phase modulation (XPM) can be mitigated in order to

optimize the fibre input power values of the DWDM channels and to maximize the transmission distance (number of fibre spans).

Dispersion management is performed by simulations, by using the Split-Step Fourier method solving numerically the non-linear Schrödinger equation which describes the propagation of the optical data pulses in a transmission fibre. Due to the complexity and impairments of non-linear effects of transmission fibres, which can depend on the transmission bit-rate, the modulation format, channel spacing, etc., until today, no simple analytical model has been proposed that could be included in this Supplement.

9.7.3 Simulation example

9.7.3.1 Computational approach

In the following, the influence of non-linear effects such as self-phase modulation (SPM), cross-phase modulation (XPM) and four-wave mixing (FWM) on $N \times 40$ Gbit/s systems is evaluated. These effects are evaluated by means of simulations for different values of input average optical power to establish the per channel power (non-linear threshold (NLT) power) that produces a 1 dB OSNR penalty at a BER of 10^{-4} with pseudo-random bit sequence (PRBS) 2^9-1 for the middle channel when only 43 Gbit/s channels with the same modulation format are present.

Furthermore, as fibre non-linear effects accumulate with the number of fibre spans, the non-linear threshold (NLT) parameter can be represented by a transmission span no. independent parameter [b-Färbert] given by the integrated power product value (IPP = (NLT_at given span no.) $\times$ (no. of spans)).

9.7.3.2 Simulation parameters

Table 9-7 shows the parameters that have been applied for the simulations.

Table 9-7 – Parameters applied the simulation

Channel bit rate	43.018 Gbit/s
Pseudo random bit sequence	2^9-1
Number of channels	5
Channel spacing	100 GHz or 50 GHz
Frequency of middle channel	193.1 THz
Fibre type	ITU-T G.652
Number of spans	6
Span length	80 km
Span attenuation	22 dB
Non-linear coefficient of fibre (n2 /Aeff):	3.0×10^{-10}/W

The typical dispersion of ITU-T G.652 fibre had been considered, and the dispersion map (pre-dispersion, in-line dispersion and post-dispersion) had been optimized for each modulation format. Non-linear effects at dispersion compensators had not been considered. The channel spacings are 100 GHz and 50 GHz for modulation formats supporting 100 GHz and 50 GHz, respectively. The ASE to adjust the OSNR had only been added in front of the receiver (optical amplifiers are without noise). The applied ASE noise filter shape had been equivalent to the shape of the filter in Figure II.6 of [b-ITU-T G.680] and the noise filter bandwidth was 1.4 times the bandwidth that gives up 2 dB OSNR penalty for each format. The per channel power values launched into the fibre spans were equal for all channels and after each optical amplifier. Finally, all channels have the same polarization throughout the link.

9.7.3.3   Simulation results

Table 9-8 summarizes the simulated integrated power product (IPP) values of 5 different 40 Gbit/s modulation formats based on the applied parameters of Table 9-7 and compares with experimentally obtained NLT values [b-Färbert], [b-Klekamp] scaled to IPP values, indicating that the simulated values are up to 1 dB more optimistic.

Table 9-8 – Summary of integrated power product values for 40 Gbit/s modulation formats, obtained by simulations (sim) and experimental measurements (exp) [b-Klekamp], [b-Charlet]

		NRZ	NRZ-DPSK	RZ-DPSK	ODB/PSBT	RZ-DQPSK	P-DPSK
		100 GHz channel spacing			50 GHz channel spacing		
IPP (sim)	dBm	12.3	15.5	17.2	14	13.1	
IPP (exp)	dBm	12.2	14.6	16.5		12	13

9.7.4   Extremes between linear and non-linear transmission

9.7.4.1   Examination with one span transmission example

In contrast to a purely linear transmission case, the optimum non-linear transmission case takes full advantage of the mitigation of non-linear Kerr effects, e.g., SPM, by suitable engineering the link dispersion by deliberate dispersion management. This is achieved by the numerical simulation via the Split-Step Fourier method prior to the installation of the link by the systems provider.

Based on the assumption of the "integrated power" behaviour, the feasible "NLT limits" of long-haul transmission over a high number of spans can be estimated via "NLT limits" obtained at transmission over lower span numbers. These limits estimations can be scaled down to simple 1 span measurement results [b-Färbert], [b-Klekamp], providing information to distinguish between linear and a non-linear transmission cases.

Measurements with NRZ 40 Gbit/s modulation format with a single channel over one span of ITU-T G.652 fibre show a non-linear threshold fibre input power at 1 dB OSNR penalty (NLT) under optimum pre-compensation of about 12.5 dBm. Figure 9-21 displays OSNR penalty data versus fibre input power showing that with optimum negative pre-compensation, a maximum NLT value can be obtained. On the other hand, looking at a linear fibre input power that is resulting in low transmission penalty of, e.g., 0.1..0.2 dB without applying any pre-dispersion optimization would be only about 5 dBm.
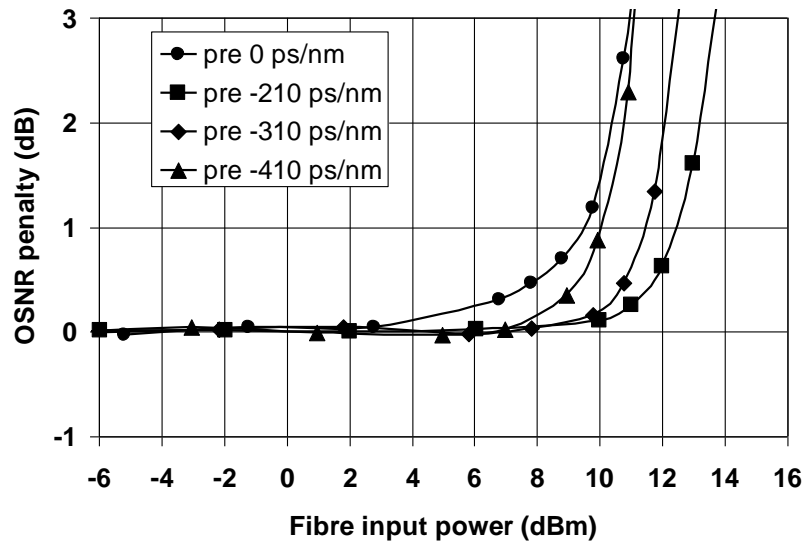
Figure 9-21 – OSNR penalty versus fibre input power for one span of ITU-T G.652 fibre with different pre-compensation values; the NLT is the power value at 1 dB of OSNR penalty

If additionally the post-compensation will be also optimized, the NLT can be increased furthermore as depicted by Figure 9-22. A maximum NLT of 15 dBm is obtained with pre-compensation of −210 ps/nm together with residual-compensation of 65 ps/nm, as shown by the curve with circles of Figure 9-22. In a real system, adaptive post-compensation will ensure low OSNR penalty for channels operating at the NLT limits. Thus, up to 10 dB higher fibre input power can be obtained by suitable optimization of pre-dispersion and (adaptive) post-dispersion compensation at the receiver end.
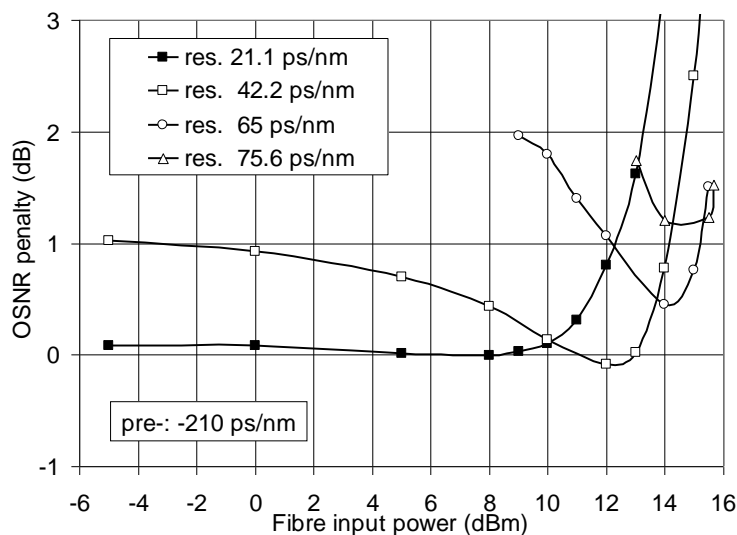
Figure 9-22 – OSNR penalty versus fibre input power for one span of ITU-T G.652 fibre with pre-compensation of −210 ps/nm and various post compensation values

9.7.4.2 OSNR simulations at multiple spans transmission

Considering the single span example for the NRZ 40 Gbit/s modulation format, the IPP values are 15 dBm and 5 dBm at the non-linear and linear transmission cases, respectively. E.g., considering 5, 10 or 20 spans transmission at the non-linear transmission case, $P_{fibre-max}$ values are 8, 5 or 2 dBm, respectively.

Applying the standard OSNR calculation (Equation 9-20) with constant span loss (22 dB) and noise figure (6.5 dB) of the in-line amplifiers together with integrated power product values of 5 dBm and 15 dBm, respectively, the OSNR behaviour in Figure 9-23 is obtained versus number of spans for the extremes of linear transmission and non-linear transmission cases.
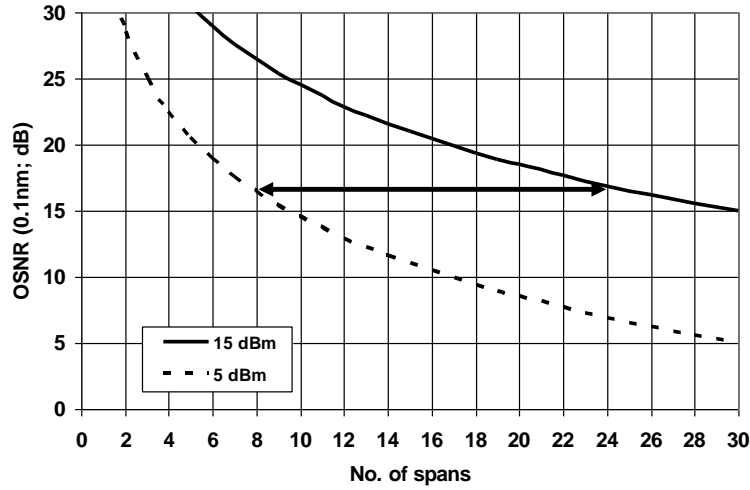

Figure 9-23 – OSNR versus number of spans considering IPP of 15 dBm and 5 dBm

Generally a three times longer transmission distance can be obtained between these examples of linear and non-linear transmission limits. E.g., looking at an OSNR sensitivity of 17 dB (enhanced FEC threshold considered in Appendix I of [b-ITU-T G.696.1]) up to eight spans can be transmitted under a linear transmission case while up to 24 spans can be transmitted under the optimum non-linear case.

9.7.5 Estimation of system non-linear effects using non-linear phase shift

Non-linear threshold (NLT) values for any one modulation format can be significantly different for different fibre types, depending on the fibre non-linear refractive index (n_2), the fibre effective area (A_{eff}) and the fibre span non-linear effective length ($L_{eff} = (1-e^{-\alpha L})\alpha$, where α is the absorption coefficient of the fibre with length L.

If different fibre types are included in a transmission system, for example, an ITU-T G.652 fibre for the transmission line and a dispersion-compensating fibre (DCF) for in-line dispersion compensation after each span, the non-linear phase shift (θ_{NL}) parameter has been derived [b-Antona] as a criterion for performance assessment of all of the fibre types of the transmission system. It has been shown [b-Antona], that the IPP (no. of spans × NLT) should be weighted by the non-linear coefficient ($\gamma = n_2/A_{eff}$) and the effective length L_{eff} of the fibre type. Considering fibre launch input power P_i, transmission over ITU-T G.652 fibre and DCF applied after each line span (of which there are N), the accumulated non-linear phase shift is given by:

$$\Phi_{NL} = \frac{2\pi}{\lambda} \sum_{i=1}^{N} (P_i \frac{n_2}{A_{eff}} \frac{1-e^{-\alpha L_i}}{\alpha})_{G.652} + (P_i \frac{n_2}{A_{eff}} \frac{1-e^{-\alpha L_i}}{\alpha})_{DCF}$$

$$\Phi_{NL} = \frac{2\pi}{\lambda} \sum_{i=1}^{N} (P_i \gamma L_{eff})_{G.652} + (P_i \gamma L_{eff})_{DCF}$$

DCF has significantly smaller effective area A_{eff} and roughly comparable non-linear refractive index n_2. If the input power values P_i into ITU-T G.652 fibre and into DCF were comparable, then the DCF would provide the dominant non-linear phase shift contribution. Since the DCF contribution to non-linear phase shift should be small compared to the ITU-T G.652 fibre contribution, it is common for implementations of in-line DCF modules to have P_i values launched into the DCFs that are much smaller than the P_i values launched into the ITU-T G.652 fibres.

A critical accumulated non-linear phase shift value is about 0.2π rad that would correspond with a system penalty of 1 dB [b-Antona]. The non-linear phase shift takes into account SPM, XPM and cross-polarization phase modulation effects but not FWM effects.

10 Statistical system design

10.1 Generic methodology

For a system with a small number of components, deterministic (or "worst case") design is useful, providing reasonable margins to the system. However, for a system with a large number of components, for example, a multi-span, and multichannel system, the margins obtained from deterministic designs may become unreasonably large. In that situation, network operators, as well as manufacturers, should consider the use of statistical design.

System parameters (e.g., maximum attenuation or maximum chromatic dispersion of the link, etc.) are distinguished from element parameters (e.g., attenuation coefficient or dispersion coefficient of fibre bobbin product, etc.). System parameters are to be determined by the system design in which statistical properties of the element parameters are considered. Examples of the relationship between system and element parameters are shown in Table 10-1.

Table 10-1 – Relationship between system and element parameters

System parameter	Element parameter	Described in
Maximum attenuation	Fibre cable attenuation coefficient, transmitter output power, receiver sensitivity, power penalty, splice loss, connector loss	10.2 Statistical design of loss
Maximum chromatic dispersion	Fibre dispersion coefficient, transmitter spectral width	10.3 Statistical design of chromatic dispersion
Maximum DGD	Cable PMD coefficient, power division between principal states of polarization, other elements in the link	10.4 Statistical design of polarization-mode dispersion
Maximum output power	Cable attenuation coefficient, fibre zero-dispersion wavelength, fibre effective area, fibre non-linear coefficient, channel spacing	For further study

In the current edition of this Supplement, however, it is proposed that only one system parameter in any particular system should be considered statistically. For example, in dispersion-limited systems, maximum chromatic dispersion is statistically considered, while the other system parameters are treated using the ordinary worst-case design approach. Statistical consideration of multiple system parameters is left for future work.

10.1.1 System outage probability

System outage probability is usually defined as the probability of BER exceeding 10^{-12} [b-Bulow]. However, since BER depends on many parameters (e.g., transmitter and receiver characteristics), it is difficult to refer to BER in generic statistical design. This clause, therefore, proposes to consider "system significance level" rather than "system outage probability", and to not refer to BER. Significance level is commonly used terminology in statistics for testing hypotheses [b-Maksoudian].

Regarding each system parameter, system significance level is defined as the probability at which the system parameter will exceed a certain value x. Of course, system significance level is a function of x. For instance, system significance level of DGD is 4.2×10^{-5}, when x equals three times the average DGD value (see [ITU-T G.691]). As another example, system significance level of maximum chromatic dispersion is 1.3×10^{-3}, when x equals the summation of the average value and 3σ (σ is standard deviation) [b-IEC SC86C].

10.1.2 Probability threshold for system acceptance

Probability threshold for system acceptance (P_{th}) is defined as maximum affordable significance level of each system parameter. The probability threshold will depend on network operation scenario, and also the trade-off relationship between probability of exceeding the value and cost.

It should be noted that for some parameters considered here, P_{th} refers to the probability that the value is exceeded at the time the link is commissioned. For example, in the case of chromatic dispersion, a P_{th} value of 10^{-3} means it is expected that, on average, one in a thousand links will exceed the specified dispersion when commissioned. For other parameters, however, P_{th} refers to the probability that the value is exceeded at any particular time in the life of a link. An example of this is PMD where a P_{th} of 10^{-5} means that, at any instant, the probability of exceeding the maximum DGD is one in one hundred thousand.

Table 10-2 contains some example values of P_{th} together with the equivalent values of the number of standard deviations away from the mean for Gaussian statistics and the equivalent maximum to mean ratio for the Maxwell distribution (PMD).

Table 10-2 – Probability threshold for system acceptance

Probability threshold, P_{th}	Gaussian: Standard deviations away from the mean [σ]	Maxwell: Ratio of maximum to mean [S]
10^{-3}	3.1	2.5
10^{-5}	4.3	3.2
10^{-7}	5.2	3.7
10^{-9}	6.0	4.2

10.1.3 Design flow chart

The generic flow chart is depicted on the left-hand side of Figure 10-1. An example of maximum chromatic dispersion is illustrated on the right-hand side of Figure 10-1.

1) *Select the system parameter to be determined*

   In the example of Figure 10-1, the system parameter is maximum chromatic dispersion.

2) *Obtain the probability distribution function for the corresponding element parameters*

   As can be seen in the histogram shown in the second right-hand side box in Figure 10-1, the average dispersion coefficient of fibre product i is assumed to be D_i, and standard deviation is σ_i.

3)   *Calculate the probability distribution for system parameter p(x) for given conditions*

In this example, the given condition is a fibre link length of 160 km. The statistical distribution of the system parameter is obtained as the concatenation of the distributions of several fibre bobbins. From the central limit theorem, the distribution of concatenated links has a Gaussian profile. In this example, the total average of chromatic dispersion is $17 \times 160 = 2720$ ps/nm, while standard deviation is 48 ps/nm. It should be noted that, by using the ordinary worst-case design, maximum chromatic dispersion is $20 \times 160 = 3200$ ps/nm.

4)   *Choose a value for P_{th}, the probability threshold for system acceptance*

In this example, it is considered acceptable if one in a thousand links has a higher dispersion than the calculated value. (P_{th} is 10^{-3}.)

5)   *Determine system parameter X from equation $P(X) = P_{th}$, where P_{th} is the probability threshold for system acceptance*

In this example, maximum chromatic dispersion is determined to be $17.9 \times 160 = 2864$ ps/nm, assuming that P_{th} is 10^{-3}. Therefore, the dispersion requirement for the transmission system is relaxed by 336 ps/nm compared to the worst-case system design.

G.Suppl.39(08)_F10-1
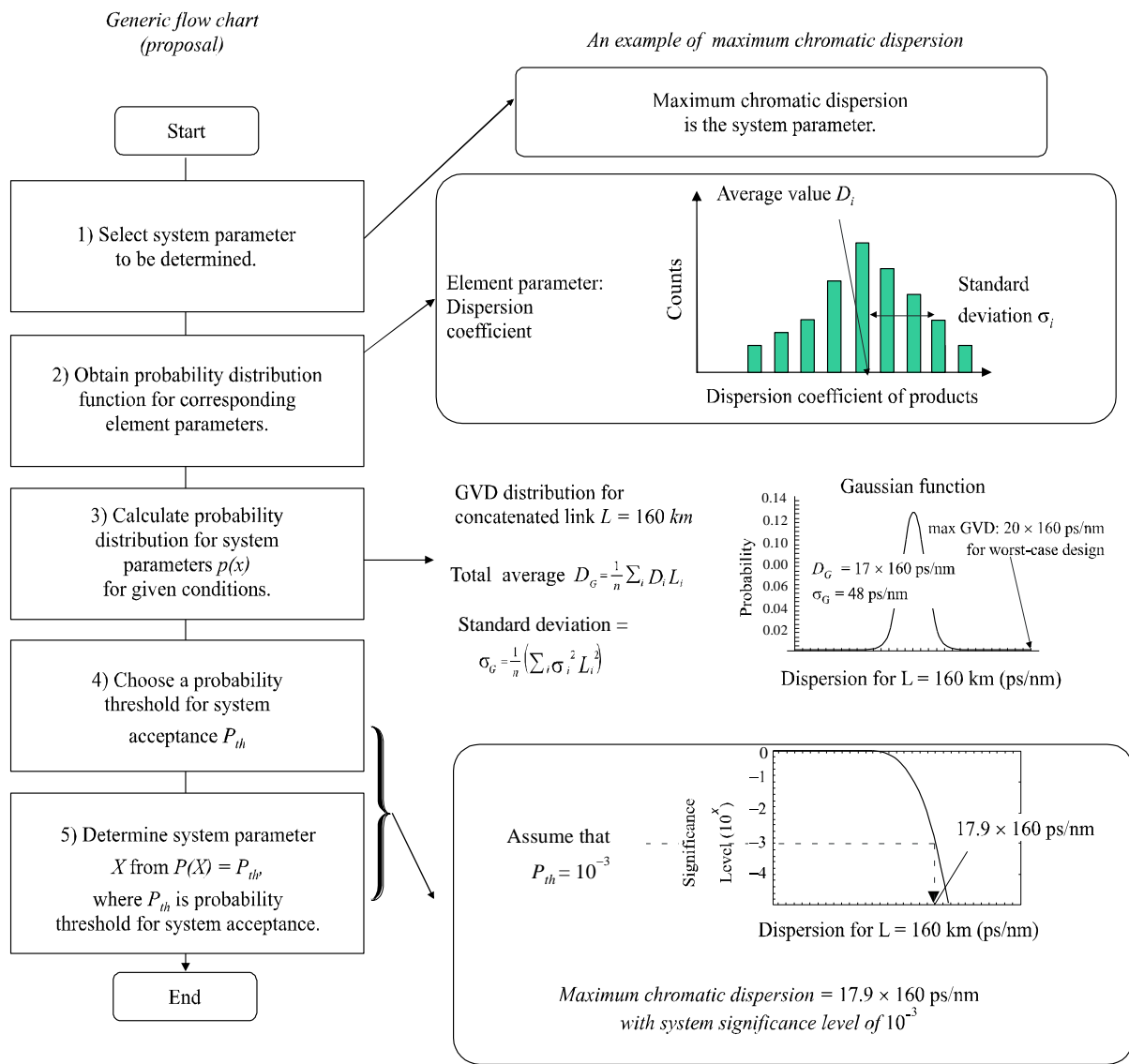
Figure 10-1 – Generic flow chart and an example of maximum chromatic dispersion

10.2 Statistical design of loss

A concatenated link usually includes a number of spliced factory lengths of optical fibre cable. The requirements for factory lengths are given in the optical fibre and cable Recommendations. The transmission parameters for concatenated links must take into account not only the performance of the individual cable lengths but also the statistics of concatenation.

The transmission characteristics of the factory length optical fibre cables will have a certain probability distribution which often needs to be taken into account if the most economic designs are to be obtained. The following paragraphs in this clause should be read with this statistical nature of the various parameters in mind.

Link attributes are affected by factors other than optical fibre cables such as splices, connectors, and installation. For the purpose of link attribute values estimation, typical values of optical fibre links are provided in an appendix of each of the fibre and cable Recommendations. The estimation methods of parameters needed for system design are based on measurements, modelling or other considerations.

The attenuation, A, of a link is given by:

$$A = \alpha L + \alpha_s x + \alpha_c y \qquad (10\text{-}1)$$

where:

α typical attenuation coefficient of the fibre cables in a link

α_s mean splice loss

x number of splices in a link

α_c mean loss of connectors

y number of connectors in a link (if provided)

L Link length

A suitable margin should be allocated for future modifications of cable configurations (additional splices, extra cable lengths, ageing effects, temperature variations, etc.). The typical values found in an appendix of each of the fibre and cable Recommendations are for the attenuation coefficient of optical fibre links.

The combination of these attenuation contributors in combination with the system maximum attenuation value lead to a variation in the length of the spans. The span length is a targeted value for Recommendations such as [ITU-T G.957] and [ITU-T G.691], but may be exceeded up to the point where length is limited by chromatic dispersion.

The typical attenuation coefficient of the fibre, α, varies with wavelength, λ, due to a number of factors: Rayleigh scattering, water absorption, macrobending loss and microbending loss. For well-designed cables, the bending loss variation with wavelength can be negligible, but generally increases with wavelengths above 1550 nm. For some cables, the microbending effect can, however, result in an elevated attenuation at higher wavelengths, which is called a bend edge. The Rayleigh scattering of ITU-T G.652 fibres is rather uniform across suppliers and time of manufacturing and follows a $1/\lambda^4$ relationship.

The peak water absorption wavelength is close to 1383 nm and can be characterized roughly as a magnitude value multiplied with a distinctive curve around 1383 nm. This peak can also be affected by hydrogen exposure and fibre hydrogen sensitivity. Over time, fibre manufacturers have learned to reduce the water absorption component, as well as the hydrogen sensitivity. [ITU-T G.652] includes two categories, ITU-T G.652.C and ITU-T G.652.D, for which the attenuation coefficient of the water peak in combination with hydrogen ageing is required to be less than or equal to the maximum value specified for the range 1310 nm to 1625 nm.

During the development of [ITU-T G.695], the overall link attenuation versus wavelength was characterized with values as measured at 1550 nm in combination with a bounding curve versus wavelength. The bounding curve was considered as a constant and the variation in values at 1550 nm took into account such factors as splice/connector quality and frequency, as well as variations in the overall cabled fibre attenuation. This type of approach resulted in clause I.1 of [ITU-T G.695] which contains a table of attenuation coefficient values that were used to relate the power levels to the target lengths of that Recommendation.

The following examples (see Figures 10-2 to 10-4), which are based on reflectometer link measurement of the core network of one network operator, illustrate the improvements in the water absorption over time.
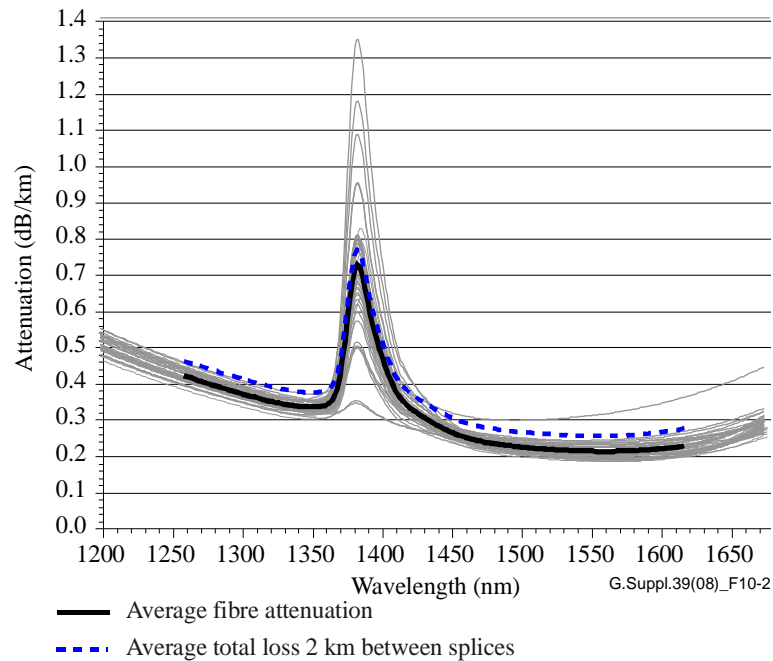
Figure 10-2 – Measured fibre attenuation and splice loss in installed
ITU-T G.652 A and B cable – Cables installed before 1990
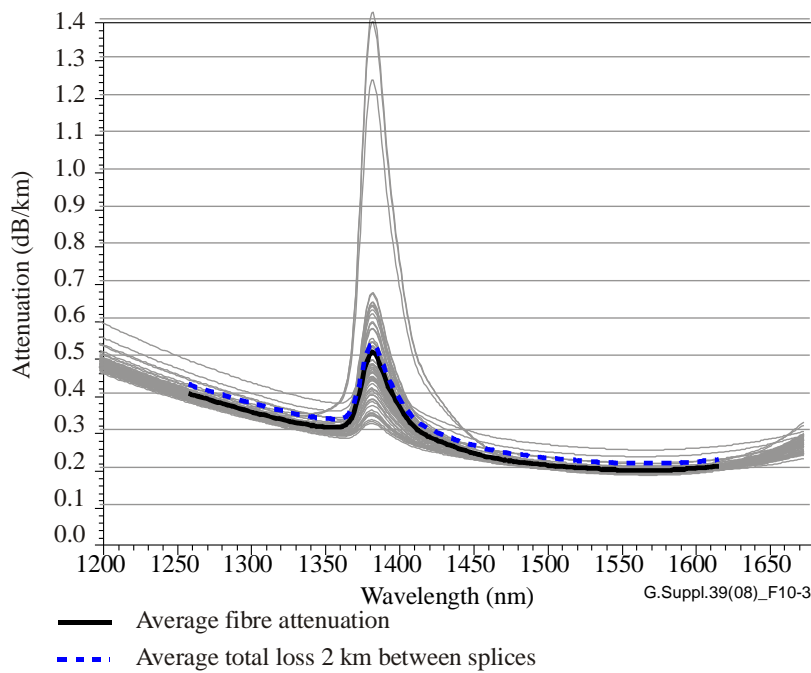
Figure 10-3 – Measured fibre attenuation and splice loss in installed ITU-T G.652 A and B cable – Cables installed around 2000
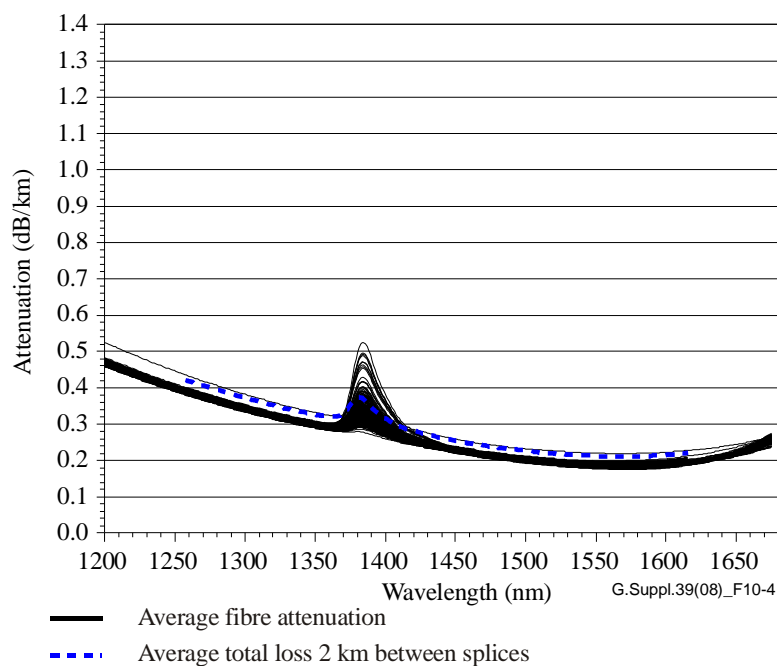
Figure 10-4 – Measured fibre attenuation and splice loss in installed ITU-T G.652 A and B cable – Cables installed in 2003

Table 10-3 summarizes the CWDM channel statistics that were deduced from the above measurements.

Table 10-3 – Core network attenuation coefficient statistics

CWDM centre wave-length (nm)	Cables installed before 1990				Cables installed around 2000				Cables installed in 2003			
	Fibre attenuation (dB/km)		Splice loss – 2 km between splices (dB/km)		Fibre attenuation (dB/km)		Splice loss – 2 km between splices (dB/km)		Fibre attenuation (dB/km)		Splice loss – 2 km between splices (dB/km)	
	Ave	Stdv	Ave	Stdv	Ave	Stdv	Ave	Stdv	Ave	Stdv	Ave	Stdv
1271	0.408	0.017	0.041	0.037	0.392	0.018	0.025	0.025	0.382	0.005	0.025	0.025
1291	0.384	0.016	0.041	0.036	0.368	0.017	0.024	0.024	0.359	0.005	0.024	0.024
1311	0.368	0.015	0.041	0.036	0.346	0.016	0.024	0.024	0.337	0.004	0.024	0.024
1331	0.341	0.015	0.041	0.035	0.326	0.015	0.024	0.024	0.317	0.004	0.024	0.024
1351	0.329	0.015	0.041	0.034	0.307	0.019	0.023	0.023	0.291	0.004	0.023	0.023
1371	0.586	0.127	0.041	0.034	0.439	0.137	0.023	0.023	0.323	0.026	0.023	0.023
1391	0.720	0.197	0.041	0.033	0.509	0.210	0.022	0.022	0.342	0.041	0.022	0.022
1411	0.436	0.074	0.041	0.033	0.348	0.082	0.022	0.022	0.280	0.016	0.022	0.022
1431	0.316	0.028	0.041	0.032	0.277	0.033	0.022	0.022	0.248	0.006	0.022	0.022
1451	0.269	0.017	0.041	0.031	0.246	0.018	0.021	0.021	0.230	0.004	0.021	0.021
1471	0.240	0.015	0.041	0.030	0.226	0.012	0.021	0.021	0.216	0.003	0.021	0.021
1491	0.225	0.017	0.041	0.030	0.213	0.012	0.021	0.021	0.205	0.003	0.021	0.021
1511	0.216	0.018	0.041	0.029	0.204	0.010	0.020	0.020	0.197	0.003	0.020	0.020
1531	0.210	0.020	0.041	0.028	0.198	0.010	0.020	0.020	0.191	0.003	0.020	0.020
1551	0.207	0.022	0.042	0.028	0.194	0.010	0.019	0.019	0.186	0.003	0.019	0.019
1571	0.206	0.025	0.043	0.029	0.192	0.010	0.019	0.019	0.184	0.004	0.019	0.019
1591	0.211	0.027	0.045	0.032	0.195	0.010	0.018	0.018	0.187	0.004	0.018	0.018
1611	0.220	0.028	0.049	0.034	0.203	0.010	0.018	0.018	0.194	0.004	0.018	0.018

NOTE 1 – Within each interval, centre wavelength ±6.5 nm, the highest value is used.

NOTE 2 – The six OTDR wavelengths used are: 1241 nm, 1310 nm, 1383 nm, 1550 nm, 1625 nm and 1642 nm.
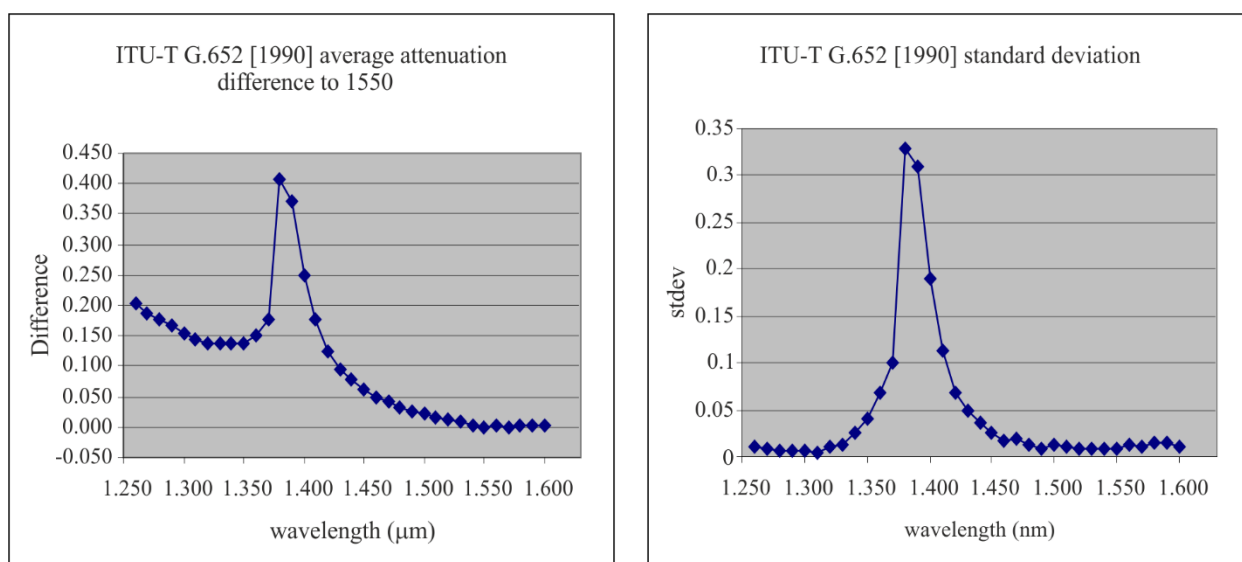
The following examples, which are also based on OTDR link measurement of the core network of the same network operator, illustrate the differences in link attenuations between ITU-T G.652 and ITU-T G.655 fibres. The measurements included two 60 km lengths of 216 ITU-T G.655 fibres, and the same lengths of 55 ITU-T G.652 fibres.

Table 10-4 – Comparison of ITU-T G.655 and ITU-T G.652 fibre attenuation measurements

| OTDR wavelength (nm) | ITU-T G.655 fibres | | | | ITU-T G.652 fibres | | | |
| | Fitted attenuation (dB/km) Typical OH-model | | Measured values (dB/km) | | Fitted attenuation (dB/km) OH-model [b-Hopland] | | Measured values (dB/km) | |
	Average	Stdv	Average	Stdv	Average	Stdv	Average	Stdv
1241	0.443	0.007	0.439	0.007	0.423	0.009	0.42	0.011
1310	0.358	0.006	0.361	0.009	0.341	0.008	0.343	0.009
1383	0.412	0.042	0.413	0.043	0.51	0.227	0.508	0.224
1551	0.211	0.012	0.209	0.012	0.194	0.004	0.192	0.005
1621	0.227	0.016	0.23	0.017	0.207	0.006	0.209	0.006
1642	0.243	0.017	0.241	0.017	0.222	0.007	0.22	0.007
1650	0.25	0.017	–	–	0.229	0.008	–	–
1660	0.261	0.017	–	–	0.241	0.009	–	–
1670	0.274	0.017	–	–	0.254	0.011	–	–
1675	0.282	0.017	–	–	0.263	0.013	–	–

The fitted attenuation values have been used to calculate attenuation statistics for both fibre types at the wavelengths covering the spectrum from 1261 nm to 1621 nm. These calculations show that ITU-T G.655 fibres have on average 0.015-0.020 dB/km higher attenuation than ITU-T G.652 fibres in the wavelength range 1261-1341 nm, and 0.016-0.021 dB/km higher attenuation in the wavelength range 1461-1621 nm.

Figures 10-5 to 10-7 represent the experience of one fibre manufacturer on the variation of attenuation coefficient with wavelength, as a difference to the value at 1550 nm. These values were used in the development of [ITU-T G.695].

Figure 10-5 – Average and standard deviation of difference in attenuation coefficient from 1550 nm – ITU-T G.652 circa 1990
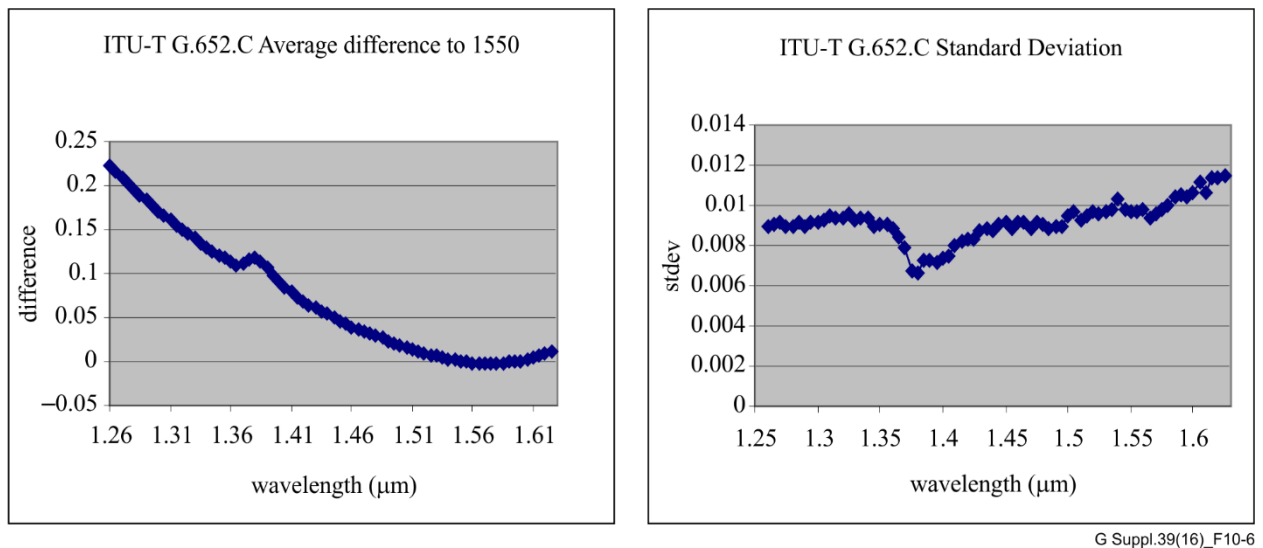
Figure 10-6 – Average and standard deviation of difference in attenuation coefficient from 1550 nm – ITU-T G.652.C
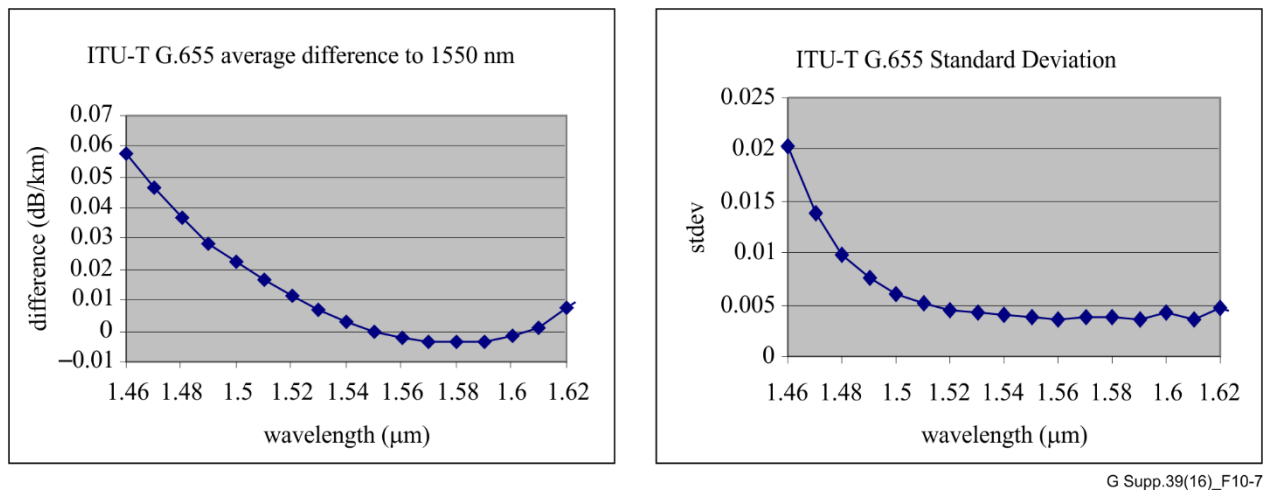
Figure 10-7 – Average and standard deviation of difference in attenuation coefficient from 1550 nm – ITU-T G.655

In the development of [ITU-T G.695], the link attenuation coefficient values at 1550 nm, obtained from some core networks in the United States, were examined, but the base value of 0.275 dB/km was retained due to the uncertainty of splice loss information for metro networks.

Figure 10-8 illustrates the experience of one network provider on the measurements of 308 links, of nine network operators, in the metro environment where the link length exceeded 20 km. These measurements, made in the period of 2003 to 2005, support the values found in [ITU-T G.695] for this environment.
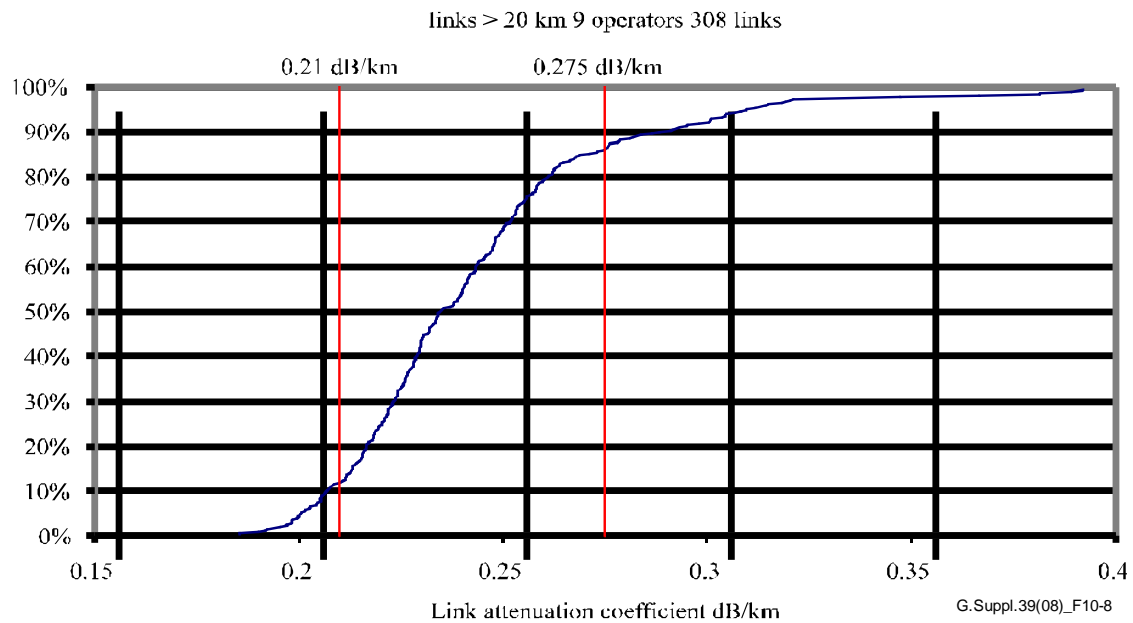
Figure 10-8 – Probability of loss being met versus link 1550 nm attenuation coefficient for links > 20 km

10.3 Statistical design of chromatic dispersion

10.3.1 Background

When different components or fibres are combined, the chromatic dispersion of the combination is the total of the chromatic dispersion values of the individuals, on a wavelength-by-wavelength basis. The variation in the total dispersion of links will depend on the distributions of the products that are used in the links.

NOTE – In the clauses that follow, there are examples given for particular fibre and component types. These examples are not necessarily broadly representative.

The fibre chromatic dispersion coefficient, $D(\lambda)$, is measured as a function of wavelength λ by methods outlined in [ITU-T G.650.1], *Definitions and test methods for linear, deterministic attributes of single-mode fibre and cable*. For a given wavelength range, it is often represented as a formula that includes parameters that can vary from fibre-to-fibre for a given fibre design. Some formulae are given in [ITU-T G.650.1], and the common units are ps/nm·km. For components, similar types of expressions can be used to characterize the chromatic dispersion, $CD(\lambda)$ in ps/nm.

10.3.2 Chromatic dispersion coefficient statistics

The characterization methodology suitable for concatenation statistics for a single distribution, or for a combination of distributions, is to calculate the dispersion coefficient for each of the wavelengths in the range of the application – for each individual fibre segment. This creates a distribution of dispersion coefficient values for each wavelength. Figures 10-9 and 10-10 show distributions for an ITU-T G.655-type fibre at two selected wavelengths.
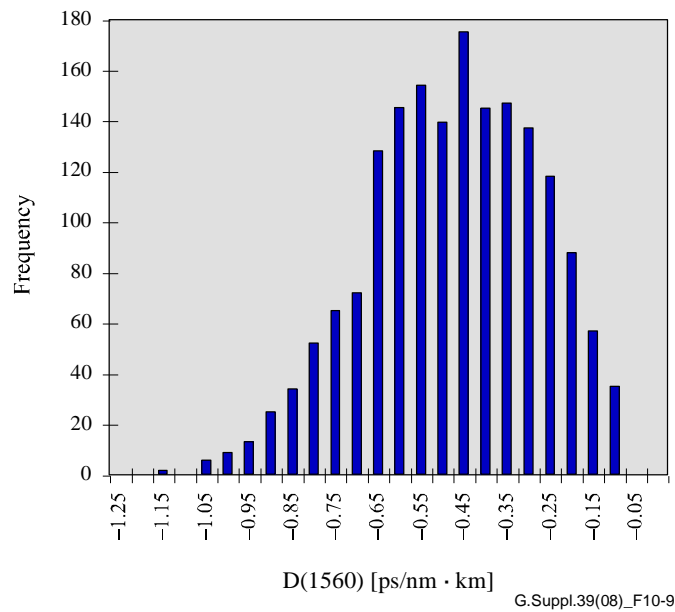
Figure 10-9 – Histogram of dispersion coefficient values at 1560 nm
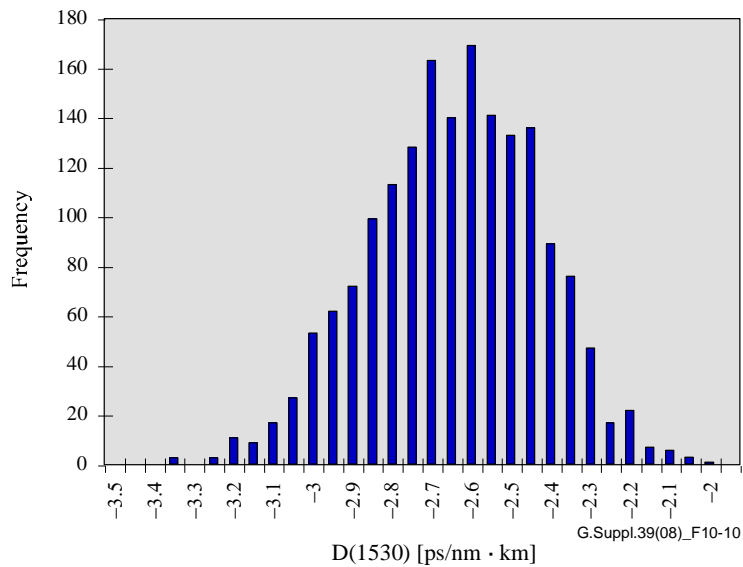
Figure 10-10 – Histogram of dispersion coefficient values at 1530 nm

The distribution for each wavelength is characterized with an average and a standard deviation value as in Figures 10-11 and 10-12.
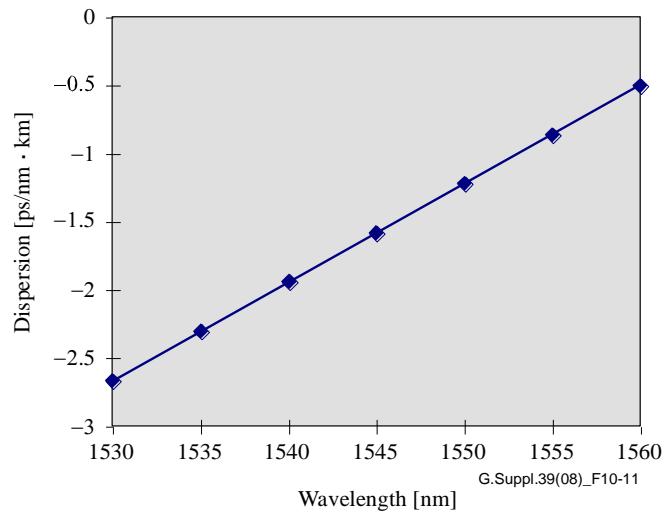
Figure 10-11 – Average dispersion coefficient versus wavelength
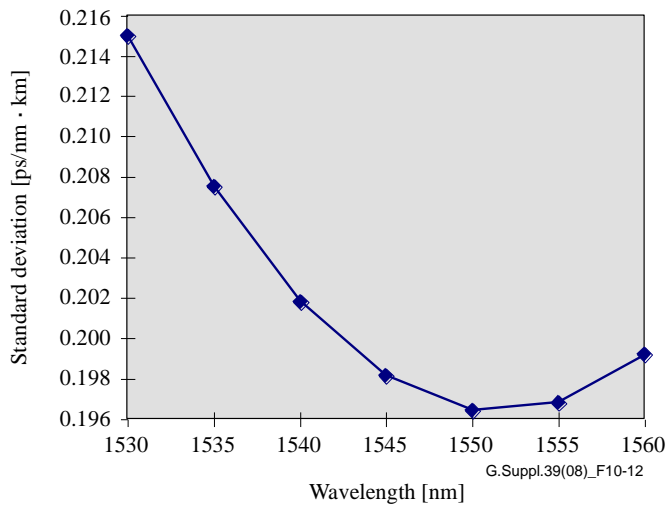
Figure 10-12 – Standard deviation of dispersion coefficient versus wavelength

Note that a linear relationship represents the average and a quadratic relationship represents the standard deviation. This is due in part to the linear representation of dispersion coefficient with wavelength. The data from the examples of Figures 10-11 and 10-12 can be empirically fitted to obtain formulae versus wavelength, λ, (nm):

$$\mu(\lambda) = 0.072(\lambda - 1567) \qquad \text{(ps/nm·km)} \qquad (10\text{-}2a)$$

$$\sigma(\lambda) = 0.1964 + 3.97 \times 10^{-5}(\lambda - 1551.6)^2 \qquad \text{(ps/nm·km)} \qquad (10\text{-}2b)$$

where μ is the average and σ is the standard deviation.

10.3.3 Concatenation statistics for a single population of optical fibres

These statistics are based on Gaussian assumptions. The examples are calculated at the "3 sigma" level for a P_{th} (probability threshold for system acceptance) of 0.13% above and below the limits. Other probability levels could be selected.

Assuming equal lengths, the dispersion coefficient of the concatenation of fibres is the average of the dispersion coefficient of the individual fibres:

$$\overline{D}(\lambda) = \frac{1}{n} \sum_i D(\lambda)_i \qquad (10\text{-}3)$$

Using the Central Limit Theorem, these averages can vary about the grand average according to a Gaussian random distribution. Using a fixed probability limit which contains 99.7% (0.13% above and 0.13% below) of the distribution, the limit of link dispersion coefficient values, D_{Tot}, is given as:

$$D_{Tot}(\lambda) = \mu(\lambda) \pm \frac{3}{\sqrt{n}} \sigma(\lambda) \tag{10-4a}$$

Assuming a conservative value of n, associated with a maximum fibre segment length of L_{Seg} within a link of L_{Tot}, Equation 10-4a can be written as:

$$D_{Tot}(\lambda) = \mu(\lambda) \pm 3 \left(\frac{L_{Seg}}{L_{Tot}} \right)^{1/2} \sigma(\lambda) \tag{10-4b}$$

The limits on the link dispersion value, CD_{Tot}, are just the limits of the link dispersion coefficient values times the link length:

$$CD_{Tot}(\lambda) = L_{Tot}\mu(\lambda) \pm 3\left(L_{Seg}L_{Tot}\right)^{1/2}\sigma(\lambda) \tag{10-5}$$

Table 10-5 shows the computed values for the population of the prior section for an assumed link length of 120 km and an assumed segment length of 5 km. These values are substantially below the –420 ps/nm value that would be deduced from the worst-case specifications.

Table 10-5

Wavelength	CD_{min}	CD_{max}
1530 nm	–336 ps/nm	–304 ps/nm
1540 nm	–249 ps/nm	–219 ps/nm

If the distribution is based on measurements of sub-sections of installed links, replace the length, L_{Seg}, by the length of the sub-sections that were measured, or a larger value representative of the length of the longest sub-sections in the link.

10.3.4 Concatenation statistics for multiple populations, including components

The notation is expanded by subscripting the average and standard deviation functions with I, II, etc., as well as adding, for example, $L_{I\text{-}Tot}$, for the link length contribution of fibre type I and n_A for the number of components of type A.

The probability limits are again done with a probability limit associated with a Gaussian of $\pm 3\sigma$, but the equations are separated into the "average part" and the "standard deviation part" before combining them. The average of the dispersion is:

$$\mu\{[CD_{Tot}(\lambda)]\} = L_{I-Tot}\mu_I(\lambda) + L_{II-Tot}\mu_{II}(\lambda) + n_A\mu_A(\lambda) + n_B\mu_B(\lambda) \tag{10-6a}$$

The standard deviation of the total dispersion is:

$$\sigma\{[CD_{Tot}(\lambda)]\} = \left[L_{I-Seg}L_{I-Tot}\sigma_I^2(\lambda) + L_{II-Seg}L_{II-Tot}\sigma_{II}^2(\lambda) + n_A\sigma_A^2(\lambda) + n_B\sigma_B^2(\lambda)\right]^{1/2} \tag{10-6b}$$

The limits are then:

$$CD_{Tot}(\lambda) = \mu[CD_{Tot}(\lambda)] \pm 3\sigma[CD_{Tot}(\lambda)] \tag{10-6c}$$

Adding more fibre or component types can be done with a simple extension of the above formulae.

Note that these formulae present the situation in a fashion that could lead one to conclude that all the compensators could be co-located. In general, this is not done. The compensators are normally distributed to reduce the maximum local dispersion along the link.

These formulae are illustrated for a combination of a distribution of ITU-T G.652 fibres and a distribution of dispersion compensation components as defined in [ITU-T G.671]. The assumed link parameters are:

$$L_{Tot} = 400 \, \text{km}, \quad L_{Seg} = 10 \, \text{km}, \quad n_{DC} = 5$$

The fibre statistics for chromatic dispersion coefficient (ps/nm·km) versus wavelength (nm) are shown in Figures 10-13 and 10-14.
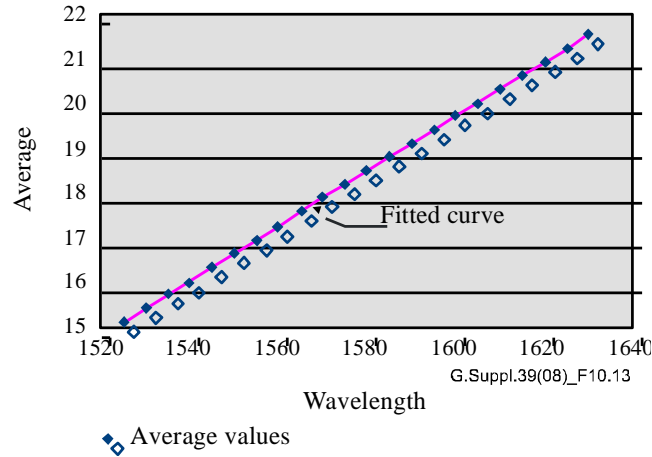
Figure 10-13 – Average chromatic dispersion coefficient of ITU-T G.652 fibre
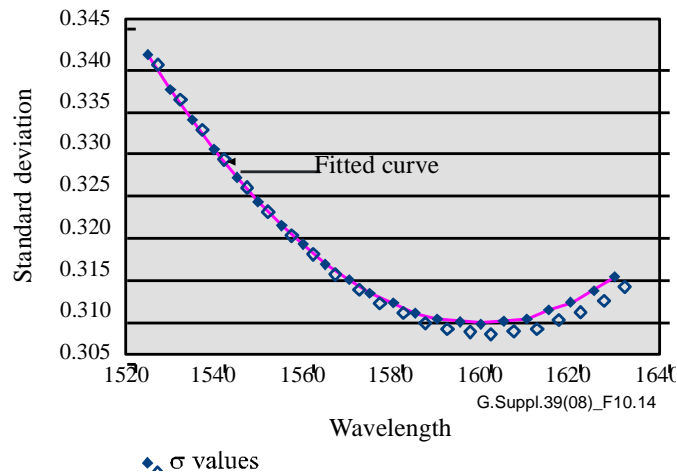
Figure 10-14 – Standard deviation of chromatic dispersion coefficient of ITU-T G.652 fibre

The formula for the fitted line in Figure 10-13 is:

$$\mu(\lambda) = -77.403 + 0.0607 \times \lambda \qquad (\text{ps/nm·km}) \qquad (10\text{-}7a)$$

where λ is in nm.

The formula for the fitted curve in Figure 10-14 is:

$$\sigma(\lambda) = 15.013 - 18.384 \times 10^{-3} \times \lambda + 5.746 \times 10^{-6} \times \lambda^2 \qquad (\text{ps/nm·km}) \qquad (10\text{-}7b)$$

The dispersion compensation statistics are shown in Figures 10-15 and 10-16.
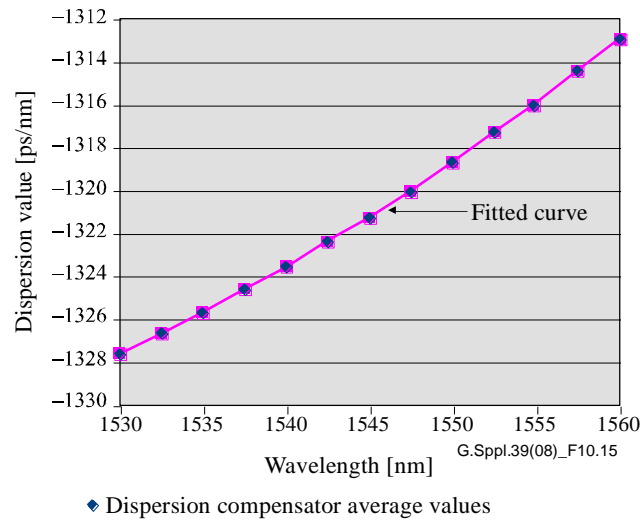
Figure 10-15 – Dispersion compensator average values
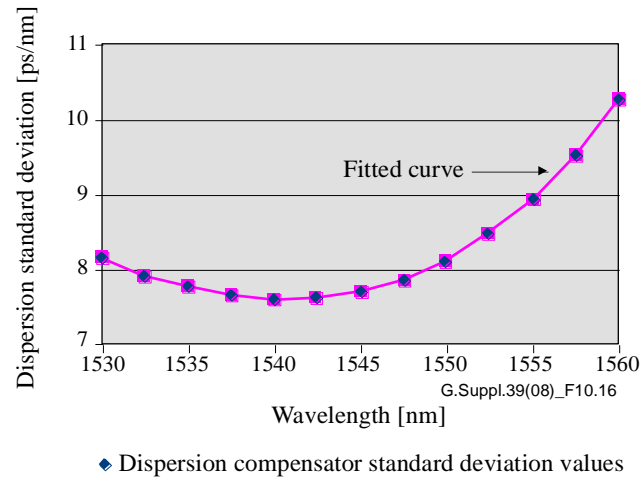
Figure 10-16 – Dispersion compensator standard deviation values

The formula for the fitted curve in Figure 10-15 is:

$$\mu(\lambda) = 8.010 \times 10^3 - 12.5698 \times \lambda + 4.227 \times 10^{-3} \times \lambda^2 \quad (ps/nm) \qquad (10\text{-}8a)$$

The formula for the fitted curve in Figure 10-16 is:

$$\sigma(\lambda) = -3.4612 \times 10^5 + 6.824 \times 10^2 \times \lambda - 0.4484 \times \lambda^2 + 9.818 \times 10^{-5} \times \lambda^3 \ (ps/nm) \qquad (10\text{-}8b)$$

Combining these statistics according to the formulae of Equations 10-6a, 10-6b and 10-6c, and using the link assumptions (400-km fibre, 10-km segments, five dispersion compensators), yields the results shown in Figure 10-17. Note that the smaller of the two wavelength characterization ranges is presented. Even though the range for fibre is broader, the range characterized for the compensator is not so broad.
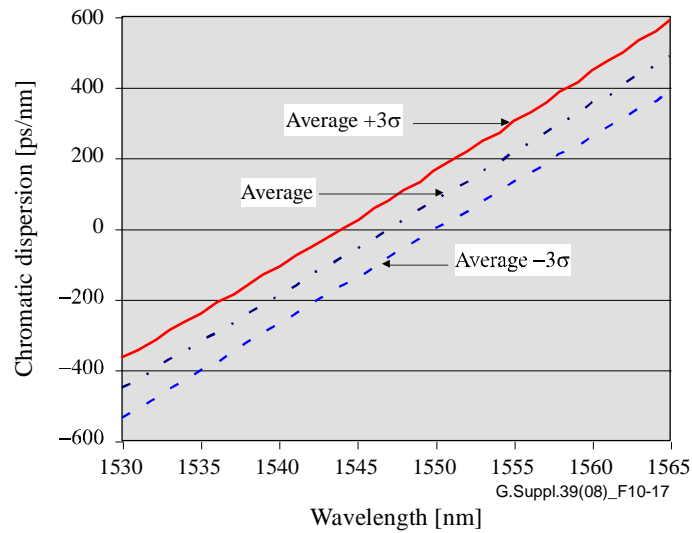
Figure 10-17 – 3 σ limits for combined ITU-T G.652 fibre and compensators

For the C-band (1530 nm to 1565 nm), the chromatic dispersion of this compensated link is within ±600 ps/nm. In [ITU-T G.691], the limit for 10-Gbit/s transmission, with respect to chromatic dispersion alone, is indicated as approximately 1000 ps/nm for transmitters and receivers that also conform with [ITU-T G.691].

10.4 Statistical design of polarization mode dispersion

The DGD varies randomly according to a Maxwell distribution characterized by the PMD value. The PMD of optical fibre cable is also specified according to a statistical format that can be combined with the other elements of the optical link to determine a maximum DGD that is defined as a probability limit. See Appendix I of [ITU-T G.650.2] for a description of the statistical specification of PMD for optical fibre cable. [ITU-T G.671] contains a description of how to combine the PMD specifications of other link elements with those of optical fibre cable to determine a combined maximum DGD for the link.

$$DGD\max_{link} = \left[DGD\max_F^2 + S^2 \sum_i PMD_{Ci}^2 \right]^{1/2} \tag{10-9}$$

where:

$DGD\max_{link}$ is the maximum link DGD (ps)

$DGD\max_F$ is the maximum concatenated optical fibre cable DGD (ps)

S is the Maxwell adjustment factor (see Table 10-2)

PMD_{Ci} is the PMD value of the i-th component (ps)

This equation assumes that the statistics of the instantaneous DGD are approximated by a Maxwell distribution, with the probability of the instantaneous DGD exceeding $DGD\max_{link}$ being controlled by the value of the Maxwell adjustment factor taken from Table 10-6.

See [IEC/TR 61282-3] for more detail, including a worked example that yields a combined link DGD maximum of 30 ps at a probability of 1.3×10^{-7}.

Table 10-6 – Maxwell adjustment factors and related probabilities

Ratio of max. to mean (S)	Probability of exceeding max.	Ratio of max. to mean (S)	Probability of exceeding max.
3	4.2×10^{-5}	4	7.4×10^{-9}
3.2	9.2×10^{-6}	4.2	9.6×10^{-10}
3.4	1.8×10^{-6}	4.4	1.1×10^{-10}
3.6	3.2×10^{-7}	4.6	1.2×10^{-11}
3.8	5.1×10^{-8}		

11   Forward error correction (FEC)

FEC is rapidly becoming an important way of improving the performance of large-capacity long-haul optical transmission systems and is already well established in wireless communication systems. Employing FEC in optical transmission systems yields system designs that can accept relatively large BER (much more than 10^{-12}) in the optical transmission line (before decoding). FEC application may allow the optical parameters to be significantly relaxed and encourages the construction of large capacity long-haul optical transmission systems in a cost-effective manner.

Definitions of FEC terminology are provided in Table 11-1:

Table 11-1 – FEC terminology

Information bit (byte)	Original digital signal to be FEC encoded before transmission
FEC parity bit (byte)	Redundant bit (byte) generated by FEC encoding
Code word	Information bit (byte) plus FEC parity bit (byte)
Code rate R	Ratio of bit rate without FEC to bit rate with FEC ($R = 1$ for in-band FEC)
Coding gain	Reduction of Q values at specified BER (e.g., 10^{-12}) assuming white Gaussian noise and a theoretical reference receiver
Net coding gain (NCG)	Coding gain corrected by the increased noise due to bandwidth expansion needed for FEC bits assuming white Gaussian noise (out-of-band FEC)
Q_b factor	Q factor corrected by the bandwidth expansion factor $1/\sqrt{R}$
BER_{in}	BER of the encoded line signal (= BER of the input signal of the FEC decoder)
BER_{out}	BER of the decoded client signal (= BER of the output signal of the FEC decoder)
BCH codes	Bose-Chaudhuri-Hocquenghem codes: the most commonly used BCH codes are binary codes
RS codes	Reed-Solomon codes: the most commonly used non-binary subclass of BCH codes
xxx (n, k) code	xxx = code class (BCH or RS). n = number of code word bits (bytes) k = number of information bits (bytes)

At present, two FEC schemes are recommended for optical transmission systems. They are "in-band FEC" for SDH systems, and "out-of-band FEC" for optical transport networks (OTNs). (Out-of-band FEC was originally recommended for submarine optical systems.) The terminology "in" or "out" refers to the client bandwidth. In-band FEC parity bits are embedded in a previously unused part of the section overhead of SDH signals, so the bit rate is not increased. In contrast to SDH, OTN signals including space for FEC bits (OTUk) have a higher bit rate than the equivalent signal before the FEC is added (ODUk). Therefore, OTN signals are encoded using out-of-band FEC resulting in a slightly

increased line-rate. [ITU-T G.709] also offers the option of non-standard out-of-band FEC optimized for higher efficiency.

11.1 In-band FEC in SDH systems

In-band FEC is described in clause 9.2.4, Annex A and Appendices IX and X of [ITU-T G.707]. The code is optional in STM-16, −64 and −256 single and multichannel systems. The code is triple-error correcting binary BCH code, more exactly a shortened BCH (4359,4320) code. Up to three bit errors can be corrected in a 4359-bit code word. The code word is an 8-bit interleaved signal stream of 270×16 bytes from one row of the STM-N frame. Therefore, up to 24-bit continuous errors in each row of an STM-16, −64 or −256 frame can be corrected.

If errors occur randomly, BER after decoding $P_c = \text{BER}_{out}$ is expressed, using raw BER $p = \text{BER}_{in}$ (before decoding), as follows for N = 4359.

$$P_c = \sum_{i=4}^{N} \frac{i}{N} \times \binom{N}{i} \times p^i \times (1-p)^{N-i} \tag{11-1}$$

11.2 Out-of-band FEC in optical transport networks (OTNs)

Out-of-band FEC is described in clause 11.1 and Annex A of [ITU-T G.709] as a modification of the out-of-band code in [ITU-T G.975]. [ITU-T G.709] specifies the network node interface (NNI) in OTN where the RS(255,239) code is optionally included. [ITU-T G.975] recommends the frame format for submarine systems and also describes the performance of the RS(255, 239) code. This code is a symbol error correcting RS code, so the byte number is used in the designation. Up to eight bytes in the code word can be corrected. The ITU-T G.709 frame employs 16-byte interleaving, so 1024 bits continuous errors can be corrected.

If errors occur randomly, BER after decoding $P_c = \text{BER}_{out}$ is expressed, using original raw BER $p = \text{BER}_{in}$ (before decoding), as follows.

$$P_{UE} = \sum_{i=9}^{N} \frac{i}{N} \times \binom{N}{i} \times P_{SE}^i \times (1-P_{SE})^{N-i}$$

$$p = 1 - (1-P_{SE})^{1/8} \tag{11-2}$$

$$p_c = 1 - (1-P_{UE})^{1/8}$$

P_{UE} is the probability of uncorrectable error, and P_{SE} is the probability of symbol (byte) error; N = 255.

11.3 Coding gain and net coding gain (NCG)

In the case of randomly distributed errors within the encoded line signal, a FEC decoder reduces the line or raw BER to a required reference BER value within the payload signal. Coding gain could therefore be regarded as the relation of these bit error ratios. In order to define a coding gain parameter as a more system-related parameter, the BER reduction by the FEC is usually transformed into a dB value based on a theoretical reference system. It is common practice to define the coding gain as the reduction of signal-to-noise ratio at a reference BER. This definition is directly applicable to an in-band FEC because its use does not imply an increase of the bit rate and therefore also no noise increase at the decision circuit due to receiver bandwidth expansion. The performance of an out-of-band FEC can be characterized better by a modified coding gain parameter. In wireless transmission systems, the net coding gain (NCG) parameter is well established for out-of-band FEC. It takes into account the fact that the bandwidth extension needed for these FEC schemes is associated with increased noise in the receiver.

Based on the NCG value, the achievable system gain in optical signal-to-noise ratio (OSNR) limited systems can be estimated accurately. In this case, the reduction of the electrical signal-to-noise ratio as a consequence of higher line BER reflects the allowable reduction in OSNR. In systems involving additional non-white noise contributions, the trade-off between sensitivity reduction due to bandwidth expansion and coding gain is much more complicated. For comparison of high efficiency FEC schemes with different (but similar) code rates used in long-haul systems, the NCG parameter is a good measure. It should be noted, however, that this comparison is only valid in systems limited by white noise sources. In the case that there is a significant penalty due to (nearly deterministic) signal degradation, the penalty may increase rapidly with increasing bit rate and invalidate the comparison. Even in systems operating in a very non-linear regime of the transmission fibre, the application of NCG is of limited value due to the fact that the associated noise cannot be characterized by white Gaussian noise.

NOTE 1 – In special cases of using the FEC coding for reducing the minimum allowable OSNR (e.g., for higher channel count), the reduction in OSNR can be higher than the net coding gain. This arises because in the case where the noise at the decision circuit has a significant contribution from a source other than OSNR, then for a given increase in total noise, the increase in the noise contribution due to OSNR alone is larger than the total increase.

Net coding gain definition

NCG is characterized by both the code rate R and the maximum allowable BER_{in} of the input signal of the FEC decoder, which can be reduced to a reference $BER_{out} = B_{ref}$ by applying the FEC algorithm. Furthermore, NCG should refer to a binary symmetric channel with added white Gaussian noise:

$$NCG = 20\log_{10}\left[\text{erfc}^{-1}\left(2\,B_{\text{ref}}\right)\right] - 20\log_{10}\left[\text{erfc}^{-1}\left(2\,B_{in}\right)\right] + 10\log_{10}R \qquad \text{(dB)} \qquad (11\text{-}3)$$

with erfc^{-1} the inverse of the complementary error function $\text{erfc}(x) = 1 - \text{erf}(x)$

NOTE 2 – $R = 1$ for in-band FEC.

See Figures 11-1 and 11-2.
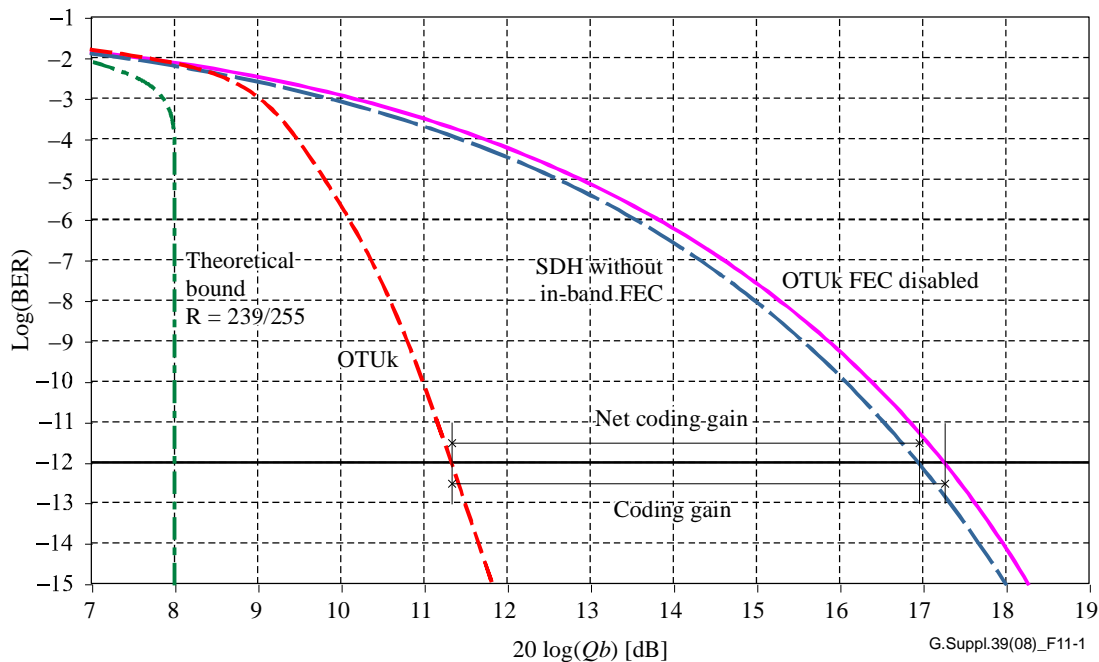
Figure 11-1 – Performance estimation of ITU-T G.709/Y.1331 FEC scheme
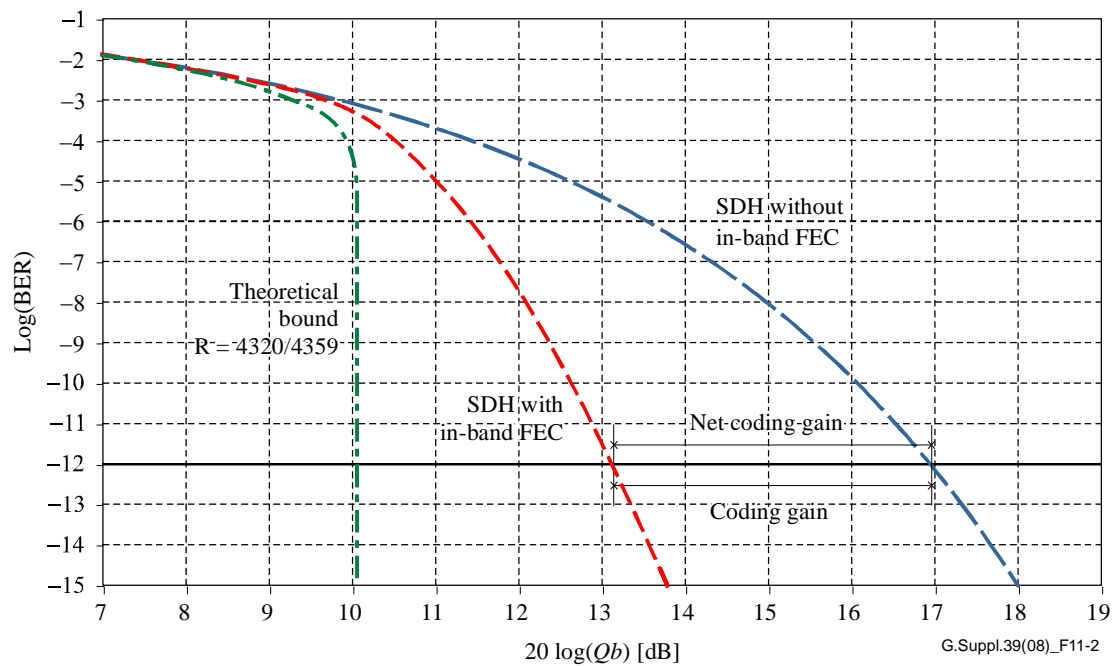
Figure 11-2 – Performance estimation of ITU-T G.707/Y.1322 FEC scheme

Note that:

$$20\log_{10} Qb = 20\log_{10} Q - 10\log_{10} R \qquad (11\text{-}4)$$

The horizontal axis is $20\log_{10} Qb$ in dB and the vertical axis is Log(BER). Net coding gain in terms of $20\log_{10} Qb$ is equivalent to allowable OSNR reduction when the line system uses optical amplifiers and ASE induced noise is the only significant noise source at the decision circuit.

See Table 11-2.

Table 11-2 – Performance of standard FECs

Application	In-band FEC BCH (4359,4320)	Out-of-band FEC RS(255,239)
	SDH	**OTN**
BER$_{in}$ for BER$_{out}$ = BER$_{ref}$ = 10^{-12}	2.9×10^{-6}	1.8×10^{-4}
Coding gain (BER$_{ref}$ = 10^{-12}) in dB	3.8	5.9
Net coding gain (BER$_{ref}$ = 10^{-12}) in dB	3.8	5.6
Code rate	1	239/255

11.4 HD-FEC and SD-FEC applications

11.4.1 Introduction

Decoding based on the output being quantized to only two levels (where each bit is considered definitely one or zero) is called hard-decision (HD) decoding.

Decoding based on the output being quantized to more than two levels (where together with the one or zero value, confidence information for the decision is also provided) is called soft-decision (SD) decoding.

Figure 11-3 illustrates HD decoding and SD decoding. In the case of HD decoding, each bit is determined to be either one or zero. In the case of SD decoding, the input analogue signal is mapped

to a number of possible states. For the case of 2-bit SD decoding, the states are [00] (strong 0), [01] (weak 0), [10] (weak 1), [11] (strong 1). That is to say, 2-bit soft-decision could be described as including 1-bit hard-decision and 1-bit confidence information. In practical implementations, more than 2 bits are generally used to improve performance.
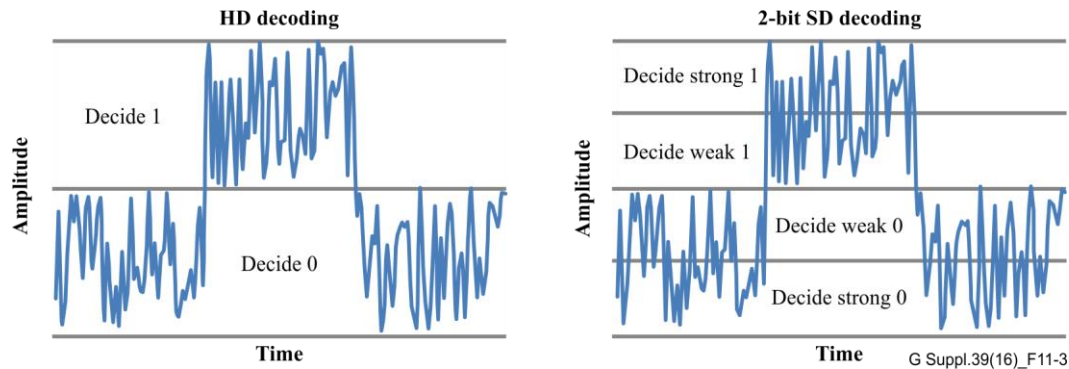
Figure 11-3 – HD decoding and 2-bit SD decoding

FEC based on HD and SD decoding are called "HD-FEC" and "SD-FEC", respectively.

11.4.2 Theoretical NCG bounds

The theoretical NCG bounds for HD-FEC and SD-FEC can be determined. For HD-FEC, NCG can be calculated based on a binary symmetric channel (BSC) model, and for SD-FEC, NCG can be calculated based on a binary input additive white Gaussian noise (AWGN) channel model [b-Mizuochi]. Some examples of theoretical NCG bounds for BERref = 10^{-12} and 10^{-15} are shown in Table 11-3.

Table 11-3 – Theoretical NCG bounds

Redundancy ratio	Code rate R	HD-FEC NCG in dB (BER$_{ref}$ = 10^{-12})	SD-FEC NCG in dB (BER$_{ref}$ = 10^{-12})	HD-FEC NCG in dB (BER$_{ref}$ = 10^{-15})	SD-FEC NCG in dB (BER$_{ref}$ = 10^{-15})
5%	0.952	8.6	9.7	9.6	10.7
7%	0.935	9.0	10.1	10.0	11.2
10%	0.909	9.4	10.6	10.5	11.6
15%	0.870	9.9	11.2	11.0	12.2
20%	0.833	10.3	11.6	11.3	12.6
25%	0.800	10.6	11.9	11.6	12.9

From Table 11-3 it can be seen that on AWGN channels more than 1 dB gain might be obtained by using SD-FEC instead of HD-FEC with the same redundancy ratio.

11.5 Statistical assumption for coding gain and NCG

The performance evaluation results in Table 11-2 are valid under the assumption that errors occur in a statistically random manner. Here, random error is defined as the following probability function.

$$P_k(t) = \frac{(\rho t)^k}{k!} \exp\{-\rho t\} \qquad (11\text{-}5)$$

Equation 11-5 is the well-known definition of Poisson random statistics, and yields the probability of the k-time occurrence of random events in time-interval t. Substituting $k = 1$ into Equation 11-5 leads

to 1-bit error statistics, and the theoretical curve of random statistics of 1-bit error occurrence is illustrated in Figure 11-4 for the average BER of 1×10^{-6}.
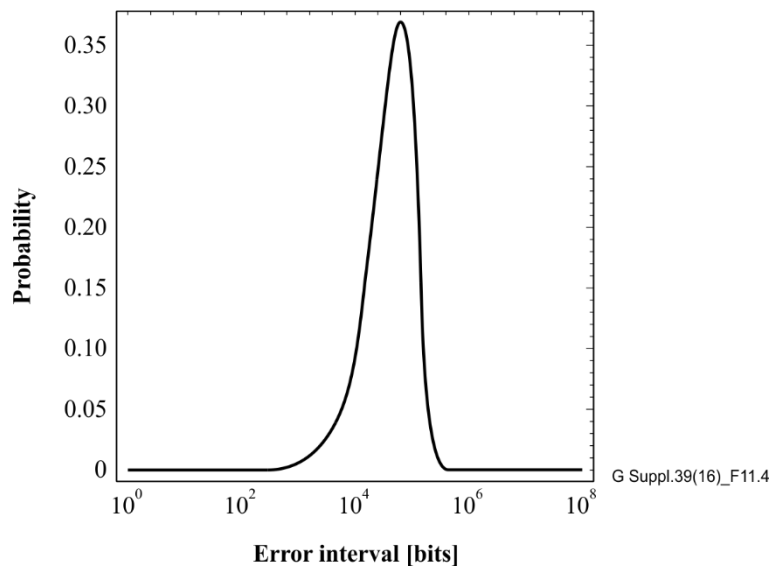
Figure 11-4 – Theoretical curve of 1-bit error probability with respect to time interval

Note that the horizontal axis is logarithmic. If error statistics follow the curve in Figure 11-2, FEC performance follows the theoretical prediction described in Table 11-2. The case in which error statistics do not follow the theoretical curve in Figure 11-2 is for further study.

There are several sources of error generation in optical transmission systems, such as ASE noise, group velocity dispersion (GVD), PMD. Moreover, non-linear effects can degrade signal performance through self-phase modulation (SPM), stimulated Brillouin scattering (SBS), modulation instability (MI) in single-channel systems, and cross-phase modulation (XPM), four-wave mixing (FWM), and stimulated Raman scattering (SRS) in multichannel systems. FEC has been proven to be effective in OSNR-limited systems as well as in dispersion-limited systems. As for non-linear effects, reducing the output power leads to OSNR limitations, against which FEC is useful. FEC is less effective against PMD, however. Thus, the treatment of PMD is a topic for further study. Candidates of optical parameter relaxation with FEC are described below. A mixture of the candidates is left for further study.

11.6 Candidates for parameter relaxation

By using FEC, optical parameters can be relaxed if the assumption of random error statistics is valid.

11.6.1 Relaxation of transmitter and/or receiver characteristics

The maximum BER can be relaxed from 10^{-12} toward the values listed in the third row in Table 11-2 at the maximum relaxation. This allows a reduced signal-to-noise ratio at the decision circuitry. Assuming a given OSNR in a reference system without FEC is sufficient to produce the required BER, the coding gain provided by adding FEC to the system can be used to relax component parameters in the transmitter and/or receiver. There are many parameters which could benefit from this such as the requirements for total launched power, eye mask, extinction ratio, electrical noise of a PIN receiver, noise figure of an optical preamplifier, isolation of demultiplex filters or, to some extent, the characteristic of the receiver transfer function determining the intersymbol interference and noise bandwidth before decision.

11.6.2 Reduction of output power levels to save pump power

Reducing the output power levels of transmitter and line amplifiers by the NCG value leads to reduced OSNR at the end of an optical amplifier chain. The associated higher electrical noise and, therefore, higher BER is compensated by FEC. The same principle can be applied to a single-span application with an optically preamplified receiver. Deploying FEC in a single-span system without an optically preamplified receiver gives a transmitter output power saving of only half of the NCG value because, in this case, the system is limited by receiver electrical noise.

11.7 Candidates for improvement of system characteristics

11.7.1 Reduction in power levels to avoid non-linearity

Reducing the output and input power levels of the optical amplifiers forces a system limited by non-linear effects to become OSNR limited, provided that the other parameters are unchanged. Power reduction according to the NCG value, and even more, is feasible as indicated in Note 1 in clause 11.3. For example, after the power levels are decreased, the multichannel system parameters for ITU-T G.652 and ITU-T G.655 fibre can also be applied to ITU-T G.653 fibre. Thus, a common system specification becomes possible that is valid for all fibre types.

11.7.2 Increase in maximum span attenuation

If the multi-span system is not chromatic dispersion limited (using ITU-T G.652 with dispersion accommodation, ITU-T G.653 or ITU-T G.655 fibre), target span distance can be extended. The input power of each line amplifier can be decreased by the amount of the net coding gain. Therefore, the maximum span attenuation can be increased by the amount of the net coding gain (maximum case). The relaxation may eliminate unnecessary repeaters in a system with slightly larger loss than that specified. Extending the distance of a dispersion-limited system is for further study.

NOTE – In a single-span system without preamplifier, the increase of maximum path attenuation is half of the NCG value only because, in this case, the system is limited by receiver electrical noise.

11.7.3 Increase in maximum number of spans for a long-haul system

The total target distance of a long-haul system can be extended enormously by increasing the number of spans (and also line amplifiers) assuming that chromatic and polarization mode dispersion do not become limiting factors (i.e., the system remains OSNR limited). Providing that the attenuation of each span is the same and remains constant, the maximum number of spans can be increased by a factor given by the NCG value. In the case of standard out-of-band FEC, the target distance may be increased by a factor of almost four. Extending the distance of a non-OSNR limited system is for further study.

11.7.4 Increase in channel count for high-capacity systems

If a multi-span system is limited by the output power of the optical amplifiers, the channel count can be increased by a factor given by the NCG value. In the case of standard out-of-band FEC, the channel count may be increased by a factor of almost four. It should be noted that this approach can be used as long as the reference system was not supported by non-linear effects which may change by reducing the channel power. For example, SPM cannot be used to compensate for chromatic dispersion if the channel power becomes less than the SPM threshold.

12 Physical layer transverse and longitudinal compatibility

This clause describes physical layer transverse compatibility as it is used in [ITU-T G.957], [ITU-T G.691], [ITU-T G.693] and [ITU-T G.959.1]. Definitions are also provided of the possible configurations that might form the basis for future standardization of multi-span systems.

All of the configurations discussed here are for point-to-point systems. Arrangements more complex than this are for further study.

12.1 Physical layer transverse compatibility

12.1.1 Single-span physical layer transverse compatibility

In [ITU-T G.957], [ITU-T G.691], [ITU-T G.693] and [ITU-T G.959.1], the applications are defined to be "transversely compatible", which implies that the ends of an optical section may be terminated by equipment from different manufacturers. This is illustrated in Figure 12-1. Therefore, a full set of parameter definitions and associated values at interface point MPI-S and MPI-R are necessary to enable such an interface.
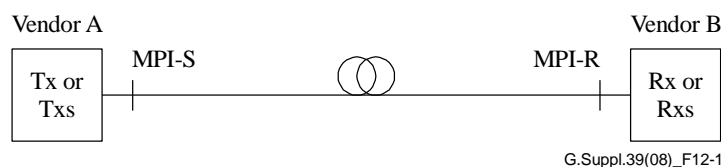
Figure 12-1 – Single-span physical layer transverse compatibility

NOTE – The interface points labelled MPI-S and MPI-R in Figure 12-1 have different labels (and different interface parameters) in the various Recommendations, but the same principle applies to both single-channel and multichannel interfaces. At present, transversely compatible multichannel applications are only found in [ITU-T G.959.1].

12.1.2 Multi-span physical layer full transverse compatibility

Currently in [ITU-T G.691], only single-span systems are specified. Originally it was the intent to also include multi-span systems employing optical line amplifiers as illustrated in Figure 12-2. When the first edition of [ITU-T G.691] was published, however, it was agreed not to include multi-span applications.
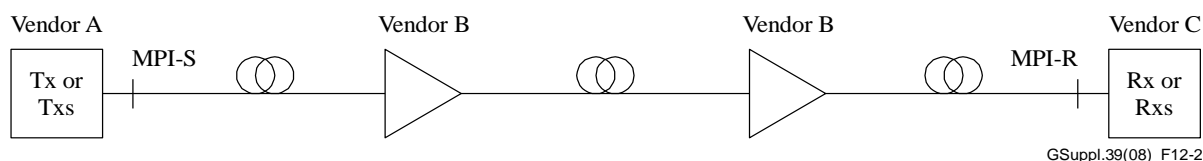
Figure 12-2 – Multi-span physical layer full transverse compatibility

Figure 12-2 shows the case for full transverse compatibility where the amplifiers are provided by a different vendor from the terminating equipment. This case requires the specification of the channel plan and full details of the optical supervisory channel (OSC) if one is used.

This case may also require the specification of some parameters such as loss and power levels on a per-span basis, and also other parameters such as chromatic dispersion, PMD and non-linearity to be "managed" over the whole link.

12.1.3 Multi-span physical layer partial transverse compatibility

It is also possible to define an additional configuration where the terminating equipment at either end of the link is provided by a single vendor. This is called partial transverse compatibility and is illustrated in Figure 12-3.
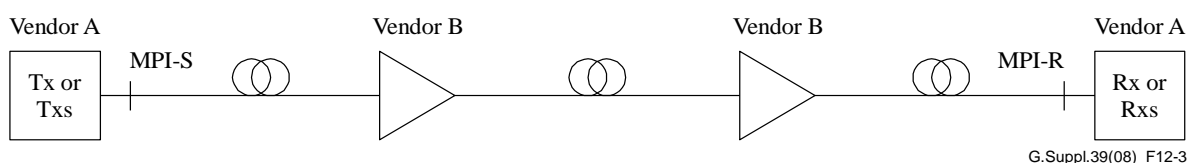
Figure 12-3 – Multi-span physical layer partial transverse compatibility

This alternative possibility could require most of the same specifications for the physical characteristics as for multi-span full transverse compatibility, except that the exact channel plan need not be specified. The operating wavelength range of the system would be required.

12.1.4 Multi-span single interface transverse compatibility

An alternative possibility (which may require less specification for the physical characteristics compared to multi-span full transverse compatibility) exists as shown in Figure 12-4. However, this configuration has not been studied within the ITU-T. Here, only a single interface point is defined for the link (at either the transmitter or the receiver) and a single vendor provides all of the equipment on one side of the interface.
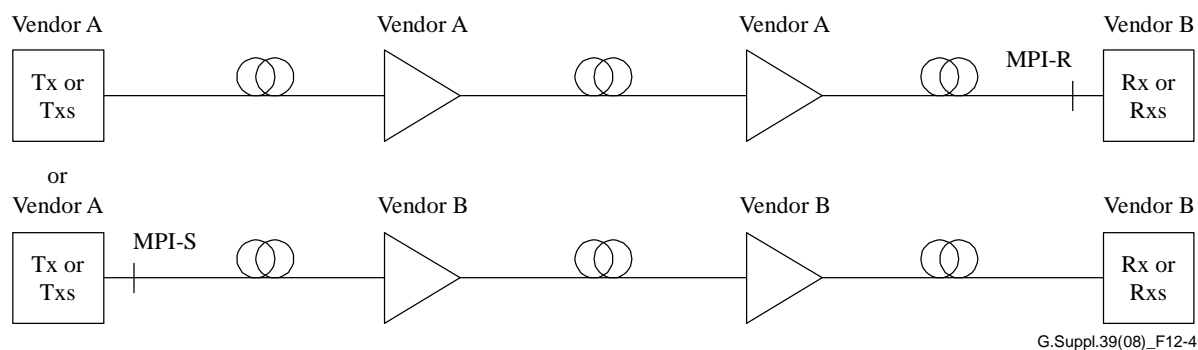
Figure 12-4 – Multi-span single interface transverse compatibility

The specifications of the physical characteristics required for this configuration are for further study, but would have to include details of the exact channel plan.

12.2 Physical layer longitudinal compatibility

In contrast to the above, an application that is defined to be "longitudinally compatible" implies that both ends of an optical section are terminated by equipment from the same manufacturer. In this case, a more limited set of parameters than for transversely compatible systems is required. Here, only the cable characteristics (attenuation, dispersion, DGD, reflections) are specified. A single-span longitudinally compatible system is illustrated in Figure 12-5.
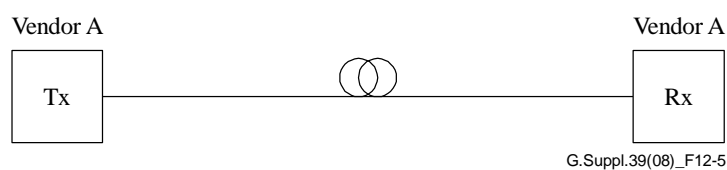
Figure 12-5 – Single-span physical layer longitudinal compatibility

For multi-span systems, longitudinal compatibility is also possible. This is similar to the single-span longitudinally compatible system, where all the active equipment comes from a single source. This is illustrated in Figure 12-6. As in the case of single span, only a very limited number of parameters are required to be specified, although chromatic dispersion and PMD must be managed on an end-to-end basis.

G.Suppl.39(08)_F12-6
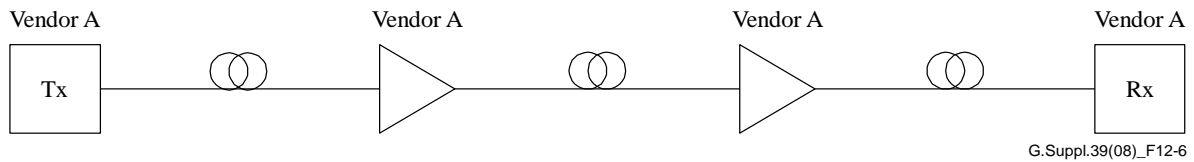
Figure 12-6 – Multi-span physical layer longitudinal compatibility

12.3 Joint engineering

Several clauses of [ITU-T G.957] address joint engineering:

–   In clause 3.1.2 of [ITU-T G.957] joint engineering is defined as: The process by which Administrations/operators agree on a set of interface characteristics of an optical link that meet agreed performance characteristics of the link when the available interface specifications in ITU-T Recommendations are insufficient to ensure the performance level.

–   In the first paragraph of clause 8.5 of [ITU-T G.957], it is stated that: For a limited number of cases, joint engineering may be envisaged to meet the requirements of optical sections where the interface specifications of [ITU-T G.957] prove inadequate. This will probably occur where the required section loss is greater (e.g., 2 dB) than that specified in [ITU-T G.957], but may also be considered for other parameters.

For those cases, it is up to the Administrations/operators concerned to specify more closely the aspects of the system where the specifications of [ITU-T G.957] are not satisfactory. It is important to stress that every situation requiring "joint engineering" is likely to be different: hence, it is meaningless to try to standardize any of the parameter values for these systems. Instead, it is for the Administrations/operators concerned to come to an agreement as to what is required and then negotiate with manufacturers as to what is actually feasible. This process is very likely to lead to both ends of a transmission link being supplied by the same manufacturer, who meets the required performance by jointly optimizing the transmitters and receivers.

It should be pointed out that, in spite of the futility of specifying any parameter values for "jointly engineered" systems, it would be advisable for Administrations/operators or manufacturers involved to follow the general guidelines and system engineering approach used in [ITU-T G.957]. In particular, it would be helpful to use the same parameter definitions (e.g., receiver sensitivity at R reference point including all temperature and ageing effects).

13 Switched optical network design considerations

An architectural foundation for switched optical networking is given in [ITU-T G.8080]. From the perspective of optical transmission systems engineering for switched optical networks, two cases can be considered, corresponding to the location of 3R terminations within the switched optical network.

In the case that the network element switching the optical signal also provides 3R termination, then the optical sections on either side of the switching network element can be separately engineered. Either worst-case or statistical design principles can be used to achieve end-to-end system performance consistent with the allocation of performance objectives given in [ITU-T G.828] and [ITU-T G.8201].

In the case that the network element performing the switching/rerouting of the optical signal does not provide 3R termination (e.g., a transparent optical cross-connect), then it is generally very difficult to ensure the bit-error rate performance of the switched optical connection without imposing severe constraints on the extent of the network. For example, the action of the transparent switching network element to effect an optical multiplex section (OMS) re-route could result in a new transmission path of different optical characteristics, possibly beyond the design limits required for the desired performance of the client signals supported by the optical transmission section (OTS). The

elimination of such cases may be addressed through pre-planning of feasible connections for the re-routed signals or through joint engineering.

The possible constraints on the time-scale to achieve switched optical networks due to the dynamic behaviour of optical amplifiers, or other optical elements within the transmission link, is beyond the scope of this Supplement.

14   Best practices for optical power safety

14.1   Viewing

14.1.1   Viewing fibre

Fibre ends or connector faces should not be viewed with unprotected eyes or with any collimating device that is not approved by the operating organization.

14.1.2   Viewing aids

Use only filtered or attenuating viewing aids approved by the operating organization.

14.2   Fibre ends

14.2.1   Termination

Any single or multiple fibre end(s) found not to be terminated (for example, matched, spliced) should be individually or collectively covered with material appropriate for the wavelength and power when not being worked on. They should not be readily visible and sharp ends should not be exposed.

Suitable methods for covering include the use of a splice protector or tape. Always attach end caps to unmated connectors.

14.2.2   Cleaning

Use only methods approved by the operating organization for cleaning and preparing optical fibres and optical connectors. Cleaning is indispensable especially for high-power systems (e.g., over 1 W). If connector end-faces are not cleaned in such systems, undesirably high temperatures may be caused that can, in some cases, lead to the "fibre-fuse" phenomenon.

Before power is activated, ensure that the fibre ends are free of any contamination.

NOTE – Fibre-fuse phenomenon is characterized by very high temperatures in association with bright white light propagation down the fibre, which may cause dangerous situations in the system.

14.2.3   Connector loss

Connector loss may induce temperature increase, especially for high-power systems. Therefore, care should be taken in the choice of connectors for high-power systems. For example, in a system where optical launched power at the connector is 2 W, a loss of 0.25 dB means that there is about 0.1 W of optical power available to cause local heating. In an example connector using ITU-T G.653 fibre, this was found to cause a 5°C rise in temperature.

14.2.4   Splice loss

Splice loss may induce temperature increase, especially for high-power systems. The power available for heating in the case of splice loss is the same as that of connector loss. The heating effect caused by this depends on where the "lost" power is absorbed. In the case that it is all absorbed local to the splice (e.g., due to contamination), then considerable temperature rises could occur.

14.3 Ribbon fibres

Ribbon fibre ends cleaved as a unit may exhibit a higher hazard level than that of a single fibre. Therefore, do not cleave ribbon fibres as an unseparated ribbon, or use ribbon splicers, unless authorized by the operating organization.

14.4 Test cords

When using optical test cords, the optical power source should be the last to be connected and the first to be disconnected.

14.5 Fibre bends

Excessive bending of the fibre can form a risk of both mechanical failure due to bending stress as well as a local heating point with high-power transmission. Local low-radius bends should be avoided.

14.6 Board extenders

Board extenders should not be used on optical transmitter or optical amplifier cards. Do not power optical sources when they are outside transmitter racks.

14.7 Maintenance

Follow only instructions approved by the operating organization for operating and maintaining the system being worked on.

14.8 Test equipment

Use test equipment of the lowest class necessary and practical for the task. Do not use test equipment of a higher class than the location hazard level.

14.9 Modification

Do not make any unauthorized modifications to any optical fibre communication system or associated equipment.

14.10 Key control

For equipment with key control, the keys should be placed under the control of a person appointed by management who should ensure their safe use, storage and overall control. Spare keys should be retained under strict control procedures by a nominated line manager.

14.11 Labels

Report damaged or missing optical safety labels to the operating organization line management.

14.12 Signs

Area warning signs are required for locations exceeding hazard level 1M. Area signs may be displayed in locations of lower classification.

14.13 Alarms

System alarms, especially those indicating that the automatic power reduction (APR) or any other safety system is inoperable, should be responded to so that repair takes place within a specified time.

14.14   Raman amplified systems

Raman amplified systems operate at sufficiently high powers that can cause damage to fibre or other components. This is somewhat described in clauses 14.2 and 14.5, but some additional guidance follows:

Before activating the Raman power

–   Calculate the distance to where the power is reduced to less than 150 mW.

–   If possible, inspect any splicing enclosures within that distance. If tight bends, e.g., less than 20 mm diameter, are seen, try to remove or relieve the bend, or choose other fibres.

–   If inspection is not possible, a high resolution OTDR might be used to identify sources of bend or connector loss that could lead to damage under high power.

–   If connectors are used, it should be verified that the ends are very clean. Metallic contaminants are particularly prone to causing damage. Fusion splices are considered to be the least subject to damage.

While activating Raman power

In some cases, it may be possible to monitor the reflected light at the source as the Raman pump power is increased. If the plot of reflected power versus injected power shows a non-linear characteristic, there could be a reflective site that is subject to damage. Other sites subject to damage, such as tight bends in which the coating absorbs the optical power, may be present without showing a clear signal in the reflected power versus injected power curve.

Operating considerations

If there is a reduction in the amplification level over time, it could be due to a reduced pump power or due to a loss increase induced by some slow damage mechanism such as at a connector interface. Simply increasing the pump power to restore the signal could lead to even more damage or catastrophic failure.

The mechanism for fibre failure in bending is that light escapes from the cladding and some is absorbed by the coating, which results in local heating and thermal reactions. These reactions tend to increase the absorption and thus increase the heating. When a carbon layer is formed, there is a runaway thermal reaction that produces enough heat to melt the fibre, which then goes into a kinked state that blocks all optical power. Thus, there will be very little change in the transmission characteristics induced by a damaging process until the actual failure occurs. If the fibre is unbuffered, there is a flash at the moment of failure which is self-extinguishing because the coating is gone very quickly. A buffered fibre could produce more flames, depending on the material. For unbuffered fibre, sub-critical damage is evidenced by a colouring of the coating at the apex of the bend.

Appendix I

Pulse broadening due to chromatic dispersion

I.1   Purpose

This appendix relates to clause 9.2.1.1. It gives an expression for bit rate as limited by chromatic dispersion. It starts with a general published result that incorporates:

–   The fibre first-order and second-order dispersion coefficients;

–   The transmitter parameters of spectral width, chirp and modulation bandwidth.

I.2   General published result

The starting general result is the paper of reference [b-Marcuse], from which equations are indicated by rectangular parentheses as [xx]. Other equations are indicated by round parentheses as (I-y). Some symbols have been changed for simplification and to avoid confusion with "standardized" symbols.

The most general form in the above paper gives the rms temporal width of the output pulse duration as a function of fibre length L to be:

$$\sigma(L) = \sigma_0 \left[(1 + AC)^2 + A^2 (1 + V^2) + E^2 (1 + V^2 + C^2)^2 \right]^{\frac{1}{2}}$$

[26]

The dimensionless symbols are:

$$V = WT, \qquad C = T\Delta\omega, \qquad A = \frac{L}{T^2} \frac{\partial^2 \beta}{\partial \omega^2}, \qquad E = \frac{L}{2T^3} \frac{\partial^3 \beta}{\partial \omega^3}$$

[21], [22]

where β is the propagation wavenumber. Also:

$$\sigma_0 = \frac{T}{\sqrt{2}}$$

[27]

is the rms duration of the input (back-to-back) pulse at $L = 0$, where the input pulse and the unchirped source spectrum are Gaussian with $\frac{1}{e}$ halfwidths T (in time t) and W (in circular frequency ω), respectively. (Note that T is not the time-slot width for a given bit rate.) The output pulse is in general non-Gaussian. The phase of the electric field of the chirped pulse is:

$$\omega_m + \Delta\omega \frac{t}{T}$$

[1]

where ω_m is the source mean circular frequency and $\Delta\omega$ is the frequency shift during the pulse.

I.3   Change of notation

Now, change to a more common standards notation and to rms widths.

The derivatives of the propagation wavenumber with respect to the circular frequency are:

$$\frac{\partial^2 \beta}{\partial \omega^2} = -\frac{\lambda_m^2}{2\pi c} D_m, \qquad \frac{\partial^3 \beta}{\partial \omega^3} = \left(\frac{\lambda_m^2}{2\pi c} \right)^2 \left(S_m + \frac{2D_m}{\lambda_m} \right)$$

(I-1)

evaluated at ω_m. Here D_m is the fibre dispersion coefficient and S_m is the fibre dispersion-slope coefficient $\left(S = \frac{dD}{d\lambda}\right)$, respectively, both evaluated at the source mean wavelength $\lambda_m\left(= \frac{2\pi c}{\omega_m}\right)$. Convert the source spectral width to an rms source width in optical frequency $\nu\left(= \frac{\omega}{2\pi}\right)$ so that:

$$\sigma_\nu = \frac{W}{2\pi \sqrt{2}} \tag{I-2}$$

Similarly, the chirp of Equation [1] is:

$$2\pi\left(\nu_m + \frac{t\Delta\nu}{\sigma_0 \sqrt{2}}\right) \tag{I-3}$$

where ν_m is the source mean optical frequency and $\Delta\nu$ is the optical frequency shift during the pulse. With the above notation, the terms in Equations [21, 22] become:

$$V = 4\pi \sigma_0 \sigma_\nu, \qquad C = 2\pi \sqrt{2} \sigma_0 \Delta\nu, \qquad A = -\frac{\lambda_m^2 D_m L}{4\pi c \sigma_0^2}, \qquad E = \left(\frac{\lambda_m^2}{2\pi c}\right)^2 \left(\frac{S_m + \frac{2 D_m}{\lambda_m}}{8\sigma_0^3 \sqrt{2}}\right) L \tag{I-4}$$

so that Equation [26] for the rms duration of the non-Gaussian output pulse becomes:

$$\sigma^2 = \left(\sigma_0 - \frac{\lambda_m^2 D_m L\Delta\nu}{c \sqrt{2}}\right)^2 + \left(\frac{\lambda_m^2 D_m L}{c}\right)^2 \left[(4\pi \sigma_0)^{-2} + \sigma_\nu^2\right]+$$

$$\frac{L^2}{8}\left\{\left(\frac{\lambda_m^2}{c}\right)^2 \left(S_m + \frac{2 D_m}{\lambda_m}\right)\left[(4\pi \sigma_0)^{-2} + \sigma_\nu^2 + \frac{1}{2}(\Delta\nu)^2\right]\right\}^2 \tag{I-5}$$

This is still the most general result, but in a more "familiar" notation. It incorporates dispersion, dispersion-slope, chirp and the widths of the input pulse and source spectrum.

I.4 Simplification for a particular case

For present purposes, ignore the chirp and second-order dispersion. Then in Equation I-4 one has:

$$C, E = 0 \tag{I-6}$$

and for notational simplicity drop the subscript m for evaluation at the mean wavelength. Equation I-5 then reduces to:

$$\sigma^2 (L) = \sigma_0^2 + \sigma_D^2 (L) \tag{I-7}$$

where the temporal broadening due to chromatic dispersion is:

$$\sigma_D = \frac{\lambda^2 DL}{c}\left[\sigma_\nu^2 + (4\pi \sigma_0)^{-2}\right]^{\frac{1}{2}} = DL\left[\sigma_\lambda^2 + \left(\frac{\lambda^2}{4\pi c \sigma_0}\right)^2\right]^{\frac{1}{2}} \tag{I-8}$$

where:

$$\sigma_\lambda = \frac{\lambda^2}{c} \sigma_\nu$$

This is written in both the frequency and wavelength representations, related by the source spectral rms width with respect to wavelength as:

$$\sigma_\lambda = \frac{\lambda^2}{c}\,\sigma_\nu \qquad\qquad \text{(I-9)}$$

Equation I-8 takes into account the bandwidths of *both* the pulse modulation and the source spectrum, which can be viewed in the frequency domain or in the wavelength domain. For example, $(4\pi\sigma_0)^{-1}$ is effectively the optical frequency width of the input pulse.

Two limiting cases correspond to known results. If the source spectral width predominates, Equation I-8 yields the usual result:

$$\sigma_D \approx D\,L\,\sigma_\lambda \qquad\qquad \text{(I-10)}$$

(This result corresponds to Equation 2.4.24 of [b-Agrawal3].) In the limit of a very coherent source, Equation I-8 gives:

$$\sigma_D \approx \frac{\lambda^2\,DL}{4\pi c\,\sigma_0} \qquad\qquad \text{(I-11)}$$

so the broadening increases as the input pulse width decreases. (This result corresponds to Equation 2.4.30 of [b-Agrawal3].)

I.5 Pulse broadening related to bit rate

Consider unchirped pulses at a bit rate B. The reciprocal of this bit rate is its time-slot. For RZ, the input pulse has a duration that is a fraction $f\,(<1)$ of the duration of an NRZ pulse; this fraction is called the duty cycle. As a special case, for NRZ one has $f = 1$. The equation:

$$N\,\sigma_0 = \frac{f}{B} \qquad\qquad \text{(I-12)}$$

states that N times the rms value of the input pulse should fit within this time-slot, reduced by the duty cycle. The value of the dimensionless shape-factor N depends on the type of input pulse as will be discussed later. With Equation I-12, the pulse broadening of Equation I-8 is then:

$$\sigma_D = \frac{\lambda^2\,DL}{c}\left[\sigma_\nu^2 + \left(\frac{N\,B}{4\pi\,f}\right)^2\right]^{\frac{1}{2}} \qquad\qquad \text{(I-13)}$$

Working in terms of optical frequency, rather than wavelength, shows the effective frequency width as the rms sum of the spectral width and the width due to the bit rate, and the broadening increases as both of these increase.

As stated in [ITU-T G.957], for a particular value of power penalty and bit error ratio (BER) at the receiver, there is an upper limit to the allowed intersymbol interference (ISI). It occurs when the maximum broadening equals some time-slot fraction $\varepsilon\,(<1)$ of the time-slot of the NRZ bit rate, i.e.,:

$$\left(\sigma_D\right)_{\max} = \frac{\varepsilon}{B} \qquad\qquad \text{(I-14)}$$

This fraction is called the epsilon value. Then Equations I-13 and I-14 yield:

$$\left(\frac{N\,B}{4\pi\,f}\right)^2 + \sigma_\nu^2 = \left(\frac{\varepsilon\,c}{\lambda^2\,B\,D\,L}\right)^2 \qquad\qquad \text{(I-15)}$$

a general result that includes source and modulation bandwidths (but without chirp or second-order dispersion), for any assumed values of the shape-factor N and the time-slot fraction ε.

I.6 Value of the shape factor

As discussed in conjunction with Equation I-12, the NRZ pulse duration is $\dfrac{1}{B}$; assuming $N = 4$ which means that twice the full-width rms of the input pulse must fit into the allowed pulse duration [b-Agrawal3]. (Examples: $N = 3.46$ would contain all the power of an NRZ rectangular pulse, while $N = 4$ contains 95.4% of a Gaussian pulse.)

Now Equation I-15 can be solved for the system chromatic dispersion as:

$$DL = \frac{\varepsilon\, c}{\lambda^2\, B\, \sqrt{\left(\dfrac{B}{\pi\, f}\right)^2 + \sigma_v^2}} \tag{I-16}$$

The allowed chromatic dispersion decreases as the duty cycle decreases since the signal bandwidth is increasing at the same time. For the limiting case of a broad spectrum/low bit rate transmitter, Equation I-15 or I-16 gives:

$$D\,L\,B\,\lambda^2\, \sigma_v \approx c\, \varepsilon \qquad \text{or} \qquad D\,L\,B\,\sigma_\lambda \approx \varepsilon \tag{I-17}$$

The duty cycle has no effect when the source spectrum dominates. The right-hand expression was used in [ITU-T G.957]. For the limiting case of a narrow spectrum/high bit rate transmitter, Equation I-15 or I-16 gives:

$$D\,L\,B^2\, \lambda^2 \approx \pi\, c\, \varepsilon\, f \tag{I-18}$$

Hence, the maximum allowed chromatic dispersion for a fixed RZ bit rate decreases along with the duty cycle. Again, this is because the frequency bandwidth of an RZ signal is greater than that of an NRZ signal at the same bit rate.

The above equations are for input pulses and source spectra that are Gaussian. It is assumed that they apply in an rms sense to more general shapes to within a reasonable approximation.

I.7 General result and practical units

Now Equations I-16 and I-9 give, in general:

$$DL = \frac{\varepsilon\, c}{\lambda^2\, B\, \sqrt{\left(\dfrac{B}{\pi\, f}\right)^2 + \sigma_v^2}} \tag{I-19}$$

broad spectrum/low bit rate:

$$\lambda^2\, B\, D\, L\, \sigma_v \approx \varepsilon\, c \qquad \text{or} \qquad B\, D\, L\, \sigma_\lambda \approx \varepsilon \tag{I-20}$$

narrow spectrum/high bit rate:

$$\lambda^2\, B^2\, D\, L \approx \pi\, \varepsilon\, c\, f \tag{I-21}$$

Usually the –20 dB full-width Γ is used in specifications. The Gaussian approximation used in [ITU-T G.957] gives the relation with the rms width:

$$\Gamma \approx 6.0697\,\sigma \qquad\qquad\qquad (I\text{-}22)$$

Also, with B in Gbits/s, D in ps/nm·km, L in km (hence DL in ps/nm), λ in µm (not nm), σ_v in GHz, σ_λ in nm, and $c \approx 299{,}792.458$ km/s (as per [ITU-T G.692]), Equation I-19 becomes Equation 9-1 in clause 9.2.1.1. The frequency and source widths of Equation I-9 are related by Equation 9-2.

For the limiting case of a broad spectrum/low bit rate, Equations I-20 and I-22 give Equation 9-3. For the opposite limit of a narrow spectrum/high bit rate, Equation I-21 becomes Equation 9-4.

Bibliography

[b-ITU-T G.680]	Recommendation ITU-T G.680 (2007), *Physical transfer functions of optical network elements*.
[b-ITU-T G.696.1]	Recommendation ITU-T G.696.1 (2010), *Longitudinally compatible intra-domain DWDM applications*.
[b-ITU-T G.982]	Recommendation ITU-T G.982 (1996), *Optical access networks to support services up to the ISDN primary rate or equivalent bit rates*.
[b-ANSI INCITS 338]	ANSI INCITS 338-2003, *Information Technology – High-performance Parallel Interface 6400 Mbit/s Optical Specification (HIPPI-6400-OPT)*.
[b-ANSI INCITS 450]	ANSI INCITS 450-2009, *Information technology – Fibre Channel – Physical Interface-4 (FC-PI-4)*.
[b-IEC SC86C]	IEC SC86C/WG1 ST-20 (2000), *Statistical treatment of chromatic dispersion*. (Submitted by T.A. Hanson.)
[b-IEC/TR 61282-1]	IEC/TR 61282-1 (2000), *Fibre optic communication system design guides – Part 1: Single-mode digital and analogue systems*.
[b-IEEE 1394b]	IEEE 1394b-2002, *IEEE Standard for a High-Performance Serial Bus – Amendment 2*.
[b-IEEE 802.3]	IEEE 802.3-2005, *Specific requirements – Part 3: Carrier sense multiple access with collision detection (CSMA/CD) access method and physical layer specifications*.
[b-ISO/IEC 9314-3]	ISO/IEC 9314-3:1990, *Information processing systems – Fibre Distributed Data Interface (FDDI) – Part 3: Physical Layer Medium Dependent (PMD)*.
[b-Agrawal]	Agrawal, G.P. (1995), *Nonlinear Fiber Optics*, San Diego, CA, Academic Press.
[b-Agrawal2]	Agrawal, G.P., Anthony, P.J., and Shen, T.M. (1988), *Dispersion Penalty for 1.3 μm Lightwave Systems with Multimode Semiconductor Lasers*, Journal of Lightwave Technology, Vol. 6, No. 5, May, pp. 620-625.
[b-Agrawal3]	Agrawal, G.P. (1997), *Fiber-Optic Communication Systems*, 2nd Edition, New York, John Wiley & Sons, Inc.
[b-Agrell]	Agrell, E., and Karlsson, M., (2009), *Power-efficient modulation formats in coherent transmission systems*, IEEE J. Lightw. Technol., Vol. 27, no. 22, pp. 5115-5126, Nov. 2009.
[b-Antona]	Antona, J.-C., Bigo, S., and Faure, J.-P. (2002), *Nonlinear Cumulated Phase as a Criterion to Assess Performance of Terrestrial WDM Systems*, Conference on Optical Fiber Communication (OFC) and Exhibit 2002, paper WX5.
[b-Barbieri]	Barbieri, A., Fertonani, D., and Colavolpe, G., "Time-frequency packing for linear modulations: spectral efficiency and practical detection schemes," IEEE Trans. Commun., vol. 57, pp. 2951–2959, Oct. 2009.

[b-Böckl]	Böckl, M. (2002), *Modulation Formats for Fiber Transmission Systems with Direct-Detection Receivers* [Dissertation],Vienna, Institut für Nachrichtentechnik und Hochfrequenztechnik.
[b-Bulow]	Bulow, H. (1998), *System Outage Probability Due to First and Second Order PMD*, Photonics Technology Letters, Vol. 10, No. 5, pp. 696-698.
[b-Buelow]	Buelow, H., (2009), *Polarization QAM Modulation (POL-QAM) for Coherent Detection Schemes, OFC 2009, paper OWG2, San Diego, CA, March 2009.*
[b-Cai]	Cai, J.-X., Davidson, C.R., Lucero, A., Zhang, H., Foursa, D.G., Sinkin, O.V., Patterson, W.W., Pilipetskii A.N., Mohs, and G., Bergano, N.S., "20 Tbit/s Transmission Over 6860 km With Sub-Nyquist Channel Spacing," Journal of Lightwave Technology, vol.30, no.4, pp.651-657, Feb.15, 2012.
[b-Charlet]	Charlet, G. et al. (2009), *Performance Comparison of DPSK, P-DPSK, RZ-DQPSK and Coherent PDM-QPSK at 40Gb/s Over a Terrestrial Link*, Conference on Optical Fiber Communication (OFC) and Exhibit 2009, Paper JWA40.
[b-Cigliutti]	Cigliutti, R. et al. (2012), *Ultra-Long-Haul Transmission of 16x112 Gb/s Spectrally-Engineered DAC-Generated Nyquist-WDM PM-16QAM Channels with 1.05x(Symbol-Rate) Frequency Spacing*, OFC 2012, OTh3A.3.
[b-Dochhan]	Dochhan, A. et al. (2013), *First Experimental Demonstration of a 3-Dimensional Simplex Modulation Format Showing Improved OSNR Performance Compared to DP-BPSK*, OFC 2013, Paper JTh2A.40, Anaheim, CA, March 2013.
[b-Färbert]	Färbert, A. et al. (1999), *Optimised Dispersion Management Scheme for Long-Haul Optical Communication*, Electronics Letters, Vol. 35, No. 21, p. 1865.
[b-Hopland]	Hopland, S., (2007), *Investigation of Wide Spectrum Losses in Installed G.655 Fibre Cables*, Proceedings of the International Wire & Cable Symposium, November 2007, Lake Buena Vista, Florida, USA.
[b-Hui]	Hui, R. et al. (2002), *Subcarrier Multiplexing for High-Speed Optical Transmission*, Journal of Lightwave Technology, Vol. 20, No. 3, March, pp. 417-427.
[b-Iannone]	Iannone, E. et al. (1998), *Nonlinear Optical Communication Networks*, New York, John Wiley & Sons, Inc.
[b-Inoue]	Inoue, K., and Toba, H. (1995), *Fiber Four-Wave Mixing in Multi-Amplifier Systems with Non-Uniform Chromatic Dispersion*, Journal of Lightwave Technology, Vol. 13, No. 1, pp. 88-93.
[b-Jansen]	Jansen, S.L. et al. (2007), *16x52.5-Gb/s, 50-GHz Spaced, POLMUX-CO-OFDM Transmission Over 4,160 km of SSMF Enabled by MIMO Processing*, 33rd European Conference and Exhibition of Optical Communication (ECOC) 2007, paper PD1.3.

[b-Jeruchim]	Jeruchim, M.C. (1984), *Techniques for Estimating the Bit Error Rate in the Simulation of Digital Communication Systems*, IEEE Journal on Selected Areas in Communications, Vol. 2, No. 1, January, pp. 153-170.
[b-Jia]	Jia, Z. et al. (2012), Field Transmission of 100G and Beyond: Multiple Baud Rates and Mixed Line Rates Using Nyquist-WDM Technology, J. Lightwave Tech., Vol. 30, No. 24, pp. 3793-3804.
[b-Kikushima]	Kikushima, K., and Hogari, K. (1990), *Statistical Dispersion Budgeting Method for Single-Mode Fiber Transmission Systems*, Journal of Lightwave Technology, Vol. 8, No. 1, pp. 11-15.
[b-Klekamp]	Klekamp, A., Dischler, R., and Idler, W. (2006), *DWDM and Single Channel Fibre Nonlinear Thresholds for 43 Gb/s ASK and DPSK Formats Over Various Fibre Types*, Conference on Optical Fiber Communication (OFC) 2006, paper OFD6.
[b-Kobayashi]	Kobayashi, T. et al. (2008), *Electro-Optically Multiplexed 110 Gbit/s Optical OFDM Signal Transmission Over 80 km SMF Without Dispersion Compensation*, Electronics Letters, Vol. 44, No. 3, pp. 225-226.
[b-Legg]	Legg, P.J., Tur, M., and Andonovic, I. (1996), *Solution Paths to Limit Interferometric Noise Induced Performance Degradation in ASK/Direct Detection Lightwave Networks*, Journal of Lightwave Technology, Vol. 14, No. 9, pp. 1943-1954.
[b-Liu]	Liu, F., Rasmussen, C.J., and Pedersen, R.J.S. (1999), *Experimental Verification of a New Model Describing the Influence of Incomplete Signal Extinction Ratio on the Sensitivity Degradation Due to Multiple Interferometric Crosstalk*, Photonics Technology Letters, Vol. 11, No. 1, pp. 137-139.
[b-Lu]	Lu, G.W. et al. (2010), *16-QAM Transmitter using Monolithically Integrated Quad Mach-Zehnder IQ Modulator*, 36th European Conference and Exhibition on Optical Communication (ECOC) 2010, paper Mo.1.F.3.
[b-Maksoudian]	Maksoudian, Y.L. (1969), *Probability and Statistics with Applications*, Scranton, PA, Scranton International Textbook Company.
[b-Marcuse]	Marcuse, D. (1981), *Pulse Distortion in Single-Mode Fibers. 3: Chirped Pulses*, Applied Optics, Vol. 20, No. 20, pp. 3573-3579.
[b-Matera]	Matera, F. et al. (2001) *Esperimenti di Trasmissione Solitonica Multicanale a 40 Gb/s: Il Progetto IST/ATLAS*, Atti Fotonica (relazione invitata), pp. 67-74.
[b-Mikkelsen]	Mikkelsen, B. et al. (2006), *Partial DPSK with Excellent Filter Tolerance and OSNR Sensitivity*, Electronics Letters, Vol. 42, No. 23, pp. 1363-1364.
[b-Mizuochi]	Nakazawa Masataka, High Spectral Density Optical Communication Technologies (Chap.17.:Forward Error Correction), Springer, 2010
[b-Pauer]	Pauer, M., Winzer, P.J., and Leeb, W.R (2001), *Bit Error Probability Reduction in Direct Detection Optical Receivers Using RZ Coding*, Journal of Lightwave Technology, Vol. 19, pp. 1255-1262.

[b-Pennickx]	Pennickx, D. et al. (1997), *The Phase-Shaped Binary Transmission (PSBT): A New Technique to Transmit Far Beyond the Chromatic Dispersion Limit*, Photonics Technology Letters, Vol. 9, No. 2, pp. 259-261.
[b-PMD]	Winzer, P.J. et al. (2002), *Effect of Receiver Design on PMD Outage for RZ and NRZ*, Conference on Optical Fiber Communication (OFC) and Exhibit 2002, pp. 46-48.
[b-Potì]	Potì, L., Meloni, G., Berrettini, G., Fresi, F., Secondini, M., Foggi, T., Colavolpe, G., Forestieri, E., D'Errico, A., Cavaliere, F., Sabella, R., and Prati, G., *Casting 1 Tb/s DP-QPSK Communication into 200 GHz Bandwidth*, ECOC'12, Amsterdam, NL, 2012, paper P4.19.
[b-Rusek]	Rusek, F. and Anderson, J. B., *The two dimensional Mazo limit*, in Proc. IEEE International Symposium on Information Theory, pp. 970–974, 2005.
[b-Sjodin]	Martin Sjodin, et al.(2012), *Comparison of 128-SP-QAM with PM-16-QAM, Optics Express*. 04/2012; 20(8):8356-66. DOI: 10.1364/OE.20.008356.
[b-Sano]	Sano, A. et al. (2007), *30 x 100-Gb/s All-Optical OFDM Transmission Over 1300 km SMF with 10 ROADM Nodes,* 33rd European Conference and Exhibition of Optical Communication (ECOC) 2007, paper PD1.7.
[b-Sano2]	Sano, A. et al. (2010), *69.1-Tb/s (432 x 171-Gb/s) C- and Extended L-Band Transmission over 240 km Using PDM-16-QAM Modulation and Digital Coherent Detection*, Conference on Optical Fiber Communication (OFC), collocated National Fiber Optic Engineers Conference (NFOEC) 2010, paper PDPB7.
[b-Secondini]	Secondini M., Forestieri, E., and Cavaliere, F. (2009), *Novel Optical Modulation Scheme for 16-QAM Format with Quadrant Differential Encoding*, International Conference on Photonics in Switching 2009.
[b-Spirit]	Spirit, D.M., and O'Mahony, M.J. (1995), *High Capacity Optical Transmission Explained*, New York, John Wiley & Sons, Inc.
[b-T11 FC]	T11 FC Project, *Fibre Channel, Physical Interfaces (FC-PI)*, Draft Rev. 8.1, 2000.
[b-Takahashi]	Takahashi, H., Oda, K., and Toba, H. (1996), *Impact of Crosstalk in an Arrayed-Waveguide Multiplexer on $N \times N$ Optical Interconnection*, Journal of Lightwave Technology, Vol. 14, No. 6, pp. 1097-1105.
[b-Weber]	Weber, W., III (1978), *Differential Encoding for Multiple Amplitude and Phase Shift Keying Systems*, IEEE Transactions on Communications, Vol. 26, No. 3, March, pp. 385- 391.
[b-Winzer]	Winzer, P.J. et al. (2003), *40-Gb/s Return-to-Zero Alternate-Mark-Inversion (RZ-AMI) Transmission over 2000 km*, Photonics Technology Letters, Vol. 15, No. 5, pp. 766-768.
[b-Winzer2]	Winzer, P.J, et al. (2010), *Generation and 1,200-km Transmission of 448-Gb/s ETDM 56-Gbaud PDM 16-QAM using a Single I/Q Modulator*, 36th European Conference and Exhibition on Optical Communication (ECOC) 2010, paper PD2.2.

[b-Yamada]	Yamada, E. et al. (2008), *Novel No-Guard-Interval PDM CO-OFDM Transmission in 4.1 Tb/s (50 x 88.8 Gb/s) DWDM Link Over 800 km SMF Including 50-GHz Spaced ROADM Nodes*, Conference on Optical Fiber Communication (OFC) 2008, paper PDP8.
[b-Yang]	Yang, Q., Ma, Y., and Shieh, W. (2008), *107 Gb/s Coherent Optical OFDM Reception Using Orthogonal Band multiplexing*, National Fiber Optic Engineers Conference (NFOEC) 2008, paper PDP7.
[b-Yonenaga]	Yonenaga, K. et al. (1995), *Optical Duobinary Transmission System with No Receiver Sensitivity Degradation*, Electronics Letters, Vol. 31, No. 4, pp. 302-303.
[b-Zitelli]	Zitelli, M., Matera, F., and Settembre, M. (1999), *Single-Channel Transmission in Dispersion Management Links in Conditions of Very Strong Pulse Broadening: Application to 40 Gb/s Signals on Step-Index Fibers*, Journal of Lightwave Technology, Vol. 17, No. 12, pp. 2498-2505.

SERIES OF ITU-T RECOMMENDATIONS

Series A   Organization of the work of ITU-T

Series D   General tariff principles

Series E   Overall network operation, telephone service, service operation and human factors

Series F   Non-telephone telecommunication services

Series G   Transmission systems and media, digital systems and networks

Series H   Audiovisual and multimedia systems

Series I   Integrated services digital network

Series J   Cable networks and transmission of television, sound programme and other multimedia signals

Series K   Protection against interference

Series L   Environment and ICTs, climate change, e-waste, energy efficiency; construction, installation and protection of cables and other elements of outside plant

Series M   Telecommunication management, including TMN and network maintenance

Series N   Maintenance: international sound programme and television transmission circuits

Series O   Specifications of measuring equipment

Series P   Terminals and subjective and objective assessment methods

Series Q   Switching and signalling

Series R   Telegraph transmission

Series S   Telegraph services terminal equipment

Series T   Terminals for telematic services

Series U   Telegraph switching

Series V   Data communication over the telephone network

Series X   Data networks, open system communications and security

Series Y   Global information infrastructure, Internet protocol aspect, next-generation networks, Internet of Things and smart cities

Series Z   Languages and general software aspects for telecommunication systems